The impact of different nourishment designs

Evaluated at the Domburg coast, the Netherlands

G.G. van Maanen

TU Delft

Front cover:

A sanderling on the Domburg coastline at dusk. (Source: Gerard van Maanen)

The impact of different nourishment designs

evaluated at the Domburg coast, the Netherlands

A case study

by

G.G. van Maanen

In partial fulfilment of the requirements for the degree of

Master of Science
in Civil Engineering

at the Delft University of Technology
to be defended publicly on Friday November 19, 2021 at 10:00 AM.

Thesis committee:	Dr. Ir. E. Brand	Rijkswaterstaat
	Drs. Q.J. Lodder	Rijkswaterstaat & TU Delft
	Dr. Ir. M.A. de Schipper	TU Delft
	Dr. Ir. B.C. van Prooijen	TU Delft

An electronic version of this thesis is available at http://repository.tudelft.nl/.

TUDelft

II

Preface

This report describes the result of my final work as a student at the Delft University of Technology. In December 2020, I started exploring the morphological features at the Walcheren coast. Almost a year later, I finalize my research on the effect of multiple nourishment strategies at the Domburg coast with still many morphological secrets to unravel. Although, I was mostly restricted to working from home, I am thankful to have completed my research with Rijkswaterstaat. Meeting people from different disciplines and learning about their passion and work was extremely valuable and motivating.

This research would not have been possible without the help of many people. I would like to thank all the people who are involved in this research, especially my supervisors for their great advice and guidance. Evelien and Quirijn, I am very grateful for your help, our lively discussions, and that you introduced me to Rijkswaterstaat. Matthieu, your enthusiasm helped me greatly to continue looking for answers. Bram, I am thankful for your insightful suggestions and questions.

Additionally, I would like to thank my colleagues from Rijkswaterstaat for their advice and help to obtain all necessary information. Specifically, I would like to show my appreciation to Ka-Way, a fellow student graduating at Rijkswaterstaat, for our thorough discussions, motivation and support.

I would like to finish off this acknowledgement with special thanks to my friends and family for their love, support and some distraction from my work. Thank you, Anne, for encouraging and supporting me and the fun we had during our breaks.

G.G. van Maanen

Leiden, November 2021

Abstract

The coastline near Domburg, in the southwest delta of the Netherlands, has been preserved with sand for three decades. Maintenance was conducted on the beach between the low water line and the dune foot every 4 years. To extent this interval, a shoreface nourishment was implemented in 2017 and was supplemented with a beach nourishment in 2019. Such a parallel shoreface bar is not a naturally occurring morphological feature, as the Domburg coast only features transverse bars.

This research investigates the hydrodynamic and morphological effects of different nourishment strategies at the Domburg coast. The study focusses on the application of the shoreface nourishment, as this strategy has not been previously applied at a coast without shore-parallel bars. The study aims at gaining more insight and knowledge on important mechanisms responsible for the spreading of nourished sediment, because this is not fully understood. Additionally, the performance of a numerical model to hindcast erosion and sedimentation in coastal zones is evaluated.

To this end, a morphological analysis based on measurements and a model analysis are conducted for three nourishment scenarios. The morphological analysis uses an extensive dataset of bathymetric surveys to compute volume changes, sediment fluxes, bar migration rates, momentary coastline (MKL) positions and nourishment longevities (defined as the period that the volume in between the dune foot and mean low water level is greater than before nourishment). The numerical model analysis is based on the output of a morphostatic XBeach model with simplified boundary conditions which computes the hydrodynamics and sediment transports.

The longevity of beach nourishments was found to be on average 3.3 years and the MKL regressed 3.9m/yr on average two years after construction. The eroded sediment did not accrete on the shoreface but was likely transported in the direction of the net sediment transport. The model output indicates that a beach nourishment only has a significant local effect on the hydrodynamics and transport rates.

The shoreface nourishment transforms from a landward skewed triangular shape into a more rounded body without the formation of a trough. The bar migrates onshore but not alongshore and the bar volume remains constant. The model shows a contraction of the tidal flow due to the shoreface bar, increasing the seaward velocity and causing a sheltered zone at the leeside and downdrift of the bar. Consequently, the alongshore transport gradients are increased. This causes extra erosion on the shoreface seaward of the bar while accretion is seen at the downdrift shoreface. The shoreface bar contributes little to the offshore dissipation of wave energy. No evidence for a wave-driven salient effect was found at Domburg from the model output.

The longevity of the 2019 beach nourishment is not prolonged by the presence of a shoreface bar, as this was found to be 3.1 years. Likewise, the MKL measured a regression of 4.3m/yr, similar to previous beach nourishments. Positively, the shoreface bar captures eroding beach sediment because accretion was found in the surf zone, as opposed to the 2014 beach nourishment. Therefore, a shoreface nourishment is moderately beneficial on maintaining the MKL but contributes to the sediment balance of the coastal cell.

Additionally, an alternative nourishment strategy was evaluated through the numerical model. A mega nourishment to the west of Domburg is a viable option as it is likely to feed the updrift and downdrift coastlines which have a sediment demand. It is recommended to further evaluate this nourishment strategy with different numerical models.

Table of Contents

Acronyms

RSP   Beach Reference Pole (Rijks Strand Paal)

BKL   Reference Coastline (Basis Kustlijn)

MKL   Momentary Coastline (Momentane Kustlijn)

JARKUS   Annual Coastal Bathymetry measurements (JAaRlijkse KUStmeting)

NAP   Amsterdam Ordnance Datum (Normaal Amsterdams Peil)

NE   Northeast

NW   Northwest

SW   Southwest

HW   High Water

MHWL   Mean High Water Level

MSL   Mean Sea Level

MLWL   Mean Low Water Level

LW   Low Water

1. Introduction

This chapter provides the background, problem description, scope and objective of this research. Subsequently, the research questions and the outline of the analysis are formulated.

1.1   Background

Natural and anthropogenic induced processes drive the structural erosion of the Dutch coastline. Among these processes are sea level rise, the closing of estuaries, and the lack of natural sediment input. This creates an imbalance of the sediment budget of the coastal cell which has consequences for coastal functions such as safety, nature, recreation and drinking water extraction (Interreg, 2021).

In 1990, the Netherlands has decided to dynamically preserve the coastline with soft measures and to halt long-term coastal recession (de Ruig, 1998). A reference coastline (BKL) was defined and by regularly compensating sediment losses, the loss of beach and dune functions are mitigated. Figure 1 shows that in the early nineties approximately 6 million m^3 sand was supplied to the Dutch coastal zone, nowadays 12 million m^3 is nourished to also compensate for sediment losses at deeper water (van der Spek & Lodder, 2015). If the rate of sea level rise increases in the future, larger yearly nourishment volumes are needed to balance the coastal sediment budget (Rijkswaterstaat, 2020).
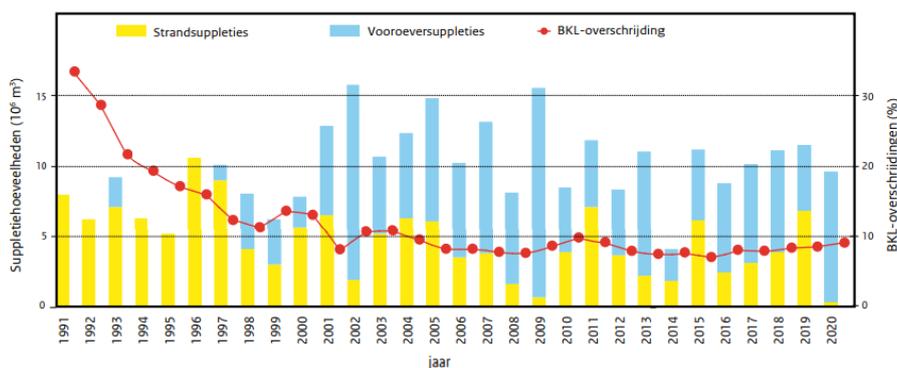

Figure 1: Nourishments at the Dutch coast, being subdivided for beach and shoreface nourishments. The percentage of BKL exceedance is depicted on the secondary y-axis. (From: Kustlijnkaarten 2021, Rijkswaterstaat)

1.2   Problem description

Originally, mainly the beach zone between the low water line and the dune foot was nourished. In the last twenty years, this has changed as shoreface nourishments became the preferred strategy to replenish the Dutch shore. Although experiences with shoreface nourishments are positive, as they positively affect the shoreline position on the long term, our understanding remains limited (Huisman, 2019). These shoreface nourishments have been applied almost exclusively at coasts with cross-shore bar behaviour. Therefore, the behaviour of shoreface nourishments at distinctive coastlines is mainly unknown.

The mechanisms responsible for the spreading of the nourished sediment are not fully understood or captured in numerical models. Huisman (2019) proposes a conceptual model for the spreading of a shoreface nourishment, but the responsible mechanisms remain unresolved. This imposes an obstacle for morphodynamic simulations. Shoreface bars are rapidly dissipated in most numerical models which imposes a challenge for the correct representation of the coastal development (Huisman, 2019). An improved knowledge of the

spreading of shoreface nourishments contributes to increasing the efficiency and decreasing the environmental impact.

1.3   Scope

The coastline of the Netherlands can be divided in three areas: The Wadden Sea in the North, characterised by barrier islands and a back-barrier intertidal flat area. The central Holland coastline, a gradually sloping uniform coastline with shore-parallel breaker bars. In the southwest, the Delta area is formed by four estuaries of which three are (semi) closed.

This research focusses on the coastline of Northwest Walcheren in the SW Delta area, amidst the Western and the Eastern Scheldt outer deltas. This is one of the few coastlines in the Netherlands without distinct shore-parallel bar behaviour. Moreover, numerous nourishments were carried out at this shoreline with diverse strategies. Numerous beach nourishments have been implemented between 1989-2014. Recently, the first shoreface nourishment has been implemented in December 2017. Additionally, in 2019, a beach nourishment was placed, resulting in a combined nourishment strategy.

The first objective is to better identify, quantify and understand the hydrodynamic and morphological processes at a shoreline without existing breaker bars. The second objective is to determine the impact of beach and shoreface nourishments on these processes. The third objective is to identify the ability of a numerical model to predict morphological changes. This knowledge aids the efficiency of shoreline nourishment strategies.

1.4   Research questions

To meet the aims and objectives, the following three research questions are answered. Each research question is supplemented with several sub questions.

1. How does a coast without shore-parallel subtidal bars develop for different nourishment strategies?

    a. What cross-shore profile changes are observed?

    b. What alongshore changes are observed?

    c. How do the sediment volumes of coastal zones change?

    d. What is the expected lifetime of nourishments?

    e. What is the evolution of the momentary coastline?

2. What processes explain the observed morphological changes of a nourished coast without shore-parallel subtidal bars?

    a. How are the wave height and direction affected by nourishments?

    b. How are tidal and wave driven currents affected by nourishments?

    c. How is the dissipation of wave energy affected by nourishments?

    d. How are sediment transport rates affected by nourishments?

3. To what extent is a morphostatic numerical model able to represent the volume changes in coastal zones posterior to a nourishment?

a. To what extent are volume changes captured accurately for a shoreface nourishment?

b. To what extent are volume changes captured accurately for a combined beach and shoreface nourishment?

The first two research questions are answered for three nourishment strategies: a beach nourishment, a shoreface nourishment and a combination of both. The first research question is answered through observations. The second question is dealt with through a numerical model study. The third research question is answered by comparing observations and model output.

The answers to these research questions lead to insight in the response of the coastal system to nourishments. With the improved understanding, an alternative nourishment strategy is assessed. The effect of this alternative nourishment strategy on the coastal system will be evaluated through a model study and compared to the antecedent outcomes.

1.5   Approach and outline

This section describes the approach and outline of this thesis. Figure 2 gives a schematization of the approach. The study starts with a literature review of theory, which is presented in chapter 2. Hereafter, a morphological analysis based on surveys and a model analysis are performed, which is an iterative process as the outcomes of one analysis raise new questions which are tackled in the other. The methods of these analyses are described in chapter 3 and the outcomes are presented in chapter 4. The outcomes are discussed in chapter 5. From these outcomes, an alternative nourishment strategy is synthesised and tested with a numerical model, which is presented in chapter 6. The research questions are answered in chapter 7. Recommendations for future nourishments and further research in the study area are given in chapter 8.

Research questions (ch. 1) → Theory (ch. 2) → Method (ch. 3) → Morphological and model analysis (ch. 4) → Discussion (ch. 5) → Alternative synthesis (ch. 6) → Conclusions (ch. 7) → Recommendations (ch. 8)
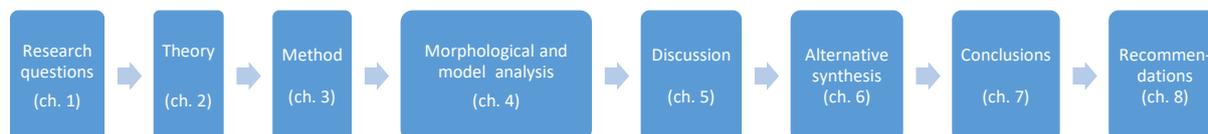
Figure 2: Approach of the conducted research.

2. Background and study area

The following chapter provides the information on natural and anthropogenic induced processes in the coastal zone. First, the coastal terminology is provided. Next, relevant hydro- and morphodynamical processes are discussed. Then, the Dutch coastal maintenance policies, nourishment strategies and how these affect the coast are explained. In conclusion, a description of the study site, the NE coast of Walcheren, is given.

2.1   Coastal terminology

The coastal zones, where land and water interact with each other, are defined by different elevation levels (Figure 3) and are further explained in Table 1.
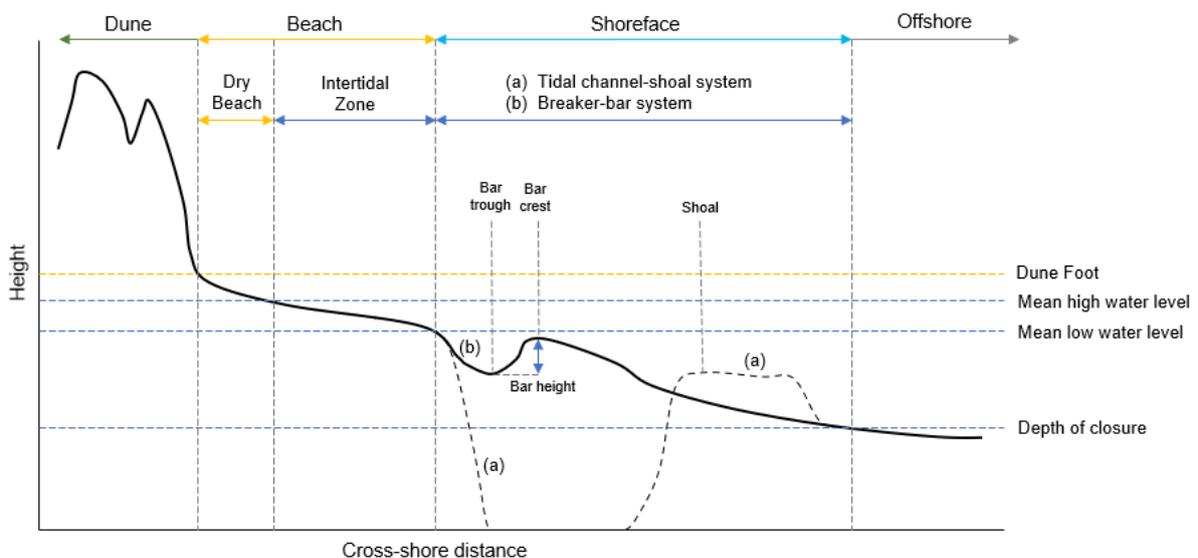

Figure 3: Definitions of coastal terms for a tidal channel-shoal system [dashed] and breaker-bar system [solid]. Adapted from: Hillmann (NLWKN).

Dune foot

The dune foot is the vertical level where the slope of the coastal profile steepens significantly. In the Netherlands, this vertical level is regularly chosen as NAP+3m (Deltares, 2018).

Depth of closure

The depth of closure is the most landward depth seaward of which no significant change in bottom elevation and no significant net sediment transport between the nearshore and the offshore is observed. Generally, the depth of closure can be either defined as the depth where different-time series show no significant bed elevation changes (Brutsché et al., 2019) or from a relation with the waves (Hallermeier, 1981).

Table 1: Definitions of morphological zones and height levels also visualised in (Figure 3).

Coastal Section	Coastal indicators	Definition
Dune	DF	Dune foot level: fixed height level where the slope is distinctly changing. In the Netherlands the DF lies around NAP + 3m.
Beach	Dry beach	Section above the Mean High-Water Level and below the Dune Foot level.
	MHWL	Mean High Water Level
	Wet beach / intertidal zone	Section between MLWL and MHWL, where often ridges and runnels are found.
	MLWL	Mean Low Water Level
Shoreface	(a) Tidal channel-shoal system	Channel: Deep section between MLWL and the front of the shoal Shoal: a relatively shallow area not connected to the beach which is shaped by tidal forces
	(b) Breaker bar system	Bar: sand accumulation created by the action of currents and waves. The bar crest and trough are the local maximum and minimum respectively. The bar height is the vertical difference between the bar crest and trough.
Offshore	Seaward limit (SL)	Sets a limit for calculating shoreface width and volume, often defined with the depth of closure.

2.2 Hydro- and morphodynamics

This section considers the near-shore hydro- and morphodynamics, largely based on the work of Bosboom and Stive (2015). It elaborates upon the water levels and currents induced by waves, tides, and winds respectively. The natural processes that are driven by the hydrodynamics and how these affect the sediment transport in the cross-shore and alongshore direction are discussed in each subsection.

2.2.1 Waves

Waves transform when travelling from deep into intermediate and shallow waters. Propagation directions, wave heights and wavelengths change, and waves start to break. These changes occur because the waves are affected by bed processes such as shoaling, refraction, and wave-breaking, discussed below in respective order.

Shoaling

As waves travel into intermediate water depth, the propagation speed is affected by the bottom. As the dissipation outside the surf zone is negligible, the energy flux remains constant. This is a function of the wave group velocity and the wave height, and thus wave heights increase or decrease when the propagation speed changes.

Refraction

Oblique incoming waves change their propagation direction in increasingly shore normal direction as the water depth decreases. This is contributed to the higher propagation speed of the wave in deeper water, and so the wave turns towards the depth contour. This phenomenon can cause convergence and divergence of wave energy, also known as wave focussing, and can contribute to larger erosion rates at certain coastal locations. Similarly, current-refraction may occur in tidal inlets where the current velocity varies over the wave crest.

Wave-breaking

Due to increasing wave heights, the crests can become unstable, and the waves start to dissipate energy through breaking. This can either be caused by steepness induced breaking, seen as the white-capping of waves in deep water, or by depth-induced breaking which is observed in the surf zone.

Cross-shore sediment transport in the nearshore

The passage of waves drives an orbital fluid motion. According to linear wave theory, these orbits are enclosed. However, due to non-linear effects, which become more apparent in intermediate and shallow water depths, non-linear effects enable a net wave-induced transport.

Skewness and Asymmetry of the surface elevation

Skewness is the asymmetry relative to the horizontal axis, where the troughs become longer and flatter while crests become higher and narrower. For skewed waves, the shoreward velocity under the crest is higher than the seaward velocity under the trough. Due to the cubed relationship between velocity and bedload transport, a net shoreward sediment transport is found under skewed waves (Henriquez, 2019).

On the other hand, asymmetry, the asymmetry relative to the vertical axis, is characterised by steepening of the wave front and a pitched-forward shape. Asymmetry causes larger onshore accelerations than the offshore accelerations due to the pitched forward wave shape (Henriquez, 2019).

Time-averaged currents

Next to the intra-wave orbital motion, progressive waves generate various types of time-averaged currents (Henriquez, 2019):

1) Longuet-Higgins streaming is a relatively small net current in the wave boundary layer in the direction of wave propagation of progressive surface waves.

2) Coined wave shape streaming is a wave boundary layer current against the wave direction, related to the non-sinusoidal wave shape in the nearshore.

3) Stokes drift is a mass flux in the direction of wave propagation, which introduces a return flow lower in the water column in the case of a boundary such as a shore.

4) In addition, undertow and rip-currents are associated with breaking waves, which dominate over Longuet-Higgins streaming in the surf zone (Bosboom & Stive, 2015).

Under non-breaking waves the turbulence above the wave boundary layer is relatively small and so sand is not in suspension, however the shearing of orbital flow does generate bedload. Therefore, bedload is dominant over suspended load under unbroken waves, which has a cubed relationship with horizontal flow velocity (Henriquez, 2019).

Alongshore sediment transport in the nearshore

In alongshore direction, obliquely incoming breaking waves induce a current in the surf zone. This current is driven by the transfer of momentum of the waves to the mean flow. Where in the cross-shore direction this force is countered by a water level gradient, that is not possible in alongshore direction. Therefore, the balancing force is supplied by bed shear stress that develops when an alongshore current is generated.

For a shoreline perturbation, gradients in the alongshore current and thus sediment transport arise. This either flattens the perturbation for mildly oblique incoming waves or causes the growth of the perturbation for high angle waves (Figure 4).
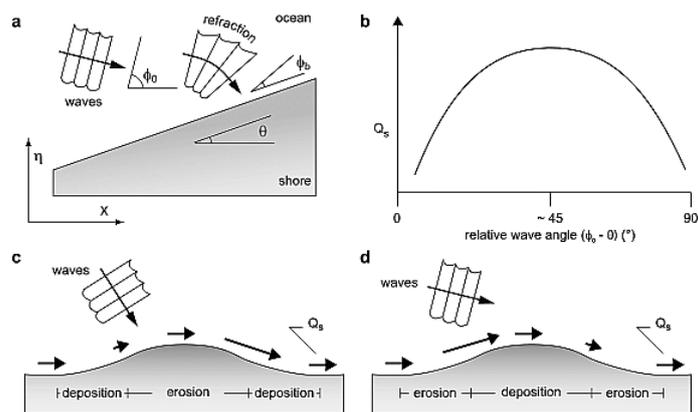
Figure 4: Response of a perturbation in the shoreline. a) Angles between incoming waves and the shoreline. b) Transport curve as a function of wave angle. c) For low-angle waves, the transport increases for higher relative angles. d) Response to high-angle waves for which the transport decreases for increasing relative angles. From: Ashton and Murray (2006).

2.2.2 Tides

The difference in gravitational pull of astronomical bodies on water masses generates the tide. In the North Sea basin, the water level varies around multiple amphidromic points in anti-clockwise direction. This results in the tidal wave propagating from the South of the Netherlands to the North, where the water level variations induce tidal currents. These currents run parallel to coast and their magnitude is proportional to the square root of the product of water depth and the alongshore water level gradient (Bosboom & Stive, 2015). This results in weaker tidal currents in shallow areas.

Asymmetry and skewness of the tidal wave

Similarly, to wind driven waves, oceanic tidal waves that propagate into shallow coastal waters are being distorted. The asymmetry induces anti-clockwise residual currents in the North Sea basin (Sündermann & Pohlmann, 2011). Likewise, the tidal wave near Walcheren deviates from a symmetrical tide (Figure 5). Looking at Figure 5, it is seen that the high-water amplitude is larger than the low water amplitude. This is a skewed tidal wave with flatter, longer troughs and peaked narrow crests. The duration of positive water levels is shorter than for negative water levels. Furthermore, the time between HW and LW is longer than between LW and HW implying an asymmetric pitched forward tidal wave shape.
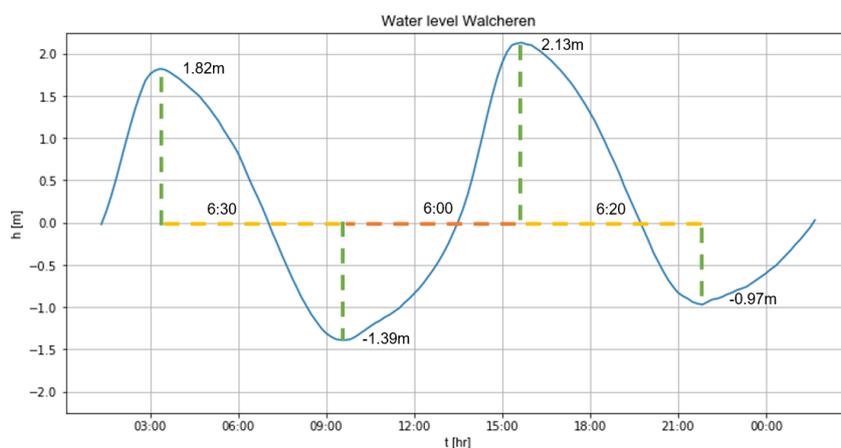

Figure 5: Example of the water level variation from the Oosterschelde11(b) measurement station in Nov 2008.

The skewness of the tide is relevant to the net sediment transport. Due to skewness, the flood velocity is higher than the ebb-velocity. Therefore, as sediment transport responds non-linearly to the velocity, a residual sediment transport in flood direction is expected.

2.2.3 Wind
The wind exerts a shear stress upon the water surface, which drives the following three processes.

Wave generation
The first process is the generation of waves by local wind fields. The wave height, period and direction are determined by the speed, duration and direction of the wind field, the fetch length and the local water depth.

Wind driven currents
Second, the wind can induce a current where the highest velocities occur at the surface and exponentially decrease in downward direction. Therefore, the impact on the morphology is limited due to the small near-bottom velocity, where the highest sediment concentrations are. Nevertheless, the residual longshore current may be largely affected during storms and in very shallow water the relative importance of wind-driven currents increases.

Water level gradients
Third, a landward wind exerts a shear stress and a mass transport in the same direction. As the coastline forms a barrier, an opposite directed mass transport is needed to compensate the onshore flow. In that manner, a water level set-up develops near the coast. This process is reinforced in the shallow coastal zone, also known as storm surge. The water level gradient drives a near-bed offshore current.

2.3   Nearshore coastal features
The previous section discussed some elemental hydrodynamic and morphodynamic processes acting on the coastal zone. The interplay between these processes creates dynamic morphological features. This section discusses some of the larger and relevant morphological features such as shoreface bars and sand waves.

2.3.1 Shore parallel bars
In the Netherlands, an often-observed coastal feature are subtidal shore parallel bars, which generally migrate in offshore direction. These bars have a multiannual lifetime and a strong alongshore uniformity (Walstra, 2016). As surf zone bars regulate the locations and rates of wave energy dissipation, their presence may dictate the morphological response of coastal systems (Bosboom & Stive, 2015).

For a breaker bar to move landward, the bar needs to erode on the seaward side and deposit on the shoreward side. In general, erosion occurs for positive transport gradients and accretion for negative transport gradients. To comply with the associated erosion and deposition pattern, the net transport needs to have a local maximum over the bar crest and unbroken waves must generate a net shoreward transport (Henriquez, 2019).

Offshore bar migration takes place during storms when large waves break on the bar and is due to the feedback between waves, undertow, suspended sediment transport, and the sandbar (Figure 6a); (Ruessink et al., 2007).

On the contrary, onshore bar migration is predominantly predicted for energetic non-breaking conditions where the skewed wave interacts with the sandbar and causes net shoreward bed-load transport (Figure 6b). The effects of infra-gravity waves and near-bed streaming are small to negligible for these conditions (Ruessink et al., 2007). For small waves, when breaking and non-breaking conditions are alternated with the tide, the sandbar can remain stationary.


(a) Offshore bar migration   (b) Onshore bar migration
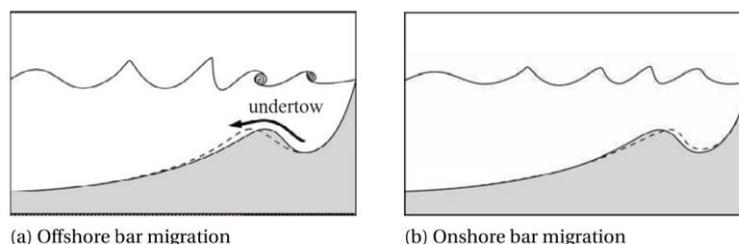
Figure 6: a) Offshore bar migration under breaking waves. b) Onshore bar migration under skewed waves (From: van den Ende, 2017)

To sum up, bars migrate offshore during storm conditions and onshore during calm conditions with a net migration from the intertidal zone to the outer shoreface in the Netherlands (Walstra, 2016).

Shore parallel bar cycles

Breaker bars migrate in net offshore direction, and thus passes through three phases forming a cyclic bar pattern (Ruessink & Kroon, 1994); (Figure 7):

1. A bar is generated at the inner nearshore zone.
2. The bar grows and migrates towards the outer nearshore zone.
3. The bar decays and disappears in the outer nearshore zone.

For steeper shoreface slopes, the offshore-directed sandbar gains faster depth, which reduces the wave breaking and the offshore migration rate. Therefore, steeper shoreface slopes lead to a longer cycle period between two successive bars (Walstra et al., 2011).

The position where the bar is decaying is called the zone of decay, which is based on the historical position where sandbars decay. Due to the decay of the outer bar, the net offshore migration of the next inner bar is stimulated which is perpetuating the cyclic system. However, it is not clear why the zone of decay exists and what processes are responsible for the position of this zone and more research can be conducted whether the position changes over time (Bruins, 2016; Walstra , 2016).
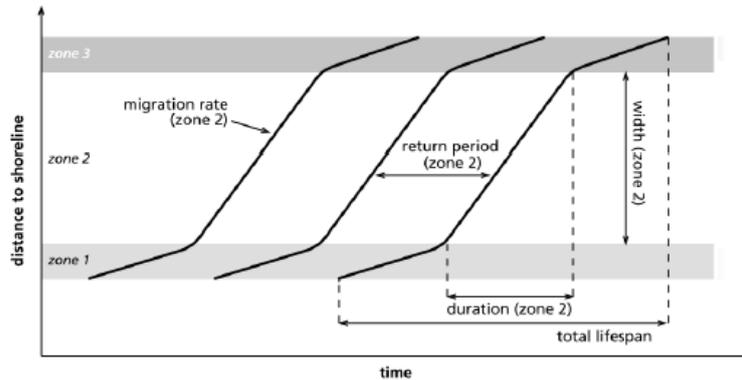
Figure 7: The cyclic pattern of multiple bars. In zone 1 the bar is initiated. When an older bar enters zone 3, the newly formed bar migrates from zone 1 to zone 2. It migrates offshore and grows larger until it reaches zone 3 where migration slows down and the bar decays. (From: Grunnet et al., 2003)

2.3.2 Transverse bars

Transverse bars, also known as finger bars, are subtidal nearshore morphological features. These bars have crests and troughs perpendicular to coastline with a typical length scale of 10-1000m. These bars are found at various coastlines, with micro- to macrotidal climates and open wave-dominated coasts to low wave energy estuaries. As these features migrate alongshore, their presence can cause remarkable yearly variations in cross-shore profiles.

There is no consensus on what exact processes form finger bars. A possible reason is through self-organization, where the bed-flow mechanism (Ribas & Kroon, 2007) or the interplay of strong tidal flows and refracted waves (Levoy et al., 2013).

2.3.3 Horizontal sand waves

Another, less distinct, coastal element are horizontal sand waves. These are alongshore shoreline fluctuations that move wave-like which are found along several stretches of the Dutch coast (Verhagen, 1989). For instance, at the North coast of Walcheren, sand waves have an amplitude of 50-150m, an alongshore celerity of 90m/yr and a period of 120yrs (Giardino et al., 2014).

2.4 Dutch policy on coastal zone management

Where the previous sections discussed the natural processes and coastal features, this section starts with a description of the Dutch coastal maintenance policy, introducing the anthropogenic modification and their effects on the coastline.

2.4.1 Strategy

Before 1990, the maintenance of the coast was aimed at solving acute erosion problems. However, coastal retreat caused an annual disappearance of 20ha of dunes (de Ruig, 1998). To halt the long-term coastal recession, the Dutch government decided to maintain the coastline at the 1990 position. The coastal functions are ensured in this manner, especially concerning the safety against flooding. This was obtained through 'dynamic preservation'. This policy aimed at supplying sand where possible and making use of hard structures where necessary. (de Ruig, 1998; van der Spek & Lodder, 2015)

2.4.2 Hard measures

Some locations require hard structures to ensure safety from flooding. For instance, the sea dike near West-Kapelle where a tidal gully runs close to the coastline. Other examples of

hard structures are the storm surge barriers in the SW Delta, the groynes at the Delfland coast, or the Eierlandse Dam at Texel.

2.4.3 Soft measures

The policy has the objective to apply soft measures, as it preserves the natural dynamics of the coastal zone. In this manner, sand is supplied where erosion threatens the coastline to retreat beyond the 1990 position, the reference coastline (BKL). To this end, the momentary coastline (MKL), defined in subsection 3.2.2, is used to decide if maintenance is required. The linear trend in MKL position is calculated for the past 10 years, except if a nourishment has been implemented in that period. In that case, the trend after the nourishment is calculated. By extrapolating the linear trend, a future coastline (TKL) position is calculated. If the TKL is expected to exceed the BKL, it can be decided to nourish the concerning transects with sand. (Rijkswaterstaat, 2020)

2.5 Nourishment strategies

This section provides an overview of the strategies applied at NW Walcheren to nourish the coastal zone, in the order of more traditional methods to recently applied methods.

2.5.1 Dune nourishment

Dune nourishments are implemented high in the coastal profile above NAP+3m. The dunes were frequently repaired in the past as a consequence of the erosion caused by severe storms.

2.5.2 Beach nourishment

Beach nourishments, implemented between the dune foot and the mean low water line, have the large advantage that they immediately replenish the shore at the correct position and so directly contribute to the MKL position. However, the lifetime of beach nourishments is relatively short: 2 to 4 years (Rijkswaterstaat and Deltares, 2019; de Sonneville & van der Spek, 2012), and therefore regular maintenance operations at erosional hotspots is necessary.

General design rules

The sand is generally supplied to the beach zone, between NAP-1m to NAP+3m. As a result, the MKL is immediately moved seaward and therefore beach nourishments are an effective solution at locations where the BKL is expected to be exceeded. It is advised that beach nourishments consist at least of 100 m^3/m (Rijkswaterstaat, 2007) and are typically in the order of 250 m^3/m (Rijkswaterstaat, 2020).
Another design aspect involves the sediment characteristics. It is advised that the grainsize of the nourished material is equal to the size of native sediment, however it is common practice that a slightly larger grain size is used (Shek, 2021). Altering the grainsize might have consequences for the beach slope, sediment transport, and the ecology. Furthermore, the nourishment slope is frequently constructed at a natural angle of 1:30 (Rijkswaterstaat, 2020), as an out of equilibrium slope is flattened out by nature (Shek, 2021).

Longevity of beach nourishments

The longevity, i.e. lifetime, is defined as the period in which the nourished volume erodes between the upper and lower bound of the beach. The dune foot and MLWL are regularly used as upper and lower limits. In the Netherlands, the lifetime of a beach nourishment is approximately 4 years (Rijkswaterstaat, 2020). The longevity might be prolonged by the combined execution of beach and shoreface nourishment (Shek, 2021).

2.5.3   Shoreface nourishment

A shoreface nourishment is implemented underwater. This type of nourishment has been implemented on a larger scale in the Netherlands since 1993. The nourishment is applied as a shore-parallel bar, at either offshore, on the crest, or in the trough of the natural bar. A nourishment that is constructed on the crest or at the seaward side of the outer bar is more efficient in protecting the beach than for nourishments in the trough (Larsen et al., 2021).

The main advantage of nourishing the shoreface is that the implementation costs are two to five times lower than a beach nourishment (Huisman, 2019). Moreover, offshore losses are limited and so almost the entire nourished volume contributes to the sediment balance (Huisman, 2019). Also, the shoreface nourishment feeds the coast especially during storms, and therefore acting as a sub-tidal buffer to mitigate storm erosion (Huisman, 2019). Furthermore, the nourishments can be applied in a wider range of weather conditions than beach nourishments and little hindrance is caused for beach recreation (Hamm et al., 2002). However, a disadvantage is the time lag between placement of the nourishment and the effect on the transgression of the coastline (Spanhoff & van de Graaff, 2007).

General design rules

General guidelines for the design of shoreface nourishments exist which state that the nourished volume per meter should be in the order of the volume of the main breaker bar (Rijkswaterstaat, 2007), which typically is 500 m^3/m. The crest is generally constructed at NAP-5m, but not shallower than NAP-3.5m (Rijkswaterstaat, 2020). The nourishment is the most effective if applied in the active zone above the depth of closure (Walstra et al., 2011; Bruins, 2016).

Lifetime of shoreface nourishments

The period of interruption of autonomous bar behaviour can be used as a measure to indicate the lifetime of shoreface nourishments (de Sonneville & van der Spek, 2012).

The lifetime of shoreface nourishments varies considerably, as the shoreface nourishments applied at Egmond aan Zee in 1999 eroded within two years (van Duin et al., 2004), at Terschelling in 1993 halted the offshore migration of sand bars for 6 to 7 years (Grunnet & Ruessink, 2005), and at Noordwijk in 1998 was detectable by wave breaking 8 years after construction (Ruessink et al., 2012). A more general statement is that the halftime of shoreface nourishments spans 3 to 30 years based on linear extrapolation of the erosion rates of 19 monitored nourishments (Huisman, 2019). Lyu (2019) argues that the larger the length of the nourishment, the lower the erosion rate per meter.

2.5.4   Combined shoreface and beach nourishment

An approach of combining beach and shoreface nourishments has been implemented since 1999 (de Sonneville & van der Spek, 2012). However, it remains unclear if these nourishments affect each other positively. In a study on 22 beach nourishments at the Holland coast, Shek (2021) demonstrates that beach nourishment longevity has increased since the implementation of shoreface nourishments, but at the same time the total supplied volumes have increased which may prolong the lifespan of nourishments.

2.6   Processes induced by beach nourishments

Regarding beach nourishments, the seaward protrusion and the out of equilibrium beach profile induce increased erosion rates. The responsible processes can be categorized in cross-shore and alongshore effects, which are considered in this section respectively.

2.6.1 Cross-shore effects

Three main cross-shore processes affect beach nourishments:

- The seaward protrusion results in a higher wave attack (Verhagen, 1992).

- Finer particles are washed out (Verhagen, 1992).

- Due to an out of equilibrium profile, a redistribution of sand in seaward direction takes place (Bosboom & Stive, 2015).

2.6.2 Alongshore effect

An alongshore redistribution of the sand takes place due to the seaward protrusion of the beach (Bosboom & Stive, 2015). This is induced by gradients in sediment transport because of the coastline orientation at the tips of the nourishment, as previously shown in Figure 4.

It was found that wave energy convergence has little effect on the alongshore redistribution of sediment (Benedet, Finkl, & Hartog, 2007). The grain size distribution can impact the evolution of a beach nourishment (Ludka, Gallien, Crosby, & Guza, 2016).

2.7 Processes induced by shoreface nourishments

This section looks closer at how the application of shoreface nourishments influences the coastal system. The first subsection discusses the general morphological behaviour of shoreface nourishments. Then, the second subsection explains the effect of a shoreface nourishment on the natural bar cycle. Finally, the third subsection considers two conceptual theories on how sediment is redistributed at shoreface nourishments.

2.7.1 Behaviour Shoreface nourishments

Shoreface nourishments behave differently per location, where they either show onshore migration, onshore and alongshore migration, or negligible migration where the nourishment remains at its execution position (Bruins, 2016; Lodder & Sørensen, 2015). Notably, independent of the dominant cross-shore or longshore migration of the original system, sediment volumes onshore of the shoreface nourishment increase due to the execution of the shoreface nourishment (Bruins, 2016).

After construction, a quick transformation into a normal bar takes place. The nourishment is reshaped to a bar with a comparable volume to bars found in the natural system and the steep seaward slope is flattened (Spanhoff & van de Graaff, 2007; de Sonneville & van der Spek, 2012). Also, the bar develops a landward skewed shaped, being caused by the larger onshore directed transport at the nourishment crest than at the bottom (Bruins, 2016). It is expected that the pronounced triangular crest ceases to exist once the seaward sediment source depletes, that is when the seaward slope gets milder (Huisman, 2019).

Cross-shore migration

At locations with original cross-shore bar behaviour, shoreface nourishments migrate towards the zone of decay. If they are placed seaward of the zone of decay, the nourishment migrates in landward direction. While if it is placed landward of the zone of decay, the nourishment migrates seaward. However, if the zone of decay in the original bar system is absent, the shoreface nourishment migrates onshore and alongshore (Bruins, 2016).

Wave skewness and asymmetry account for most of the onshore sediment transport. This was confirmed by a model simulation with disabled wave skewness and asymmetry, which

provided 50% of the erosion at the nourishment and no nearshore accretion (Huisman, 2019).

Significant bar migration is not necessarily linked to individual energetic wave events. However, from a broader perspective, relative offshore bar migration was found with energetic wave conditions while onshore migration was found for both energetic and non-energetic wave conditions (Onnink, 2020).

Longshore migration

A combination of onshore and alongshore directed migration occurs mainly southward of the outer deltas of the Wadden Sea inlets. This was mostly observed at locations where originally no dominant cross-shore migration was present. Notably, these bars migrate alongshore without the development of a deep trough, nor a zone of decay can be determined (Bruins, 2016)

2.7.2 Influence of shoreface nourishments on the natural bar cycle

The coastal profile responds quickly to a shoreface nourishment applied around NAP-5m. If a nourishment of the same magnitude as the existing breaker bars is applied at or outside the location of the outer bank, the natural offshore bar cycle is halted or reversed as breaker bars and troughs will move onshore. This results in an increase in volume in the breaker, beach and dune zones. (Rijkswaterstaat, 2007; Bruins, 2016; de Sonneville & van der Spek, 2012).

A similar development has been observed where no bars are present in the original coastal profile. The nourishment reshapes as a breaker bar but no trough is formed (Bruins, 2016). As the coastal profile reshapes, a net increase in sediment volume landward of the nourishment is found. The first shoreface nourishment at Callantsoog, a profile without an existing bar pattern, functioned as a bar and migrates landward over time. The introduction of a second nourishment, within 2 years, showed that the first bar behaved as natural bars would. (Rijkswaterstaat, 2007)

In the case of an onshore migrating shoreface nourishment, which connects to the outer bar, a shoreward propagating accretionary wave (SPAW) can be observed due to the remaining shoaling waves. Next the SPAW can connect to the inner sandbar, which initiates on its turn a second SPAW which attaches to the shoreline (Radermacher et al., 2018; Onnink, 2020).

2.7.3 Mechanisms for sediment redistribution at shoreface nourishments

This subsection presents two conceptual mechanisms for the redistribution of nourished sediment.

Salient effect

The presence of a shoreface nourishment might directly contribute to offshore dissipation of incoming storm wave energy, acting as a submerged breakwater, creating a sheltered area at the leeside of the nourishment (Figure 8:left panel). This causes a difference in alongshore sediment transport nearshore, being called the salient effect. The littoral drift is reduced locally and sediments are trapped in the leeside of the nourishment (van Duin et al., 2004).

The effect of the nourishment on the wave induced depth averaged return flow is negligible for accretive wave conditions landward of the shoreface bar, derived from physical model tests. Nonetheless, for erosive wave conditions in the physical model test, the depth-averaged velocities in the nearshore have reduced considerably for a shoreface nourishment. As a result, the reduced wave induced return flow transports less suspended sediment offshore (Walstra et al., 2011).

Onnink (2020) observed downdrift erosion after the placement of a shallow bar, suggesting a presence of the salient mechanism on the morphology. On the contrary, Huisman (2019) did not observe clear adjacent coastline changes for 19 nourishment sites.
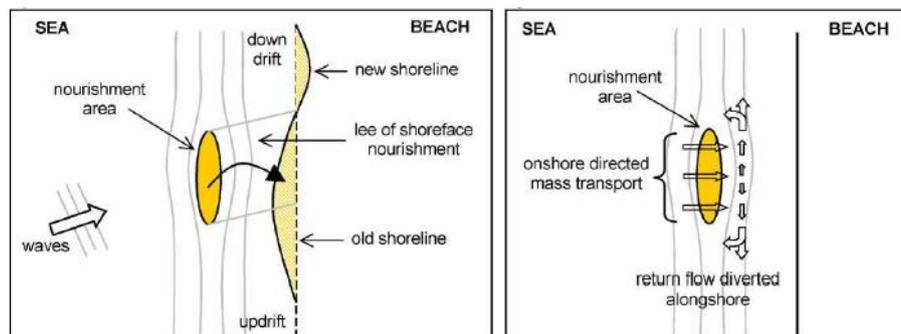

Figure 8: Left panel: Salient effect affecting the alongshore transport rate. Right panel: Feeder-bar affected by both cross- and alongshore processes. (From: van Duin et al., 2004)

Active feeder bar

The purpose of an active feeder bar is that the dispersed volume feeds the landward coastline to increase the beach width. (van Duin et al., 2004; Radermacher, et al., 2018).

The right panel in Figure 8 portrays the concept of an active feeder bar. The sand is transported onshore over the bar by shoaling non-breaking waves. Also, a residual circulation is formed due to the mass transport by waves over the nourishment. The water level gradient forces strong lateral and seaward directed currents at the landward side of the nourishment which forms a trough.

Nourished sediment that reaches the trough is either expelled at the sides by water-level gradient driven currents during shore normal to mildly oblique wave conditions or brought to the nearshore zone as a result of enhanced onshore transport (Huisman, 2019).

The sediment that is expelled by rip currents is spread over a large zone and therefore the effect of the shoreface nourishments on the adjacent coastlines is hard to distinguish. The expelled sediment is expected by be transported back to the surf zone by onshore sediment transport over time (Huisman, 2019).

The efficiency of shoreface nourishments implemented at depths of 5-6m, defined by percentage of the nourished volume that reaches the coast within five years, is estimated to be between 20-30% in the nearshore zone (between NAP-1m and NAP-5m). The efficiency with respect to the beach is low, in the order of 2-5% after 3-5 years. (van Rijn, 2011)

Erosion due to oblique stormy conditions contributes to roughly 15- 40% of the total erosion of shoreface nourishments, where the sand is lost in alongshore seaward direction, based on numerical model results (Huisman, 2019).

2.8   Study area

This section elaborates upon the NW coast of Walcheren, the area studied in this thesis. First, a summary of the historic evolution of the SW Delta is given. Next, the study site is described with its morphological features. Then, the influence of the semi-closure of the Eastern Scheldt is considered. Finally, an overview is given of the nourishments near Domburg and how these have affected the coastline.

2.8.1 Historic evolution of the NW Walcheren coastline

Around 100AD, the Delta area was covered by an extensive coastal peat layer and dissected by distributaries of the Rhine, Meuse and Scheldt (Figure 9a). Man-made and natural causes increased the drainage of the peat layer. Consequently, this led to significant subsidence and a transgression of the sea. Around 800AD, estuaries with branching channels were present in the landscape (Figure 9b). In the period hereafter, sedimentation accreted the intertidal areas to supratidal levels and smaller channels silted up. These areas were embanked which resulted in the formation of islands (Figure 9c). Larger tidal channels became more distinct due to the formation of islands and extensive ebb-tidal deltas developed, despite the limited riverine sand supply. The scouring of the subsurface by growing tidal channels likely provided the sediment. (Elias, van der Spek, & Lazar, 2016)
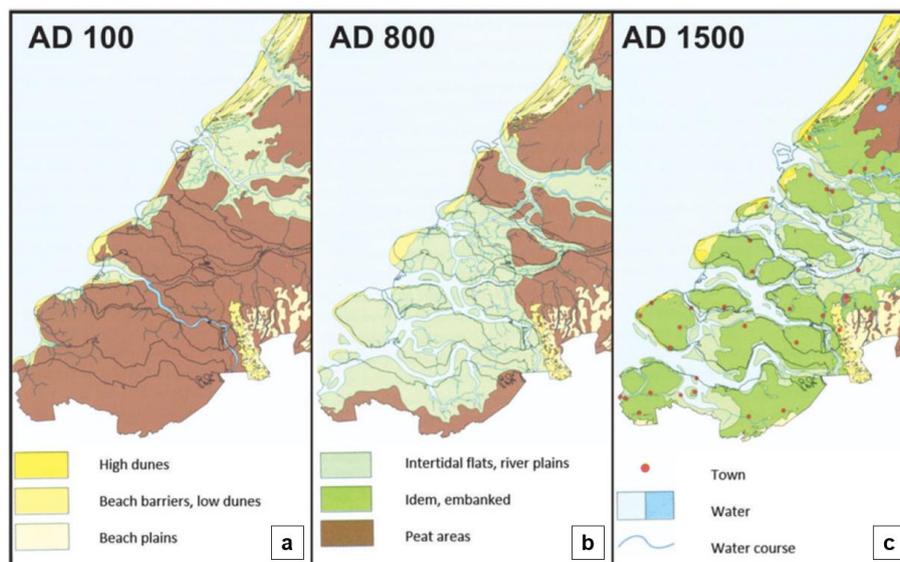
Figure 9: Palaeographic reconstructions for the SW delta of the Netherlands. (From: Voset al., 2011)

Numerous storm surge disasters, frequent embankment failures due to the composition of the subsurface and relocation of dikes due to tidal channels cutting into island's shorelines illustrate the lasting battle between mankind and the sea. (Elias, van der Spek, & Lazar, 2016)

During the late Middle Ages, the weakening of the sandy coast due to erosion and subsidence of the land behind the barrier coast caused major flood disasters. Large parts of the province of Zeeland were inundated and lost to the sea. (Bosboom & Stive, 2015)

The Dutch coast is a sediment importing system. During the Holocene, an estimated 200 to 250 billion m^3 sediment was deposited in the Dutch coastal zone which originates for roughly 10% from the Holocene Rhine and 90% was eroded from the Pleistocene area of the present North Sea. (Bosboom & Stive, 2015)

Western Scheldt ebb-tidal delta

Since 1955, large volumes of sediments have been dredged and dumped and 114 million m^3 of sand was extracted from the Western Scheldt. As the channels increased in depth and sills were removed, the hydraulic efficiency increased, and the tidal prism of the Western Scheldt was raised with 5-7%. Meanwhile, the central part of the ebb-tidal delta, the Vlakte van de Raan, is eroding with the delta front slowly migrating landward. Although the Western Scheldt ebb-tidal delta is subject to significant anthropogenic changes, the system is robust and resilient if the relative importance of the tides and waves is not adjusted significantly (Elias, van der Spek, & Lazar, 2016).

Eastern Scheldt ebb-tidal delta

Before the storm surge barrier was constructed, the ebb-tidal delta grew as the tidal prism increased following the completion of the Volkerak dam and the Grevelingen dam. Succeeding the construction of the Eastern Scheldt storm surge barrier, which partly blocks the cross-sectional area of the tidal channel, the tidal prism reduced with circa 28% (Rijkswaterstaat and Deltares, 2019). Another consequence of the barrier is the complete blockage of sediment import and export (Geurts van Kessel, 2004). The decrease in tidal currents and lack of sediments from the estuary give way to waves to erode the front of the ebb-tidal delta. The sediments were mainly transported to the North, following the direction of the dominant flood tidal currents. (Elias, van der Spek, & Lazar, 2016)

The volume in the outer delta follows the following relationship, where a decrease in tidal prism prescribes a decrease in outer delta volume and vice versa. (Bosboom & Stive, 2015)

$$V_{od} = C_{od} \cdot P^{1.23}$$

Therefore, the reduction of tidal volumes reduces the sand supply by the ebb current and so, the relative importance of wave-driven transport increases. This results in in net landward sediment transport, erosion of the delta front and building of sand bars on the outer rim of the ebb tidal delta. Moreover, shore-parallel flow is promoted as the shore-normal tidal flow is reduced. (Elias, van der Spek, & Lazar, 2016)

A loss of 72 million m³ is observed in the ebb-tidal delta of the Eastern Scheldt since the completion of the storm surge barrier. (Elias, van der Spek, & Lazar, 2016)

2.8.2 Site description

The Northwest coast of Walcheren is located between the ebb-tidal deltas of the Western- and Eastern-Scheldt estuaries (Figure 10). Therefore, the coast is characterised by tidal morphological features such as deep tidal channels and shallow sand bars. The Oostgat, near West-Kapelle, and the Oude Roompot, near Oost-Kapelle, are two tidal channels which embrace coastline of Walcheren. In between, the Domburger Rassen arise, a shallow area with depths ranging from NAP-12m to NAP-5m. The coastline at the Northwest coast of Walcheren is characterised by sandy beaches and dunes between West-Kapelle and Oost-Kapelle and the sea-dike at West-Kapelle. The seaward protrusion at Domburg generates a gradient in the alongshore current, resulting in a continuous eroding coast.

Figure 10: Overview of NW Walcheren. The villages of West-Kapelle, Domburg and Oost-Kapelle are indicated, as well as some distinct bathymetric features such as the tidal gully of the Oostgat and the Domburger Rassen. The locations of several transects are depicted [red] with the number increasing from the Eastern Scheldt storm surge barrier towards West-Kapelle. The transect number indicates the alongshore distance [dam].

Figure 11 shows the coastal profile near Domburg, before the placement of large nourishments. Moving from the top to bottom in the profile, the following features are found. The dune face retreats and likewise the dune foot moves approximately 15m landward in 18 years. The variability in the intertidal area indicates the formation of ridges and runnels. In the same area, shore-perpendicular permeable groynes are found, existing of a double row of wooden poles every 200m (Figure 12). These groynes slightly reduce the littoral drift in the inner surf zone (Bosboom & Stive, 2015). The wet beach is connected to the upper shoreface with a relatively steep slope. Historically, no distinct breaker bars are found on the upper shoreface near Domburg. On the contrary, transverse bars are present near Domburg. Their passage causes significant variability in coastal profiles. Figure 11 shows that below NAP-5m the bed rises and drops again in the order of 1m. Both the lack of breaker bars and the occurrence of transverse bars can be contributed to the dominance of the tide on the Domburger Rassen. Another noticeable, but difficult to observe, feature are the sand waves at the NW coast which propagate from West-Kapelle in NE direction along the coast to Oost-Kapelle. However, the sand wave amplitude is negligible for transects 2000-1300 (Giardino, den Heijer, & Santinelli, 2014).
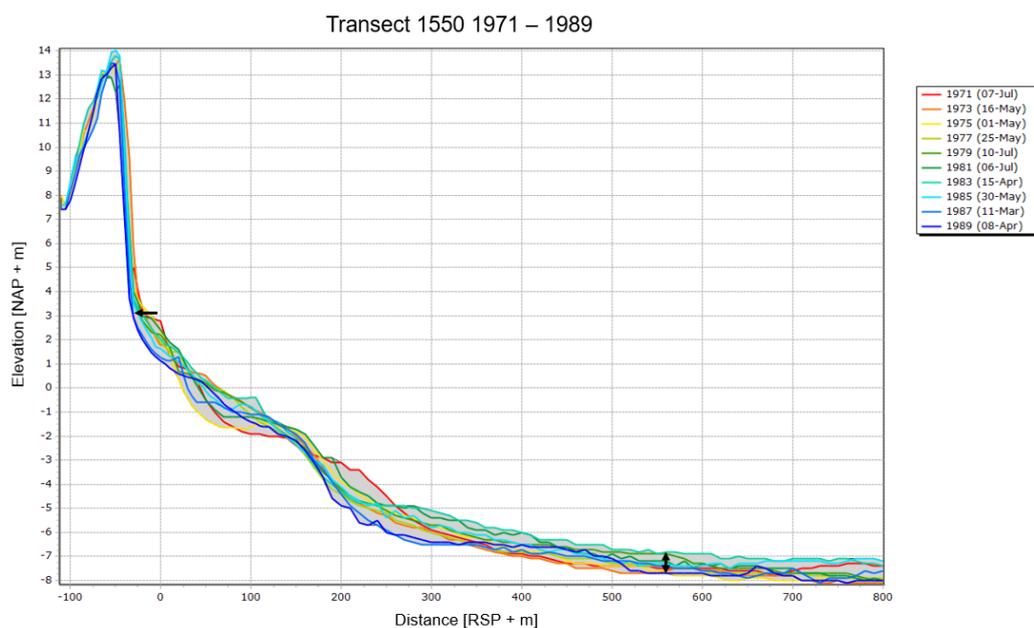
Figure 11: The cross-shore profiles at transect 1550 in the period 1971-1989, before large sand nourishments were applied. The arrows indicate the retreating dune face and the passage of transverse bars.

Figure 12: The coast of Walcheren with its typical shore-perpendicular permeable wooden groynes. Taken at Domburg, November 2020. From: Gerard van Maanen

2.8.3 Influence of the Eastern Scheldt

After the partial closure of the Eastern Scheldt in 1986, and consequently completing the Delta works, multiple responses have been observed.

For instance, due to the decreased tidal currents and a lack of sediment supply from the estuary, waves started to erode the front of the outer delta, with an estimated sediment loss of 72 million m^3 from the outer delta since the completion of the storm-surge barrier. The eroded sediment was mainly transported to the North in the direction of dominant flood tidal currents. (Elias, van der Spek, & Lazar, 2016; Rijkswaterstaat and Deltares, 2019)

Also, a reduction of the shore-normal currents resulted in a dominance of shore-parallel currents promoting scour in the North-South running channels. (Elias, van der Spek, & Lazar, 2016)

Although the tidal prism decreased by 28% as a consequence of the partial closure, the tidal flows have been found to be sufficient to maintain the main channels on the ebb-tidal delta. (Elias, van der Spek, & Lazar, 2016; Rijkswaterstaat and Deltares, 2019)

Nonetheless, the main changes in nearshore erosive and sedimentary coastal indicator trends for Walcheren are predominantly a result of the nourishment scheme and not due to the Delta works (Giardino, den Heijer, & Santinelli, 2014).

2.8.4 Nourishments near Domburg

To counteract the erosion at Domburg, numerous beach nourishments were placed, spanning on average a period of 4 years. Table 2 provides an overview of the sand nourishments at Domburg, where approximately 5.5 million m^3 was supplied over the period 1990-2020. At a relatively short distance upstream of Domburg, the coastline at the Westkappelse Zeedijk is regularly maintained. Recent nourishments at this coastal stretch are enclosed in Table 3.

Table 2: Nourishments conducted at Domburg.

Start construction	End construction	Type	Start Transect	End Transect	Length [m]	Volume [m^3]	Volume [m^3/m]
Apr-89	May-89	Dune	1481	1583	1020	9.272	9
Apr-89	May-89	Beach	1481	1583	1020	201.258	197
Jan-90	Dec-90	Beach-Dune	1481	1583	1020	245.517	241
Jan-92	Dec-92	Beach	1280	1742	4620	637.000	138
Jan-93	Apr-93	Beach	1430	1585	1550	318.000	205
Jan-94	Dec-94	Beach	1433	1605	1720	453.000	263
Jan-00	Apr-00	Beach	1406	1883	4770	886.127	186
Apr-04	Nov-04	Beach	1465	1885	4200	777.565	185
May-08	Jul-08	Beach	1406	1633	2265	369.565	163
Feb-12	May-12	Beach	1489	1632	1430	250.399	175
Nov-14	Dec-14	Beach	1469	1612	1430	304.000	212
Jun-17	Dec-17	Shoreface	1448	1632	1840	665.000	361
Apr-19	May-19	Beach	1448	1632	1840	416.000	226

Table 3: Recent nourishments conducted at the Westkappelse Zeedijk.

Start construction	End construction	Type	Start Transect	End Transect	Length [m]	Volume [m^3]	Volume [m^3/m]
Jan-15	Feb-15	Beach	1755	1948	1930	600.000	310
Jun-17	Dec-17	Shoreface	1735	2215	4800	2.400.000	500
May-19	Jun-19	Beach	1735	1948	2130	600.000	281

Beach nourishment 2008

An analysis of the 2008 beach nourishment at Domburg concluded that the longevity of the nourishment was approximately 4 years with a halftime of 1 year. After 4 years, 35% of the nourished sediment is still present on the shoreface or the beach. (Interreg, 2019)

Shoreface nourishment 2017

After numerous beach nourishments, a shoreface bar was implemented in 2017 for the first time at Domburg. The shoreface nourishment was constructed between transects 1632-1448 with an initial volume of 361m^3/m over 2km bringing it to a total nourished volume of 665.000m^3. The nourishment is placed at a depth of NAP-7m with a slope 1:10 up until a

depth of NAP-4m. Notably, the shoreface nourishment is not implemented parallel to the coast, but slightly tilted (Figure 13). Moreover, considering the limited water depth at the Domburger Rassen, the shoreface bar is interrupted around transect 1550 because the dredging vessel could not navigate over the local transverse bar. Therefore, the nourishment is effectively split into two separate nourishment bodies. The shoreface nourishment is not constructed on behalf of the erosion trends but is aimed at nourishing the coastal foundation, i.e. the lower shoreface, to extend the longevity of regular beach nourishments.
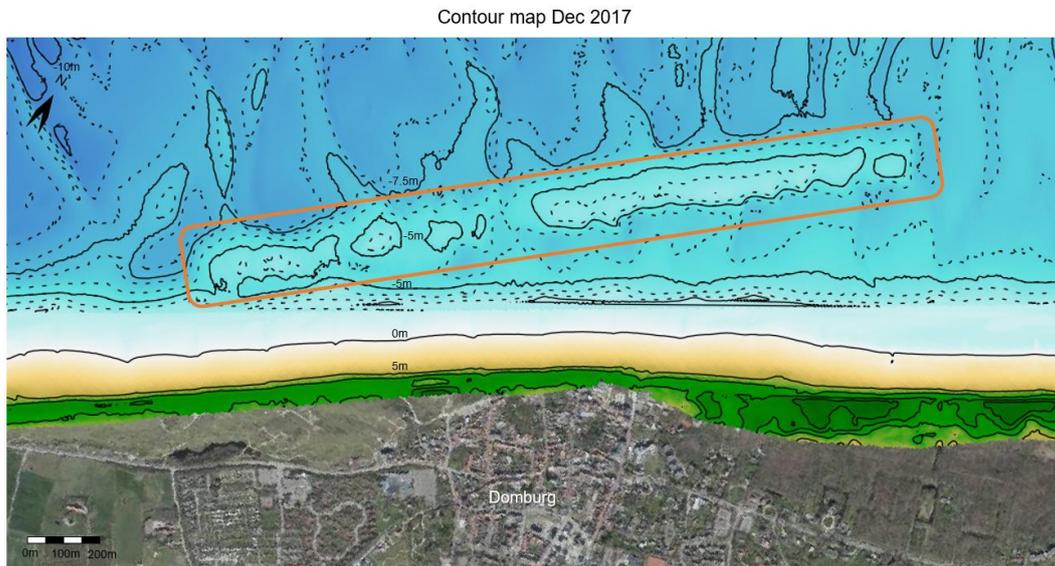
Figure 13: Contour map near Domburg, shortly after construction of the shoreface nourishment in Dec 2017 [Orange]. The subtidal contour intervals are 1m [dashed] and 2.5m [solid]. Besides the nourishment body, the transverse bars can be recognized seaward and landward of the nourishment.

Coastline evolution

Although the coast near Domburg has a tendency to erode, the coastline is maintained by nourishing the coastline (Figure 14). The large seaward migration of the coastline near West-Kapelle is explained by the large nourishments carried out to strengthen the Westkappelse Zeedijk (McCall, van Santen & Huisman, 2014). The coastline advance at the east of Domburg is a result of the numerous nourishments. Moreover, it is observed that the dunes are growing at various locations and the erosion of the beaches is limited due to the nourishments (Rijkswaterstaat and Deltares, 2019).

The coastline evolution is dominated by longshore sediment transport (McCall, van Santen & Huisman, 2014). The average daily conditions are the driving force that cause morphological changes. (Interreg, 2019)
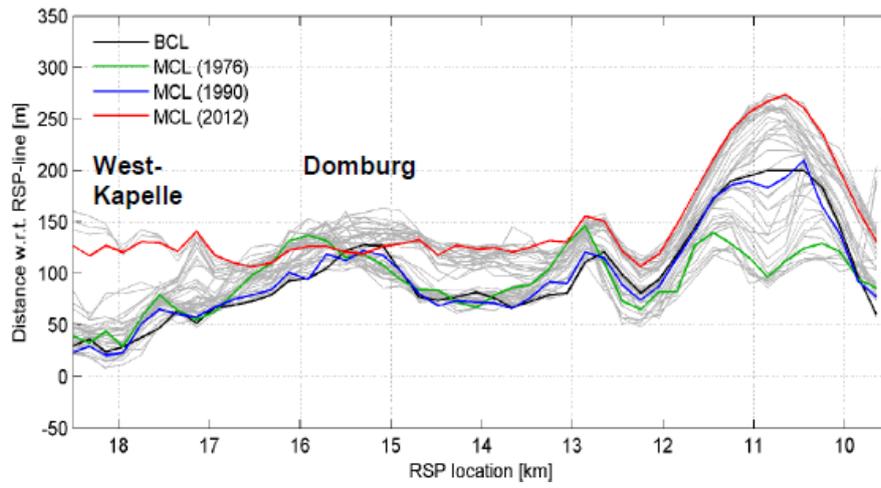
Figure 14: Overview of MKL-positions at the North-West coast of Walcheren for the period between 1970-2012. (From: McCall et al., 2014)

3. Methodology

This research is based on two pillars: data analysis and numerical modelling. The first section describes the data sources and the data handling. The second section explains the methods for the morphological analysis. The third section discusses the numerical model, which is set up within the XBeach package. The results from the data and model analysis are presented in chapter 4.

3.1 Data selection

Measurements form the basis for the conducted research. The morphological analysis is based solely on measurements, whereas the measurements form a starting point for the numerical model setup. The following two subsections elaborate on the used hydrodynamic data and morphological data.

3.1.1 Hydrodynamic data

The used hydrodynamic data can be divided in wave, water level and wind measurements. All data was acquired through Rijkswaterstaat water info. The locations of the measurement stations are shown in Figure 15.
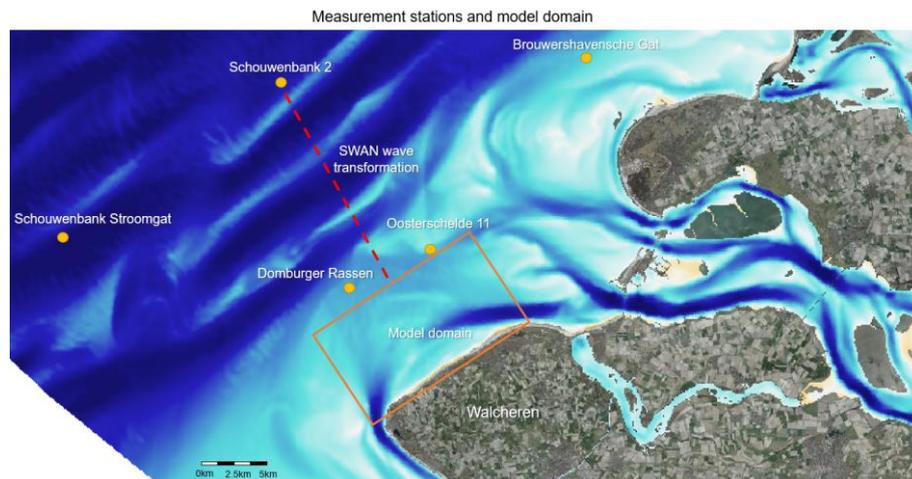
Figure 15: Overview of the measurement stations [yellow], XBeach model domain [orange] and the transect used for wave transformations in SWAN [red dashed].

Wave data

The Southwestern delta of the Netherlands is continuously measured by multiple wave buoys. Because of the varying bathymetry, wave conditions can vary strongly over short distances. The significant wave height (H_s) and the wave direction (Θ_w) were acquired from the Schouwenbank 2 and the Domburger Rassen wave buoys. The Schouwenbank 2 wave buoy is located relatively far offshore in 25m water depth and has an extensive timeseries of wave measurements.

The Schouwenbank 2 wave measurements are used to schematize the wave climate for NW Walcheren and to assign wave classes for the numerical model.

Although, the Domburger Rassen wave buoy is situated close to the coast of NW Walcheren, the length of the timeseries is limited. Therefore, this measurement station is used to validate the transformation of wave conditions through SWAN.

Water level data

The water level data is solely used in the numerical model. Subsection 3.3.4 elaborates upon obtaining water levels at the model boundaries from the zuno4-ASTRO model.

As the tide is the primarily responsible for offshore currents, the flow measurements from Schouwenbank Stroomgat are used to validate the currents in the numerical model.

Wind data

Wind data, the wind speed and direction, is available from the Brouwershavensche Gat station. This data is used for creating wind roses and as model input.

3.1.2 Bathymetric data

The utilised bathymetries originate from four sources: Vaklodingen, JARKUS surveys, Verdichte JARKUS surveys, and post-construction surveys. The study focusses on the 2014 beach, 2017 shoreface and 2019 beach nourishments and therefore the datasets in the period 2014-2021 are handled in this research.

The Vaklodingen are surveys of the entire coastal foundation, conducted until a water depth of NAP -20m. This survey is done every three years for the entire coast and the Western Scheldt estuary and every six years for the Waddenzee and the Eastern Scheldt estuary. It consists of single beam measurements with transects interspacing of 1000m along the coast and 200m in the Waddenzee, Western Scheldt estuary and tidal inlets. The transects are interpolated to produce a bathymetry map covering the entire coastal zone with a resolution of 20x20m. The JARKUS survey is an annual bathymetric measurement consisting of shore-perpendicular transects covering the dunes to approximately 1km offshore with intervals of 200-250m for the entire Dutch coast. These measurements have been done since the 1960's and therefore offers a long timeseries of morphological data. Figure 16 portrays the positions of the JARKUS transects near Domburg. Moreover, extra measurements are conducted with intervals of half a year and an interspace of approximately 100m, known as the 'Verdichte JARKUS' (Rijkswaterstaat, 2020). For Domburg, the Verdichte JARKUS (V. JARKUS) is not consistently measured as some data sets are missing or do only cover the dry or the wet profile. Finally, a valuable dataset are the post-construction surveys originating from the construction companies. These cover, depending on the nourished zone, either the dry or the wet part of the profile. Consequently, this data is combined with another recent dataset to allow for morphological analysis.

Table 4: Overview bathymetric datasets

Dataset	Date Beach	Date Shoreface	Remarks
JARKUS	3-2-2014	21-5-2014	
Nov 2014 Beach nourishment			
Post-construction	24-12-2014	21-5-2014*	*Bathymetric shoreface data is added from the previous JARKUS survey
JARKUS	11-3-2015	11-5-2015	
JARKUS	1-1-2016	21-4-2016	
JARKUS	19-1-2017	28-3-2017 / 15-6-2017	Transects 1571-1775 are measured in June
V. JARKUS	22-3-2017	15-6-2017	
Dec 2017 Shoreface nourishment			
Post-construction	29-3-2018*	23-12-2017	*Bathymetric beach data is added from the succeeding V. JARKUS survey. Multibeam 1x1m data.
V. JARKUS	29-3-2018	29-3-2018	
JARKUS	31-5-2018	29-3-2018	
V. JARKUS	1-4-2019**	1-4-2019**	**Measurement date is not certain
JARKUS	23-2-2019	4-4-2019	
Apr 2019 Beach nourishment			
Post-construction	24-4-2019	4-4-2019	
V. JARKUS	1-10-2019***	1-10-2019***	***Measurement date is not certain, only shoreface data available
JARKUS	7-2-2020	4-5-2020	
V. JARKUS	7-2-2020	20-5-2020	
V. JARKUS	1-10-2020**	1-10-2020**	Measurement date is not certain
JARKUS	29-3-2021	23-3-2021	

The datasets described in Table 4 and are used in the morphological analysis. In addition to these data sets, the Vaklodingen from February 2019 and the June 2019 North Sea bathymetric map are used for the numerical model set-up in the offshore domain.
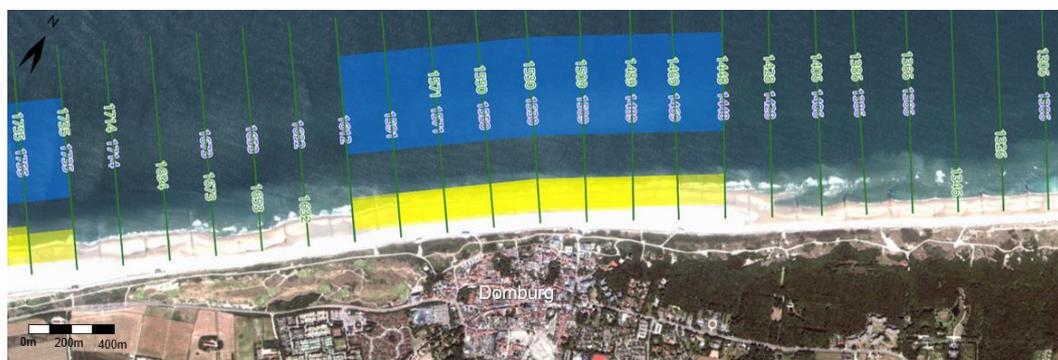
Figure 16: JARKUS transects at Domburg with the beach and shoreface nourishments indicated [yellow and blue].

3.2 Morphological analysis

This section describes the approach for the data analysis. The data, described in the previous section, was used to define the wave climate, calculate the positions of coastal indicators, and to calculate the sediment volumes.

3.2.1 Hydrodynamics

Wave and wind roses

The wave and wind roses are created with measurements from respectively the Schouwenbank 2 wave buoy and the Brouwershavensche Gat measurement station. The wave/wind direction and the wave height/wind velocity are used to produce these

hydrodynamic charts. A general wave and wind rose are made to define the wave climate. Also, wave and wind roses are made to characterize the wave climate in between nourishments.

Incoming wave energy

An estimation of the incoming wave energy flux is made by calculating the wave energy at Schouwenbank 2. First, as the wave period could not be retrieved from the wave buoy, an estimation of the significant wave period is made for wind waves (Schiereck & Verhagen, 2019):

$$T_s = 0.9 \cdot \left(3.6 \cdot \sqrt{H_s} \right)$$

The wavelength is calculated with the following formula (Schiereck & Verhagen, 2019):

$$L = \frac{g \cdot T_s{}^2}{2 \cdot \pi}$$

- T_s Significant wave period   [s]
- H_s Significant wave height   [m]
- L   Wavelength   [m]
- g   gravitational constant   [m/s^2]

Then, a discrimination is made for deep water ($h/L > 0.5$) and for intermediate water ($h/L < 0.5$). The group velocity of waves is calculated for both cases according to the dispersion relationship. Next, the wave energy flux is calculated with:

$$U = \frac{1}{16} \cdot \rho \cdot g \cdot H_s^2 \cdot c_g$$

- U   Wave energy flux   [MW/m/s]
- ρ   Density   [kg/m^3]
- c_g Group velocity   [m/s]

Next, a summation of the wave energy flux during nourishment intervals is made. In this way, the difference in incoming wave energy during certain periods can become evident.

3.2.2 Coastline indicators

The development of the coast can be followed through the analysis of coastal indicators. These can be divided in two categories. The first category contains indicators such as the dune foot (DF), mean high water level (MHWL) and mean low water level (MLWL), which are the cross-shore location of a prescribed vertical level. The second category contains indicators that are based on a volume between two vertical levels, from which a cross-shore location is calculated. Examples are the MKL and the centroid of a shoreface nourishment. Where the first category is susceptible to natural variations, the latter shows less variation as it is based on a volume. Because this analysis considers short term coastal development with few measurements in time, the focus is shifted towards the second category of coastline indicators.

Momentary Coast Line

The momentary coastline position is computed every year from surveyed cross-shore transects. The MKL is a function of the volume of sand between the dune foot level and the upper part of the shoreface (Figure 17).
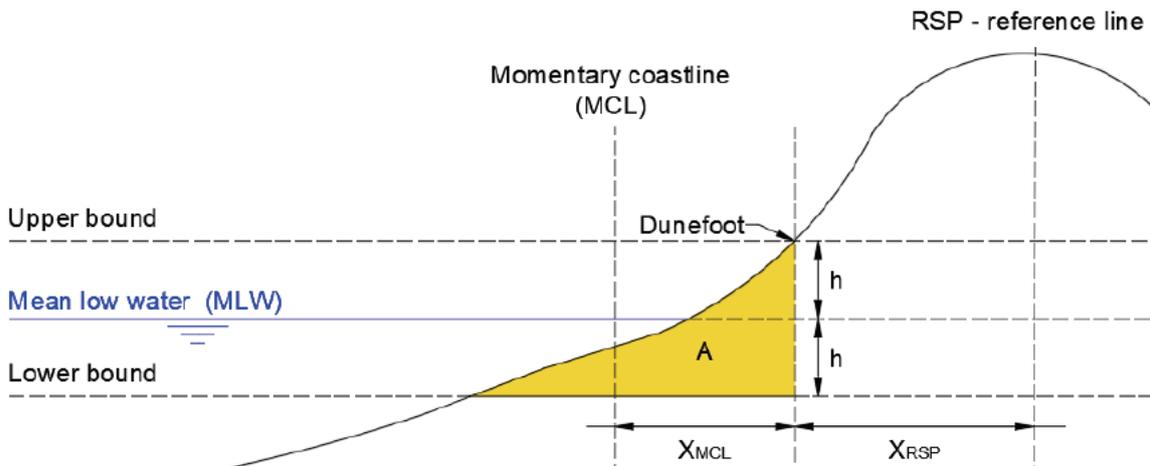
Figure 17: Calculation of the Momentary Coastline (MKL). From: Shek (2021).

$$MKL = X_{MKL} + X_{RSP} = \frac{A}{2 \cdot h} + X_{RSP}$$

- h   height difference between DF and MLW   [m]
- A   area MKL volume   [m²]
- X_{RSP} distance between DF and RSP   [m]
- X_{MKL} distance between MKL position and DF   [m]

The MKL provides a robust method to determine the coastline position. The MKL data was retrieved through MorphAn, which calculates the volumes and MKL position for each transect for JARKUS, Verdichte JARKUS and the post-construction surveys.

Centroid of a shoreface nourishment

To more closely follow the development of a shoreface nourishment, the position of the bar's centroid is calculated. The first step is to determine a base profile. For a coast with natural migrating bars, a mean profile of preceding years can be used (Bruins, 2016). Nonetheless, as there is no shore parallel bar pattern at Domburg, the most recent profile prior to the placement of the shoreface nourishment is used.
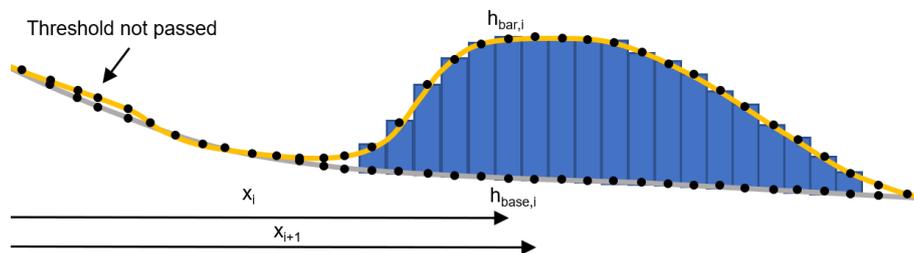
Figure 18: Visualisation of the midpoint Riemann sum to calculate a volume of a shoreface bar in a cross-shore profile. The volume is approximated by the volume of the slices between the base profile [grey] and the bar [yellow]. The XYZ data points [black] determine the slice's size. A threshold is applied to exclude small variations.

Next, the difference on the shoreface between the base profile and consecutive profiles is used to calculate the bar area and the static moments. To exclude small perturbations a threshold is chosen of 0.3m. The area is calculated by utilising a midpoint Riemann sum. In this procedure, the area is approximated with the area of rectangles under each profile point (Figure 18). The static moment is calculated in a similar manner, only that each rectangle is

multiplied with its cross-shore distance with respect to the RSP. The following formulas are used to determine the cross-shore position of the bar's centroid:

$$A = \sum \left(h_{bar,i} - h_{base,i}\right) \cdot (x_{i+1} - x_i)$$

$$S_x = \sum \left(h_{bar,i} - h_{base,i}\right) \cdot (x_{i+1} - x_i) \cdot x_i$$

$$Centroid_x = \frac{A}{S_x}$$

The result is the volume and the cross-shore position of the bar's centroid for each transect and in time. In this way, the cross-shore migration and the volume development can be followed in time.

3.2.3 Volume calculation

Similar as for the calculation of the centroid, a midpoint Riemann sum was employed to calculate the sediment volume in coastal zones. The upper, lower, landward, and seaward boundaries of the coastal zones are specified in Table 5, whereas an overview of the coastal zones is given in Figure 19.
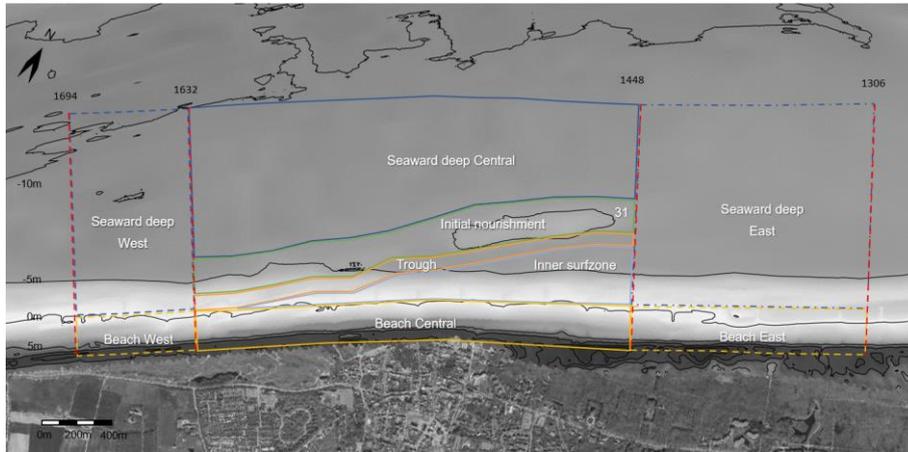
Figure 19: Top view of the coastal zones at Domburg.

The defined coastal zones can be separated in three alongshore sections: West (transects 1694-1632), Central (transects 1632-1448), and east (transects 1448-1306). Where the west and east sections exist of a beach zone and a deep zone, the central part is divided into more zones as the shoreface was nourished. Accordingly, an initial nourishment zone, trough zone, and inner surf zone are defined based on the position of the shoreface bar.

*Table 5: Boundaries for the volume development of coastal zones. *The limits for the central deep zone are adjusted due to the presence of the shoreface nourishment in transects 1632-1448.*

Zone	Upper boundary	Lower boundary	Landward boundary	Seaward boundary
Beach	NAP + 5m	NAP - 1.14m	RSP - 50	RSP + 150
Inner surf zone	NAP -1.14m	NAP - 10m	RSP + 150	RSP + 165-430
Trough	NAP - 3m	NAP - 10m	RSP + 140-430	RSP + 240-530
Initial nourishment	NAP - 3m	NAP - 10m	RSP + 240-530	RSP + 430-705
Seaward deep	NAP - 1.14m / NAP - 3m*	NAP - 10m	RSP + 150 / RSP + 430-705*	RSP + 1000
Total	NAP + 5m	NAP - 10m	RSP - 50	RSP + 1000

Estimated sediment fluxes

As explained in the previous section, the volumes of coastal zones for each cross-shore profile are calculated. Therefore, the volume development through time is tracked for each transect. From the volume development of coastal areas, the net sediment fluxes near Domburg can be estimated with a box model based on a system of linear equations. An example of a simple box model is given in Figure 20.

Figure 20: Example of a simple box model for a beach nourishment and the equations to find the unknown sediment fluxes [Red].

This model links the volume changes of multiple polygons to in- and out-going sediment fluxes. The box model makes use of the following assumptions and simplifications:

- The outgoing sediment flux (S_{out}) from the MKL layer is approximated as 100.000 m^3/year, based on sediment volume changes and nourishment volumes (McCall et al., 2014). This is a loss of sediment from the MKL layer and is assumed to be in in alongshore NE direction.
- Based on a single line model, the incoming alongshore sediment flux (S_{in}) is an estimated 30.000 m^3/year in the MKL layer (McCall et al., 2014).
- It is assumed that there is no alongshore sediment exchange between adjacent beaches. Beach volume changes can only be due to a cross-shore exchange with the subtidal polygon or a nourishment.
- The alongshore sediment flux ($S_{deep,west}$) is separated into four fluxes from west to central ($S_{deep,central}$, $S_{nourishment,central}$, $S_{trough,central}$, $S_{lee,central}$) and again joined from central to east ($S_{deep,east}$) because of the division in multiple subtidal coastal zones. The magnitude of the fluxes is determined by the cross-shore length of the coastal zones, and so it is assumed that the alongshore sediment transport in the subtidal zone is equally distributed in the cross-shore. This simplification is based on sediment transports computed with a numerical model (Section 3.3), which indicates a year averaged alongshore transport which is similarly distributed over the subtidal cross-shore (Figure 21).
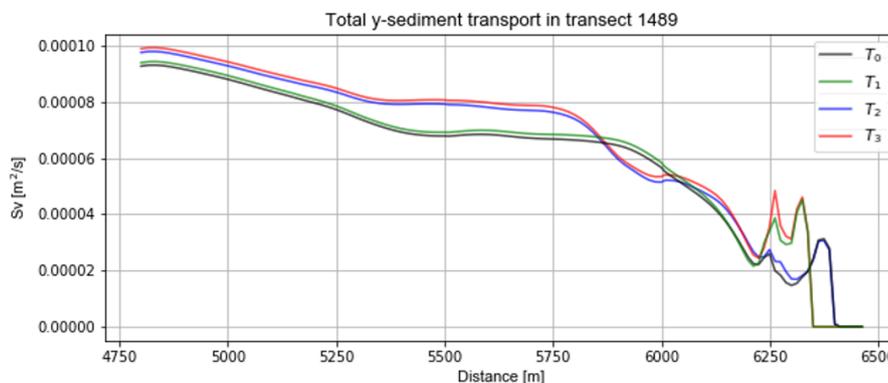
Figure 21: Computed alongshore annual sediment transport from a numerical model. The subtidal zones range between 5400m < x < 6250m, where the sediment transport remains almost constant and starts to decrease at 5800m. The legend portrays the different nourishment scenarios, described in section 3.3.3.

- Likewise, the exchange with the seaward boundary is based on a ratio according to the polygon alongshore length. For the west, central and east deep zones this was respectively 15%, 50%, 35%. According to the numerical model, the exchange is seaward directed and an order of magnitude smaller than the alongshore transport.
- Furthermore, the model is simplified by ignoring other sources and sinks, such as aeolian transport to the dunes and subsidence.
- In the case a nourishment was completed in the considered period, the volume measured by the contractor was added in the respective coastal zone.

Erosion rate and longevity of beach nourishments

The erosion rates of the 1994, 2000, 2004, 2008, 2012, 2014 and 2019 beach nourishments are approached through linear regression. The beach volume was calculated for each transect for each instance in time. As there are post-construction surveys available for the 2014 and 2019 beach nourishments, their starting volume is certain. Similarly, the 1994 and 2000 JARKUS measurements were conducted shortly after construction, and so these measurements provide a good starting point. This was not the case for the 2004, 2008, and 2012 beach nourishments. The JARKUS survey was measured before the nourishment, and no post-construction survey was available. To solve this, the following procedure was followed:

- It was checked if a JARKUS survey was performed maximum 3 months prior to the start of the nourishment.
- If that was the case, an extra data point per transect was created. The datapoint contains the most recent beach volume and the date is set in between the start and end of nourishment construction.
- The nourished volume/m was obtained from the nourishment database and added to the datapoint.

In this way, the beach nourishments have comparable data from which their erosion rates can be determined (Figure 22). Although an exponential fit would better suit the erosion rate of beach nourishments (Dean, 2003), due to the limited number of data points in time it was chosen to use a linear fit. According to Shek (2021), using a linear instead of an exponential fit leads to a small underestimation of the longevity.

The longevity is defined as the time that the nourished volume is still partially evident after the nourishment is completed. It is assumed that morphological changes during the construction period are negligible as the nourishments are regularly completed within two months. The longevity is determined based on an extrapolation of the linear fit. Likewise, the halftime of a nourishment is the period that half of the nourished volume is still evident after the completion of the nourishment.
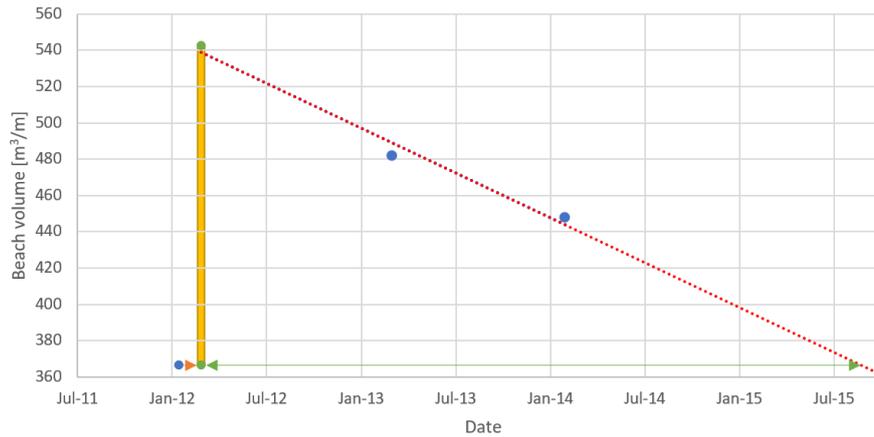
Figure 22: Example of linear fitting an erosion trend for the 2012 beach nourishment, where the volume was manually adjusted. The beach volume based on JARKUS measurements [Blue] was adjusted. The date was adjusted [Orange] and the nourished volume was added [Yellow] to create new data points [Green]. Then, a linear line [Red] was fitted through the datapoints from which the longevity [Green Arrow] was determined when the line intersects the pre-nourishment volume.

3.3 Numerical model setup

This section describes the numerical model setup. First the choice of model is explained. Second, the computational grid is presented. Third, an overview of the bathymetries for each nourishment strategy is given. Fourth, a description of the boundary conditions is provided, including the morphological tide, wave and wind conditions. Fifth, an overview of the output parameters from the model are given. Sixth, the SWAN output for the wave conditions and the model currents are validated.

3.3.1 XBeach

XBeach is a process-based numerical model, especially suited for the computation of nearshore hydrodynamics and morphodynamical response during storm-events. Wave breaking, surf and swash zone processes, dune erosion, overwashing and breaching are included in XBeach (Roelvink, et al., 2009) . The model handles temporal scales of hours to days well. The model is computationally expensive as it is long wave resolving and uses shortwave averaged values (Deltares, 2020). This model package is handled in surf beat (instationary) mode, where the short-wave variations on the wave group scale and their associated infra-gravity waves are resolved.

Hence, the first shortcoming of the model is the limitation to simulate periods longer than a couple of days. Therefore, a brute-force simulation, modelling the complete period with a measured timeseries of boundary conditions, is not feasible. To work around this shortcoming, eleven representative wave conditions and the morphological tide are used to simulate the sediment transport, which are then multiplied with their yearly occurrence. This procedure, previously applied in Fockert (2008) and Lesser (2009), drastically reduces the computational time compared to brute-force simulations.

Although process-based models are a valuable tool in understanding and predicting morpho-dynamics, the model-physics have a tendency to flatten out sub-tidal bars over time (van Duin et al., 2004; Grunnet & Ruessink, 2005). Artificial flattening of bar and trough features in the numerical model is prevented by applying a morpho-static approach. This approach uses a static bathymetry to prevent the morpho-dynamics from influencing the hydrodynamics.

31

This approach has been validated for multiple shoreface nourishments to represent realistic accretion in the inner surf zone (Huisman, 2019).

The scope of the analysis of the XBeach simulations is on gaining insight in the dominant sediment transport patterns around a shoreface nourishment at a coast without pre-existing bar pattern. Therefore, a calibration of the numerical model is not performed and either default settings, or the settings for the safety evaluations of the Dutch primary water defences were used (Appendix C.1).

3.3.2 Grid

XBeach requires a computational grid to transfer energy from the offshore boundary to the nearshore. The grid was created with RGFGRID. The grid size varies in x- and y-direction from 50*50m furthest offshore to 25*12.5m in the surf zone near Domburg (Figure 23). In this way computational times are minimized while a high grid resolution is obtained in the nearshore. Furthermore, a gradual refinement of the grid, in both cross- and alongshore direction, is applied to smoothly transfer energy between grid cells.
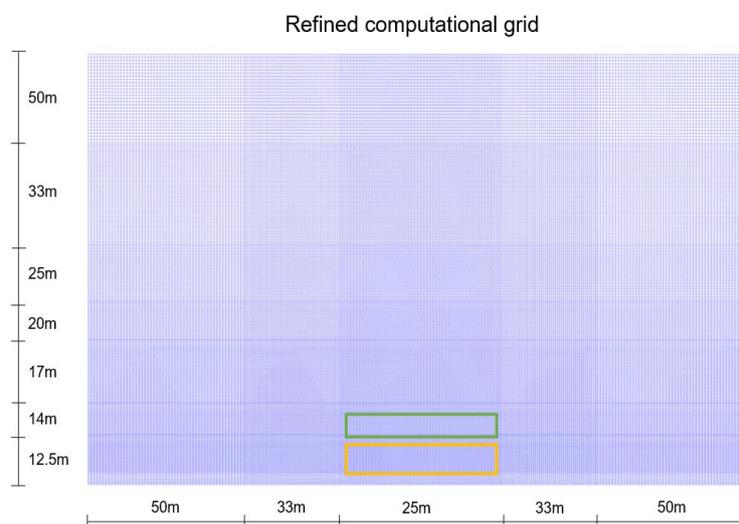
Figure 23: Overview of the computational grid used in XBeach. The grid was built with RGFGRID with a refinement towards the coastline near Domburg. The x – and y-axis represent the dx and dy grid sizes. The yellow and green enclosed zones show the areas where respectively beach and shoreface nourishments are applied.

3.3.3 Bathymetries

To investigate how nourishments affect the hydrodynamics and transport patterns at the Walcheren coastline, the only variable that is changed in the simulations is the bathymetry. As the shallow Domburger Rassen are subject to morphological changes, it is chosen to base all simulated bathymetries on one survey in which locally adjustments are made to include nourishments. In this way, solely the effect of nourishments is taken into account and larger morphological processes are excluded, such as the erosion of the Eastern Scheldt outer delta.

Bathymetry construction

The bathymetries are constructed with the use of multiple surveys which are explained in Table 6. The bathymetries were created by interpolating the xyz data to the model grid through the QUICKIN software. Subsequently, a smoothing operation is applied to prevent instabilities and unrealistic model output.

Table 6: Surveys on which the bathymetries are based.

Survey	Date	Description
North Sea bathymetry	Jun 2019	100x100m raster data. Used for offshore areas not covered by Vaklodingen.
Vaklodingen	Feb 2019	20x20m raster data covering the bathymetric features of the Western and Eastern Scheldt.
Nourishment monitoring	Mar/Jun 2017	5x5m raster data covering the area of interest between transects X. The dry profile was measured in March, the wet profile in June 2017. No nourishment was present in the bathymetry.
Post-construction bathymetry shoreface nourishment	Dec 2017	1x1m raster data covering the vicinity of the shoreface nourishment between transects 1428-1653.
Post-construction bathymetry beach nourishment	Apr 2019	5x5m raster data covering the vicinity of the beach nourishment between transects 1428-1653.

The bathymetries used for the model analysis are described in Table 7 and shown in Figure 24. The order of the simulations represents the history of the Domburg coastline.
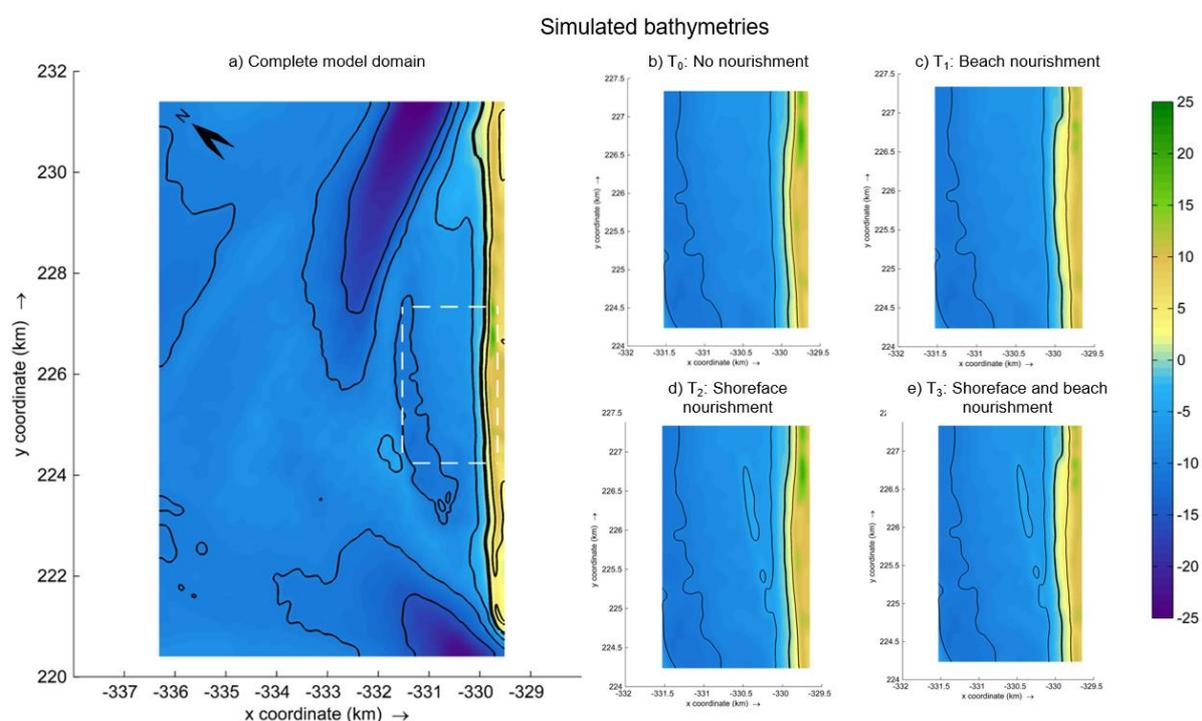
Figure 24: Overview of the simulated bathymetries with 5m contours and the thick solid line represents the 0m line. a) Complete bathymetry of the model domain. The white dashed line represents the area of interest near Domburg where nourishments are applied. b) T_0: No nourishment. c) T_1: Beach nourishment. d) T_2: Shoreface nourishment. e) T_3: Shoreface and beach nourishment.

Table 7: Simulated scenarios. In these scenarios, the bathymetry is the only variable.

Name	Nourishment	Description
T_0	None	An autonomous scenario without the influence of a nourishment.
T_1	Beach nourishment	The conventional strategy at Domburg, where the beach is nourished.
T_2	Shoreface nourishment	The scenario where only a shoreface nourishment is evident.
T_3	Beach and shoreface nourishment	The scenario where both a shoreface and beach nourishment are present.

Wooden groynes

A remarkable feature of the NW Walcheren coastline are the shore perpendicular wooden groynes (Figure 12), which are successful to decrease erosion rates near Domburg (Lazar, Elias, & Spek, 2017). It is believed that oblique incoming waves are partly dissipated, and the tidal current is contracted due to the pole rows and consequently affects the littoral drift. XBeach contains a vegetation module, which enables taking into account the effect of pole rows. However, the vegetation module introduced instabilities and lead to erroneous outcomes. To overcome this issue, it was decided that the vegetation module in XBeach would not be utilised. This introduces inaccuracies in the nearshore zone regarding alongshore sediment fluxes and hydrodynamics. However, it is believed that the influence of the shore perpendicular groynes is indirectly accounted for in the static bathymetry. Namely, the pole rows influence the shape of the nearshore, and so this influence is present in the surveyed bathymetries.

3.3.4 Boundary conditions

A morphostatic model is setup with three major hydrodynamic forcings: waves, wind and tide. This section elaborates on the boundary conditions applied in the numerical model. In this manner, wave input, wind input, morphological tide and the lateral model boundaries are discussed. The boundary input is based on timeseries from measurement stations close to the model domain (Figure 15).

Wave input

The morphology of the coast is largely shaped by average wave conditions, these must be included in the simulations to find realistic yearly sediment transports. However, a brute-force simulation of wave and wind conditions would be computationally too expensive.
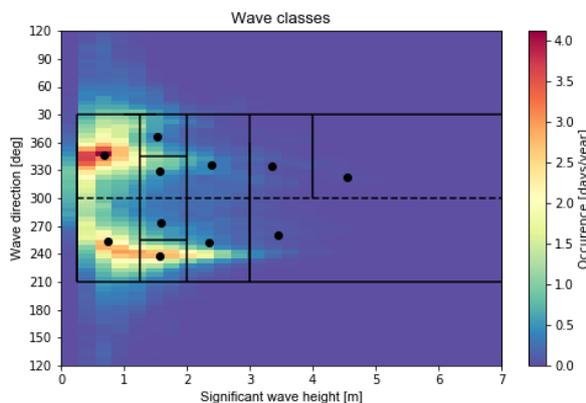
Figure 25: Wave climate at the Schouwenbank. The selected wave conditions, averaged per black square, are represented by black dots.
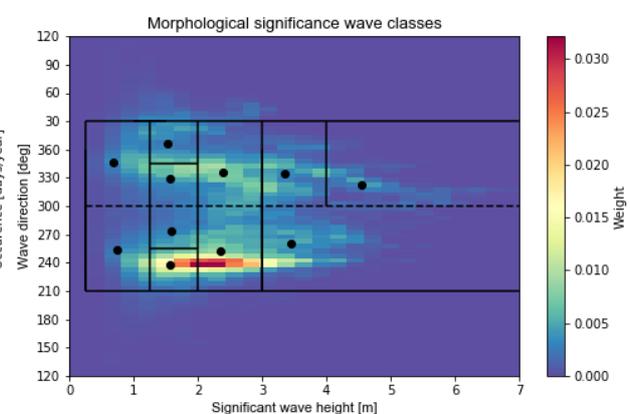
Figure 26: Morphological significance of wave conditions at the Schouwenbank.

Eleven wave classes are selected manually which represent the wave climate of the NE coast of Walcheren (Figure 25). In order to choose representative conditions, the morphological significance was taken into account (Figure 26). This is estimated by raising the wave height to the power 2.5, proportional to the wave driven sediment transport.

The selected wave conditions are based on significant wave height and wave direction measurements from the Schouwenbank 2 buoy, located in 25m water depth and amidst local shoals, in the period January 2016 – January 2021.

The wave climate is mainly characterised by two oblique directions from the NNW and the SW. The wave climate is schematized by assigning eleven wave classes, based on averaging the wave directions and wave heights per wave class. In this manner, each wave class is represented by a single significant wave height and direction.

Waves smaller than 0.25m are excluded as their morphological significance is negligible due to their low occurrence, shore normal wave angle and their low morphological significance. Also, waves with an incoming wave angle larger than 90° to the shore normal are not considered due to their low occurrence and low morphological significance. Moreover, these cannot be treated by the wave transformation models such as SWAN.
A similar wave selection procedure has previously been applied by Lesser (2009). An overview of selected offshore wave conditions at the Schouwenbank can be found in Appendix C.2.1.

Considering the offshore location of the Schouwenbank wave buoy, the selected wave conditions were transformed from the Schouwenbank to the model boundary with the use of the SWAN wave model. The computed nearshore wave conditions can be found in Table 8.

Table 8: Nearshore wave and wind boundary conditions after a SWAN computation, their probability of occurrence and their morphological weight.

	Wave class [°N]	H_s [m]	Θ_{wave} [°N]	T_p [s]	U_{wind} [m/s]	Θ_{wind} [°N]	P [%]	Weight [%]
	$0.25 \leq H_s < 1.25$							
1.	210-300	0.62	267	4.65	6.38	230	24.73	6.79
2.	300-30	0.64	342	5.79	4.90	331	32.21	7.25
	$1.25 \leq H_s < 2.0$							
3.	210-255	1.24	262	5.79	10.80	221	8.90	12.93
4.	255-300	1.24	284	5.79	9.29	263	2.87	4.21
5.	300-345	1.33	328	6.46	7.29	313	3.84	5.54
6.	345-30	1.32	3	6.46	8.78	27	3.24	4.37
	$2.0 \leq H_s < 3.0$							
7.	210-300	1.76	272	6.46	13.28	242	5.48	21.45
8.	300-30	1.99	334	7.20	10.75	337	3.10	12.66
	$3.0 \leq H_s$							
9.	210-300	2.46	283	7.20	16.85	256	1.00	10.23
	$3.0 \leq H_s < 4.0$							
10.	300-30	2.80	335	8.03	13.81	342	0.68	6.36
	$4.0 \leq H_s < 7.0$							
11.	300-30	3.21	335	8.96	16.77	329	0.16	3.19
	Total						**86.21**	**94.98**

Wind input
The modelled domain spans a large area where shoals are omnipresent. Considering the energy transfer from wind to waves and wind-driven currents on the shallow Domburger Rassen, this cannot be neglected in the numerical model. Accordingly, a timeseries from the Brouwershavensche Gat between January 2016 and January 2021 was used to find the average windspeed and direction associated with every wave class (Table 8). A spatially and temporally uniform wind is given as model input.

Tide input
The meso-tidal regime near Domburg has a semi-diurnal character with M2, S2, and M4 as the main tidal constituents (Rijkswaterstaat and Deltares, 2019). The tidal wave deforms from West-Kapelle to Domburg from a progressive wave into a standing wave (McCall et al., 2014). Furthermore, the mean tidal range decreases from 2.62m at West-Kapelle to 2.55m near Oost-Kapelle (Rijkswaterstaat, 2021).

The tidal variation has an influence on the transport processes in the coastal zone. For instance, low water during spring tide exposes the foreshore nourishment more to the largest waves. On the other hand, a storm during neap tide can cause more dune erosion as the water level remains relatively high for a longer period of time.

The project area lacks water level stations near the west and east model boundaries. Therefore, water level timeseries were obtained through the zuno4-ASTRO model, which is being computed by Rijkswaterstaat. The model provided astronomical water levels for the west and east model boundaries in the period 22/1/2017 to 7/2/2017. This period represents a characteristic spring-neap tidal cycle near Domburg (Figure 27).
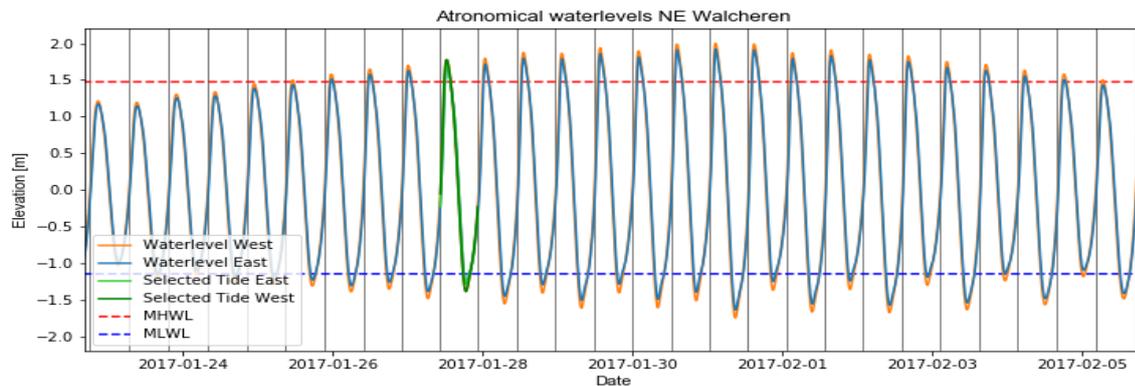
Figure 27: Spring-neap tidal cycle at the west and east model boundaries the mean low and high-water levels indicated.

Considering the computational effort of simulating complete spring-neap tidal cycles for every wave condition, a simplification is used for the tidal input. The method of deriving a morphological tide is previously applied by de Fockert (2008) and is relies on the following procedure:

1. For every tidal signal in a spring-neap tidal cycle, the bed level development at the coast is computed with a morphodynamic model. Individual tidal signals were used due to the small daily inequality and the absence of intertidal flats in the study area, which are primarily influenced by the highest high waters.

2. The cumulative bed level development of all computations is averaged over the number of tides.

3. The average bed level development is compared to all individual computations. The tidal signal with the highest correlation to the average tidal signal is chosen as the morphological tide. This signal represents the complete neap-spring tidal cycle best.

To carry out the above procedure, the numerical XBeach model is applied. In which the bathymetry is based on the 2017 spring survey, conducted three years after a beach nourishment. Furthermore, the model made use of a coarse grid with a *dx* varying from 100m to 25m in the surf zone in cross-shore direction and a *dy* of 100m in alongshore direction. A normally incident wave of $H_{m0}=1.8$m with $T_p=5$s was forced at the offshore boundary. Furthermore, the water level variations were imposed at the moment the first waves reach the coastline, because the model requires spin-up time. In adddition, the default settings for the safety evaluations of the Dutch primary water deffences were used (Appendix C.1).

Accordingly, the tenth tidal singal in the spring-neap tidal cycle represents the average bed development the best with a correlation of $R^2 = 0.98$ (Figure 28). Hence, the tenth tidal signal, with a tidal range of 3.18m and 3.02m at the west and east model boundary

respectively, is further used in the morphostatic model simulations to investigate the effects of nourishments. Appendix C.2.2 elaborates on the correlation for all individual tidal signals.
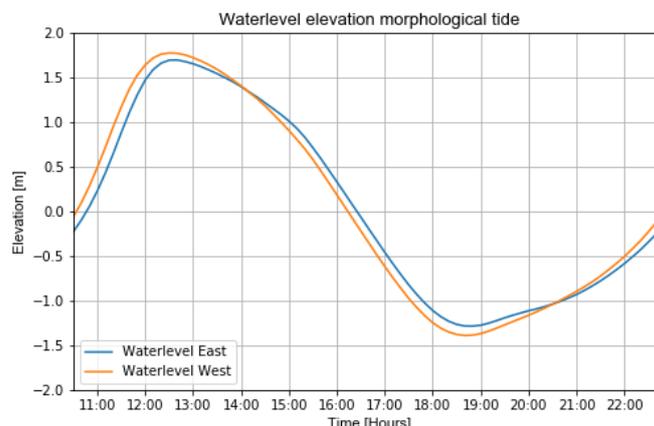
Figure 28: The water level elevations at the west and east model boundaries that represent best the bed level development during a complete tidal cycle. The signal's tidal range is a factor 1.2 larger than the mean tidal range at Walcheren.

Lateral boundaries

To prevent the lateral boundaries from influencing the results in an adverse way, information needs to be prescribed at these boundaries. It was chosen to use a 'no-gradient' Neumann boundary, which states that there is locally no change in surface elevation and velocity. Furthermore, a shadow zone is taken into account. Thus, the lateral model boundaries are located 4km away from the area of interest to exclude results from regions where the boundary conditions are not fully enforced. (Deltares, 2020)

3.3.5 Model output

The bathymetry is not updated in the numerical model, therefore the focus of the output is on the hydrodynamics and the potential sediment transport. The computed hydrodynamics can help explain observed morphologic changes from data. The potential sediment transport is used to find gradients in sediment transport. Consequently, these gradients will be used to compare different bottoms and provide insight in various nourishment strategies at Domburg. The computed output parameters are listed in Table 9.

Table 9: Output parameters XBeach.

Type	Description	Keyword	Unit
Hydrodynamics	Wave height rms	H	m
	Flow velocity, x-component	u, ue	m/s
	Flow velocity, y-component	v, ve	m/s
	Wave angle	$thetamean$	°
	Dissipation	D	W/m^2
	Wave energy	E	W/m^2
Morphology	Sediment transport, x-component	$Subg, Susg, Sutot$	m^2/s
	Sediment transport, y-component	$Svbg, Svsg, Svtot$	m^2/s

The model produces realistic hydrodynamic output, however the model is not calibrated and so the results must be interpreted with caution.

3.3.6 Model validation

To validate the model, a comparison of model output with data from nearshore measurement stations (Figure 15) is made. First a comparison of the wave transformation in SWAN and data from the Schouwenbank 2 wave buoy and the Domburger Rassen wave buoy is made. Then, the current velocities at an offshore point in the model and the data from the Schouwenbank Stroomgat are compared.

Waves

Where the Schouwenbank 2 wave buoy provides a long timeseries of wave heights, periods and directions, the Domburger Rassen wave buoy has a very limited timeseries solely wave heights. In this manner, only the wave heights are compared for the same time instances to the wave heights from the SWAN wave transformation. Figure 29 portrays a good resemblance of the wave data and the transformed wave conditions. The wave heights at the Domburger Rassen are consistently lower than at the Schouwenbank 2, which is also observed for the SWAN wave transformation. Notably, storm waves larger than 5m are not correctly represented by the wave conditions. These waves are primarily from the NW. An explanation is the variability in storm conditions during the limited dataset. Therefore, considering the low probability of occurrence of storm conditions and the similarity of mild and energetic wave conditions, the SWAN wave transformation is found to be sufficient.
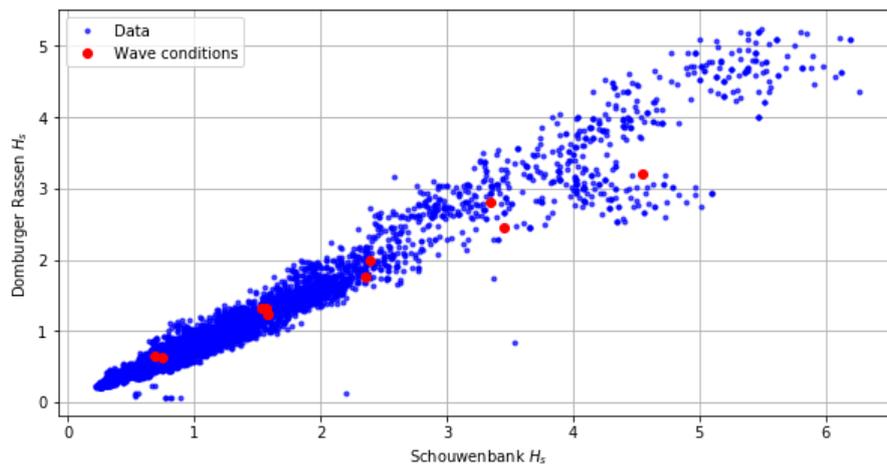
Figure 29: Significant wave height of the Schouwenbank 2 Wave buoy and the Domburger Rassen [Blue] compared to the transformed wave conditions from SWAN [Red].

Currents

The currents that are enforced by the numerical model are validated through measurements from the Schouwenbank Stroomgat station. In the numerical model, an offshore location is selected to evaluate the velocities for the two wave conditions with the highest probability of occurrence. The Schouwenbank Stroomgat station is located further offshore and in deeper water than the model domain (Figure 15). The measured currents from three arbitrary tidal cycles are used for the comparison. Figure 30 shows overall similar velocities and duration for the measured and the modelled currents. Therefore, the tidal currents are captured accurately in the model.
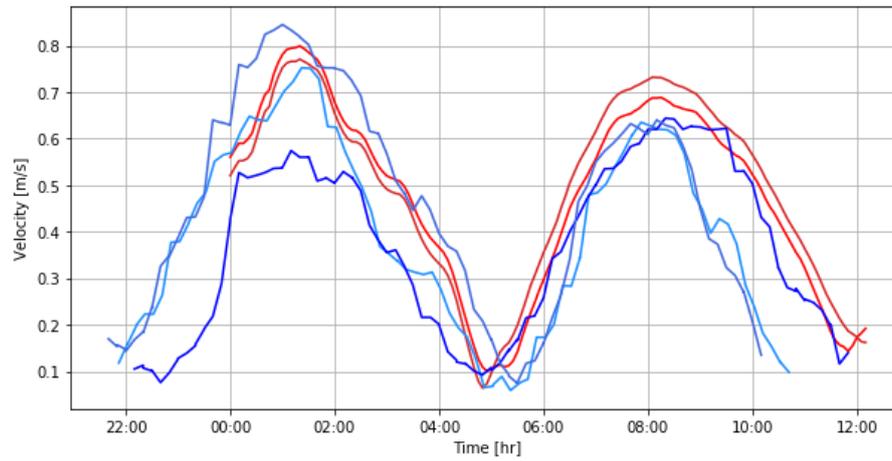
Figure 30: Comparison of measured current velocities and modelled current velocities. The measured current velocities are three random time instances from the Schouwenbank Stroomgat station [blue]. The [red] lines represent boundary conditions c1 and c2 near the offshore and west lateral model boundary.

4. Results

This chapter presents the analysis of four coastal maintenance strategies of the NW Walcheren coastline. The considered bathymetries are an unnourished coast (T_0), with a beach nourishment (T_1), with a shoreface nourishment (T_2), and with both a beach and shoreface nourishment (T_3). Section 4.1 deals with a morphological data analysis which examines cross-shore and alongshore developments, the volume development of coastal zones and the development of the momentary coastline (MKL). Following the morphological analysis, the results from the morphostatic numerical model are presented in section 4.2. It addresses the effect of nourishments on the nearshore hydrodynamics and sediment transport patterns which help explain the observations done in the first section. Thereafter, section 4.3 draws a comparison between the observed volume change of coastal zones and the modelled volume change.

4.1   Morphological data analysis

This section focusses on the morphological development of the NW coast of Walcheren under the influence of multiple nourishment strategies. The analysis is based on bathymetric and hydraulic data. The section starts with elaborating on the wave climate for the considered periods. Following, an examination of cross-shore developments, for instance profile changes, migration of a shoreface bar, and the beach slope is done. Next, alongshore developments are considered, such as erosion and sedimentation zones in the nearshore, the migration of transverse bars. Then, the volume development in the nearshore is presented. Following, the lifetime of beach nourishments is reviewed. Hereafter, the momentary coastline evolution is examined. The section concludes with a review of the main observations.

4.1.1   Wave climate

The general wave climate for the Walcheren coastline is illustrated with the use of measurements from the Schouwenbank 2 wave buoy, the Oosterschelde 11 water level station and the Brouwershavensche Gat wind station. Following, a differentiation is made for the wave climates in the periods spanning the nourishment strategies.

General wave climate

The wave climate at Walcheren has a bi-directional character with an average significant wave height of 1.1m and a significant period of 5.9s. The wave climate is dominated by wind waves that are formed locally in the shallow North Sea (Deltares, 2018) where occasionally waves larger than 6m and water levels higher than NAP+2.5m are measured during storm conditions (Figure 31). Waves mainly originate from the SWW and NNW. The more energetic waves originate from the SWW, while milder waves are mainly from the NNW, normal to the coastline (Figure 32). The dominant wind direction is from the southwest, especially for winds stronger than 12 m/s (Appendix A.2).
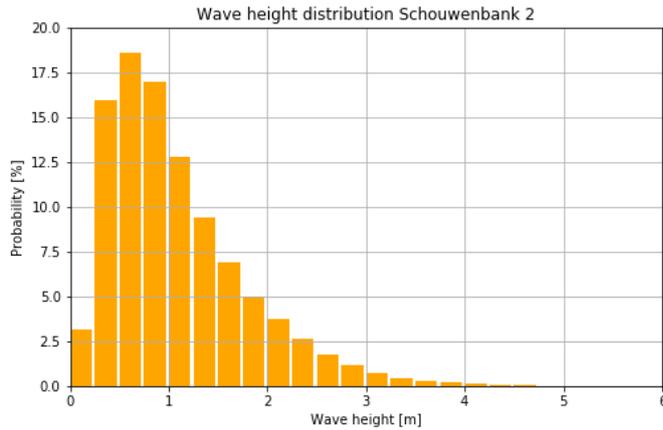
Figure 31: Wave height distribution Schouwenbank 2 in the period Jan 2008 – Jan 2021.
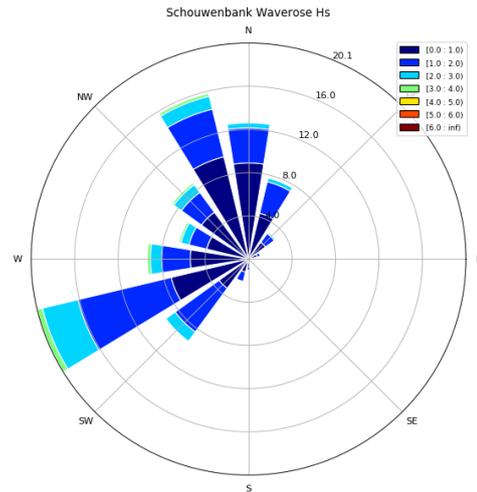
Figure 32: Wave rose Schouwenbank 2 in the period Jan 2008 – Jan 2021 [m].

Wave climates nourishment intervals

The natural variability in the weather can cause the wave climate to be different from one year to the other. This might affect coastlines as the erosion rate of nourishments increases for stronger wave climates. Therefore, the wave climate in the periods between nourishments is compared to the general wave climate. In this manner, the correlation coefficients for all wave conditions and for more energetic wave conditions, H_s>2m, is determined for the bins of the wave height and direction (Table 10). This results in the observation that wave climates during nourishment intervals is similar to the general wave climate with the exception of Dec 2017-May 2019. The storm conditions show good correlation for the beach nourishments, thus the incoming wave energy per directional bin was not susceptible to large variations. Appendix A.1 Wave climate provides timeseries, wave roses and wave height distributions for each nourishment interval.

Table 10: Correlation coefficients of the significant wave height distribution and wave direction bins for the periods between nourishments compared to the general wave climate.

Period	R^2 H_s	R^2 Θ_{wave}	R^2 $H_{s\ storm}$	R^2 $\Theta_{wave\ storm}$
Jun 2008 - Mar 2012	1.00	0.99	1.00	0.98
Mar 2012 - Dec 2014	1.00	0.98	1.00	0.98
Dec 2014 - Dec 2017 (T_1)	1.00	1.00	1.00	0.99
Dec 2017 - May2019 (T_2)	0.99	0.97	1.00	0.83
May 2019 - Jan 2021 (T_3)	1.00	0.99	1.00	0.98

4.1.2 Cross-shore development

Two beach nourishments and one shoreface nourishment were completed in the period 2014-2021. This subsection reviews the cross-sectional morphological developments in this period. It includes an examination of cross-shore profiles, migration of the shoreface nourishment and the beach slope. An overview of the transect locations can be found in Figure 16.

Central: Cross-shore profiles T_1

The Dec 2014 beach nourishment has a post-construction survey available. Figure 33 illustrates the fast response of the coastal profile, as a third of the sediment is already eroded after three months, and the beach profile returns to the original profile in 1 year. Initially, the linear sloping beach is reshaped into the characteristic exponential beach profile. Meanwhile, the nourishment plateau at NAP+4m remains. The year hereafter, this plateau was eroded and the beach profile returned to its original shape.

A substantial part of the supplied sand is distributed on the shoreface between -3m and -7m. However, the passage of transverse bars, causing an elevation or depression of the shoreface, obscures where the nourished sand remains.
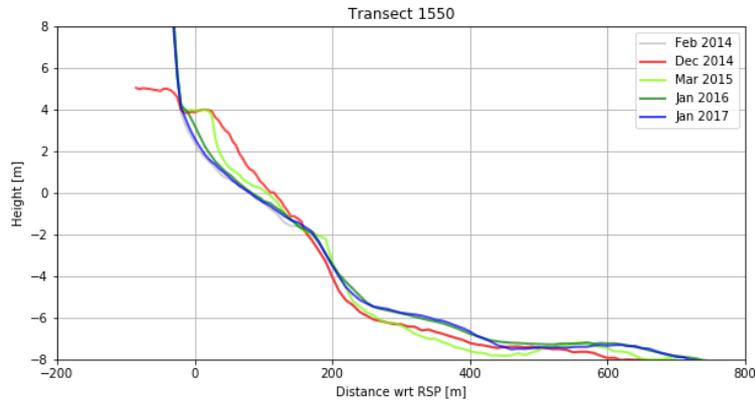
Figure 33: Cross-shore profiles of transect 1550, after the 2014 beach nourishment. The Dec 2014 survey between -100 - -50 was added manually for the beach volume calculation and does not represent reality.

Central: Cross-shore profiles T$_2$

The first shoreface nourishment near Domburg was implemented in Dec 2017 as a shore-parallel bar, spanning transects 1632-1448. Due to difficulties in the construction process, no nourishment body is evident in transect 1550 (Figure 40). This effectively splits the shoreface bar in two separate segments, where the west segment is close to the steep shoreface (Figure 34), the east segment lies further offshore on the plateau of the Domburger Rassen (Figure 35).

The west segment, characterized by transect 1591 in Figure 34, shows a quick response after the completion of the shoreface nourishment. Initially, the top and seaward side of the shoreface bar quickly erode, but no clear landward migration of the bar is observed nor the development of a trough. Hereafter, between Mar 2018-Feb 2019, the shoreface bar continues to flatten and also displaces sediment at the landward shoreface. Generally, at the west segment, the shoreface bar merges with the steep subtidal shoreface and decreases in volume in the first 1.5 years.
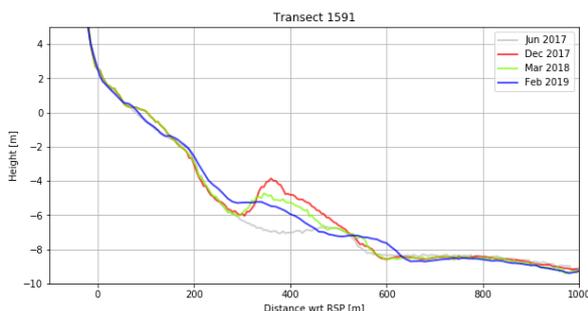
Figure 34: Cross-shore profiles of transect 1591, including the 2017 shoreface nourishment between 250-500m.
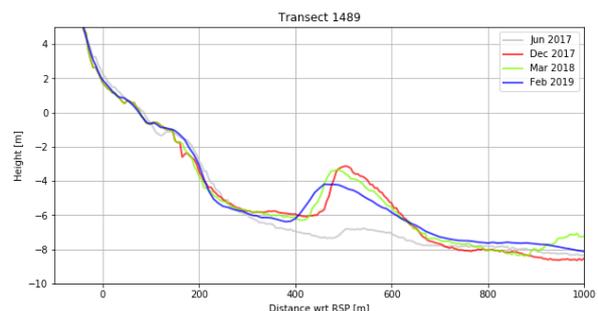
Figure 35: Cross-shore profiles of transect 1489, including the 2017 shoreface nourishment between 400-700m.

The east segment, represented by transect 1489 in Figure 35, portrays multiple developments in the period Dec 2017-Feb 2019. To start with, the consecutive profiles show an onshore migration of the shoreface bar between 400-700m. Additionally, the crest height decreases slightly to -4.5m. It is also seen that the landward and seaward slopes become gentler and the bar transforms from a sawtooth into a more rounded body. Remarkably, no trough is formed landward of the shoreface bar. Seaward of the shoreface bar, the observed

variability is mainly due to the passage of transverse bars, with crest heights in the order of 1.5m. Other transects depict that these bars also cause variability landward of the shoreface bar. These observations are generally made for all transects 1530-1448 before the construction of the 2019 beach nourishment.

Central: Cross-shore profiles T₃

In May 2019, a beach nourishment was completed between transects 1632-1448 while the shoreface bar was still evident. Despite the presence of the shoreface bar, a quickly eroding beach is visible in Figure 36 and Figure 37. After one year, approximately half of the nourished volume is still present at the beach and after two years about one third remains. The beach profile returns to a smooth profile with some ridges and runnels causing the variability in the intertidal zone.

Looking at the shoreface, the west segment shows continuous fusion of the shoreface bar and smoothening of the coastal profile (Figure 36). However, a small breaker bar is formed with the crest at -2m in the period Oct 2020-Mar 2021, which is also occasionally observed in other transects such as 1612 and 1489.
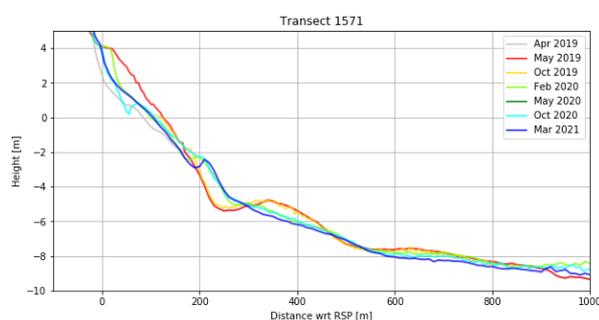
Figure 36: Cross-shore profiles of transect 1571, including the 2019 beach nourishment.
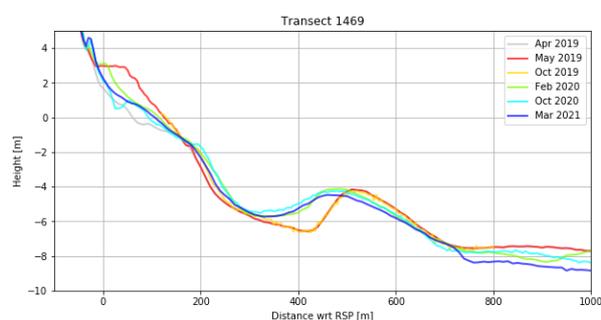
Figure 37: Cross-shore profiles of transect 1469, including the 2019 beach nourishment.

Meanwhile, the east segment depicts the apparent shoreface bar with sedimentation at the landward side (Figure 37). This sediment mainly originates from the beach nourishment and settles at the steep shoreface below -2m, at 180-280m, and in the trough zone of the shoreface bar, at 330-450. This effectively causes the crest to displace landward and leeside slope becomes gentler. In the period Feb 2020 – Mar 2021, after the beach nourishment was largely eroded, the shoreface bar remains mostly stationary. At 700-1000m in Figure 37, the passage of a crest and trough of a transverse bar explains the decreasing elevation.

Central: Remarkable transects

The previously described observations generally apply to all transects, but some transects demonstrate different developments. For instance, near the upstream ends of the two sections, strong erosion of the shoreface bar is seen (Figure 38 and Figure 39). Where the shoreface bar remained in most transects, a large volume of nourishment erodes in transects 1632 and 1530.
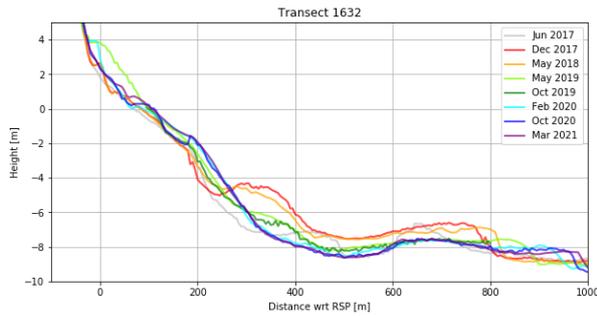
Figure 38: Cross-shore profiles transect 1632.
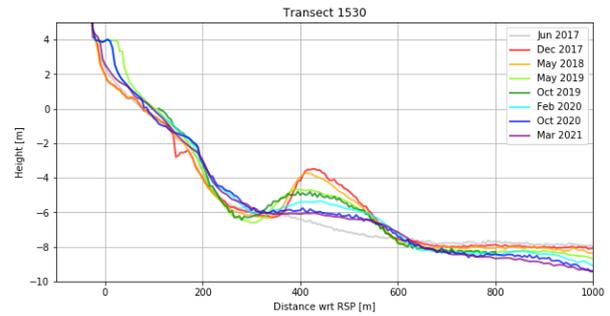
Figure 39: Cross-shore profiles transect 1530.

Another remarkable transect is 1550, where two small shoreface bars appear after the 2017 nourishment (Figure 40 at 450m and 750m). The contractor encountered difficulties in navigating close to the coast due to shallow water depths above transverse bar crests. Similarly, the 2019 beach nourishment is not found in transect 1612 (Figure 41). The reason why this transect was not nourished is not known.
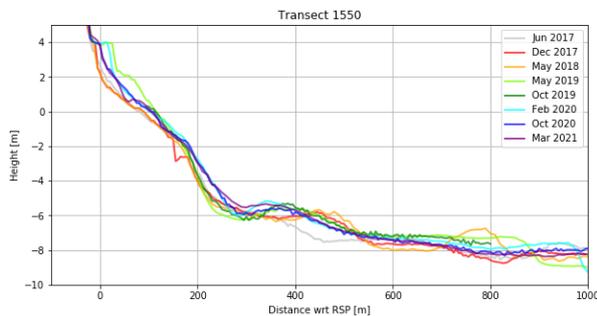
Figure 40: Transect 1550 shows no large shoreface bar but two small bodies at 450m and 750m after the 2017 nourishment.
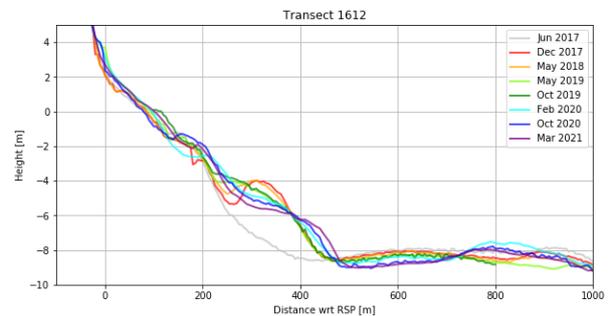
Figure 41: Transect 1612 where the 2019 beach nourishment is not present in the profile.

West

In upstream direction of the nourished zone, no unambiguous effects of the nourishments at Domburg are seen (Figure 42 and Figure 43). Small ridges and runnels are present in the intertidal zone and an advance of the steep shoreface at 200m is observed. It must be noted that the upstream transects 1948-1735 near the Westkappelse Zeedijk are nourished simultaneously. Possibly, these nourishments supply sediment to transects1694-1653. Another observation in transect 1673 is the highly variable shoreface at 600m (Figure 43). This is the crest of a curved transverse bar that migrates through this transect, causing a seaward extension of the upper shoreface.
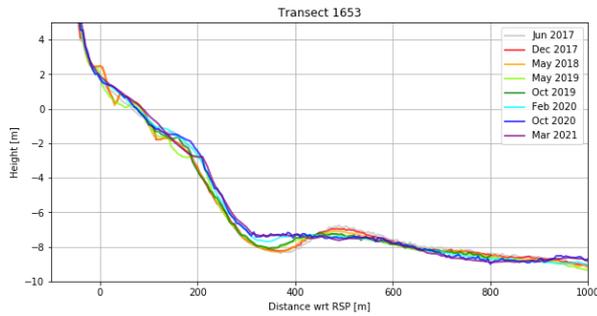
Figure 42: The first transect upstream of the nourished zone.
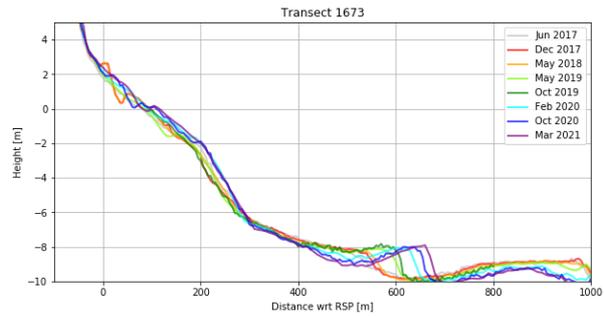
Figure 43: The second upstream transect portraying small variably ridges and runnels and the large variability on the shoreface at 600m.

East

Eastward of the nourished zone, the first downstream transect shows accretion on the shoreface, intertidal zone and beach (Figure 44). This indicates that the nourishments dispose sediment in downstream direction. However, this effect is not seen for further downstream located transects 1366-1306. Additionally, shoreface bar emerges in transect 1428 after a year and remains relatively stable afterwards. Contrarily, no shoreface bar has developed after three years in transect 1406. This suggests that the alongshore migration of the shoreface nourishment is limited.

Considering the coastal profile between -50 – 300m in transects 1428 and 1406 (Figure 44 & Figure 45), an advance of the coast is observed as the profiles move in seaward direction over time. A negative transport gradient for hydrodynamic and aeolian processes can explain the accretion found between NAP+4 and NAP-5.

Furthermore, variable ridges and runnels are found in the intertidal zone. These features are more extensive than the ones found in the central intertidal zone at Domburg.
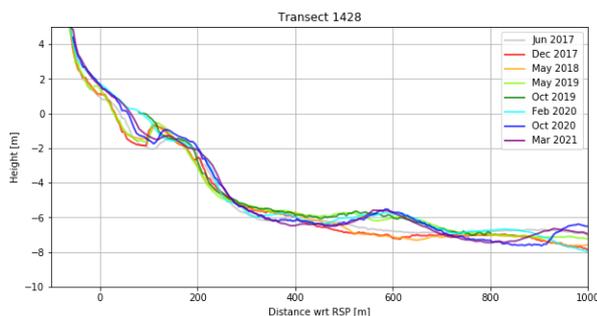
Figure 44: The first transect downstream of the nourished zone shows an emerging shoreface bar after a year.
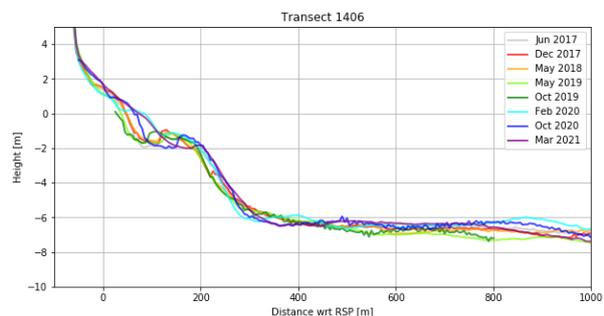
Figure 45: The second downstream transect shows extensive ridges and runnels but no emerging shoreface bar

Cross-shore migration of the shoreface nourishment

The cross-shore migration of the shoreface nourishment is followed through the position of the bar's centroid. In the period Dec 2017 – Apr 2019, when the bar was undisturbed, an initial migration rate of 18.8m/yr in landward direction was found (Figure 46). As mentioned before in section 2.8.4, the nourishment effectively consists of two bodies of sand separated at transect 1550. Looking at the migration rates of those two bodies between 1632-1571 and 1530-1448, the migration rates are 25.9m/yr and 14.6m/yr respectively. Therefore, initially the bar closer to the shoreline moves faster.
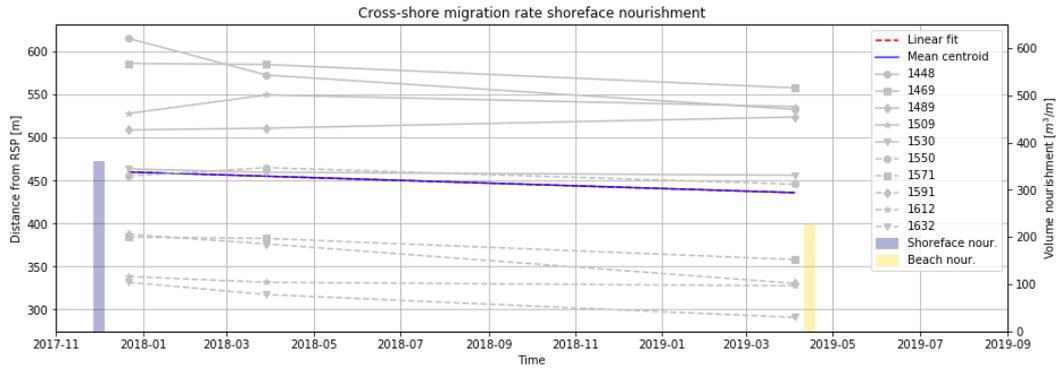
Figure 46: Cross-shore migration of the shoreface nourishment near Domburg based on the position of the centroid of the shoreface bar. The mean migration rate is 18.8 m/year in landward direction. The nourishment volumes are depicted on the secondary y-axis.

Remarkably, transect 1509 shows an initial seaward movement. This is explained by the passage of transverse bars, which shows a large volume increase at the seaward side of the shoreface bar (Figure 47). A comparable situation occurs at transect 1448, where landward of the nourishment a transverse bar arises, causing a more rapid landward shift of the centroid.
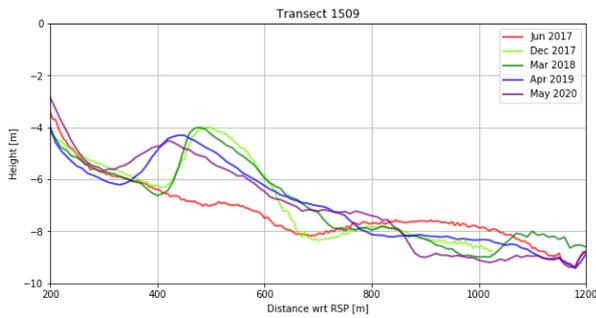
Figure 47: Cross-shore profiles of transect 1509, where the variability between 700m-1000m indicates the passage of transverse bars.
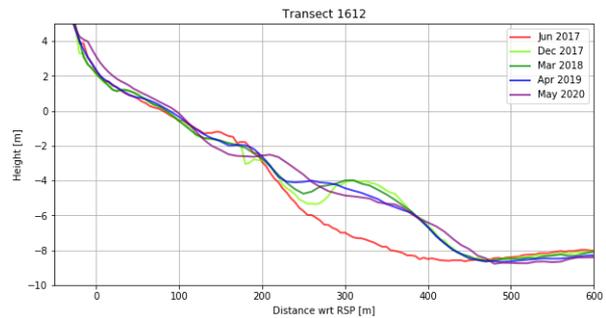
Figure 48: Cross-shore profiles of transect 1612, where the 2017 shoreface nourishment is evident between 250m - 450m and the 2019 beach nourishment at -50m – 150m.

In May 2019, the coast was disturbed by a beach nourishment. In the following period, a mean migration rate of 17.8m/yr is observed, comparable to the situation before, but the transects show more variability. For instance, the sandbar is displaced seaward in transects 1448 and 1550, being the ends of the east shoreface bar. The intermediate transects migrate in landward direction on average with 16.1m/yr.
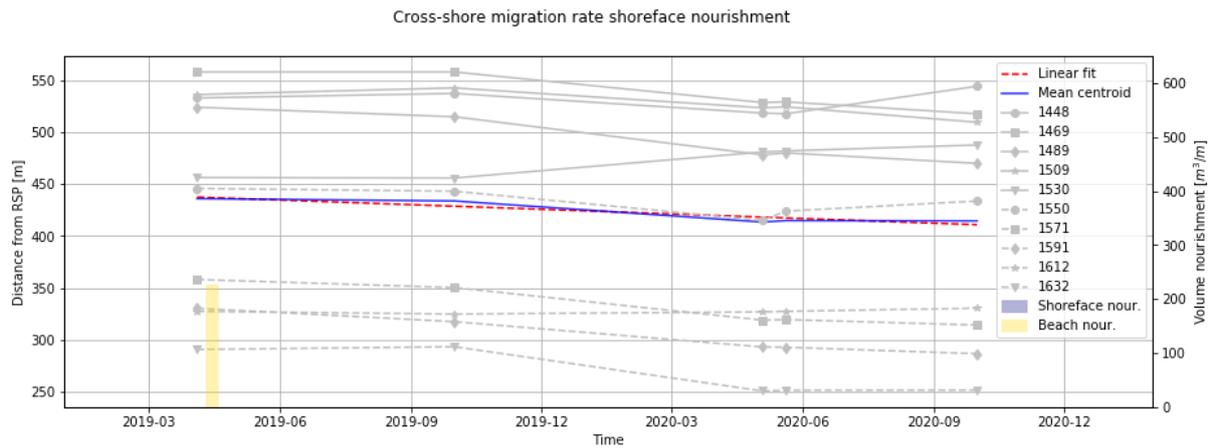
Figure 49: Cross-shore migration of the shoreface nourishment near Domburg posterior to the 2019 beach nourishment, based on the position of the centroid of the sandbar. The mean migration rate is 17.8 m/year in landward direction. The nourishment volumes are depicted on the secondary y-axis.

Initially, transects 1571-1632 in the west section remain stationary. However, a rapid landward displacement is seen between Oct 2019 – Apr 2020. This is a result of the redistribution of nourished sediment which fills up the subtidal zone landward of the shoreface bar (Figure 48 at 200-250m). Due to the nourished sediment at the landward side, the centroid of the sandbar shifts in landward direction.

Overall, a landward directed mean migration of 17.7m/yr is found for the period Dec 2017-Oct 2020 (Table 11). The variability per transect is contributed to, either the passage of transverse bars at the landward or seaward side, or to the redistribution of nourished beach sediment. However, this does not apply to the seaward directed migration of transects 1530 and 1448 in the period Oct-2019 – Oct-2020 (Figure 49).

The volume of the shoreface bar decreases with -2.5m³/yr on average. However, the volume trend is highly variable per transect (Table 11). Again, this is due to the passage of transverse bars or due to a volume of nourished beach sediment attaching to the bar. Nonetheless, transects 1530 and 1632 do not comply, as they show a remarkably strong volume decrease. Transect 1530 shows erosion of the bar, where notably the asymmetric shape develops into a round bulge (Figure 50). Transect 1632 displays a quick volume decrease at the seaward side of the bar (Figure 51).

Table 11: Mean migration rate and volume change of the sandbar for each transect.

Transect	Bar migration rate [m/yr]	Bar volume change [m³/m/yr]
1448	-26.8	54.6
1469	-25.0	32.7
1489	-14.5	-24.5
1509	-8.0	29.9
1530	9.1	-84.0
1550	-13.9	-1.6
1571	-27.2	11.7
1591	-37.6	0.9
1612	-2.8	19.2
1632	-29.8	-64.1
Mean	-17.7	-2.5
Std	13.5	41.4
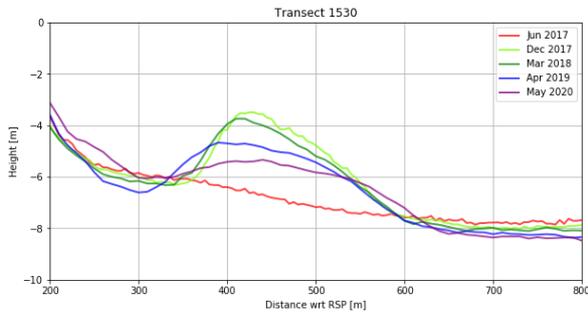
Figure 50: Cross-shore profiles of the shoreface nourishment in transect 1530.
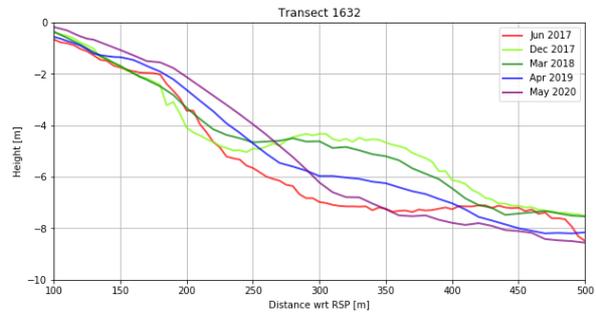
Figure 51: Cross-shore profiles of the shoreface nourishment in transect 1632.

Beach slope development

The beach slope, defined as the slope between the NAP+3m and NAP-3m height levels, is influenced greatly by beach nourishments. For the 2014 and 2019 beach nourishments, post-construction surveys are available. The nourishments result in a post-construction slope of 1/27. The beach slope adjusts quickly within one year to a gentler slope of 1/35, which is near equilibrium for the NW Walcheren coast.

No noticeable effect of the shoreface nourishment on the beach slope can be determined.
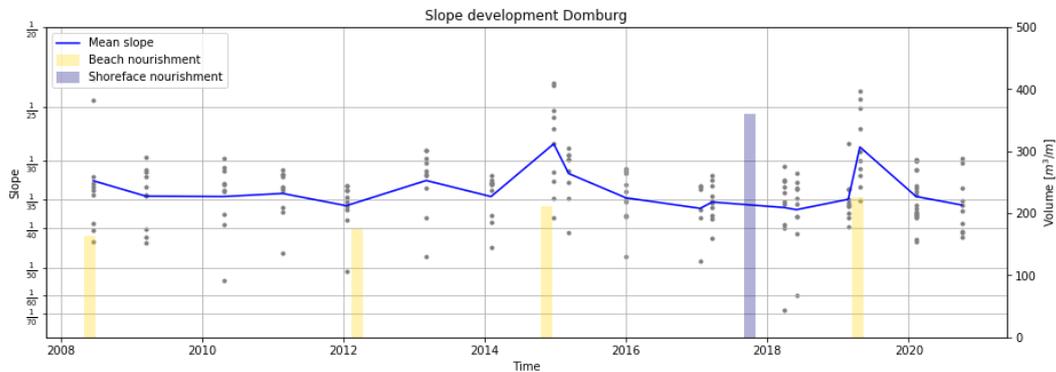
Figure 52: Slope of the coastal profile between NAP+3m and NAP-3m of transects 1448-1632. The nourishment volumes are depicted on the secondary y-axis.

4.1.3 Alongshore development

This sub section considers morphological alongshore developments. First, the erosion-sedimentation maps are analysed and interpreted. Second, the alongshore migration rate of transverse bars is quantified. Third, the alongshore migration of the shoreface nourishment is studied.

Erosion sedimentation

In the period after a beach nourishment (T_1), strong erosion between the 0m and 5m contours occurs. A large volume of sediment is eroded from both nourished beaches at Domburg and at the Westkappelse Zeedijk (Figure 53a). Meanwhile, in downstream direction of the nourishment at West-Kapelle, the shoreface accretes around the -5m contour line (Figure 53b). More seaward, a pattern of accreting and eroding patches emerges near Domburg, being explained by the migration of transverse bars in northeast direction (Figure 53c). To the east of Domburg, small shore parallel subtidal bars cause variability on the shoreface (Figure 53d). The bar heights are in the order of 1m. The erosive and accretive patches in the dunes to the east of Domburg are likely to be a result of measurement or interpolation errors due to the high spatial variability in the dunes (Figure 53e).
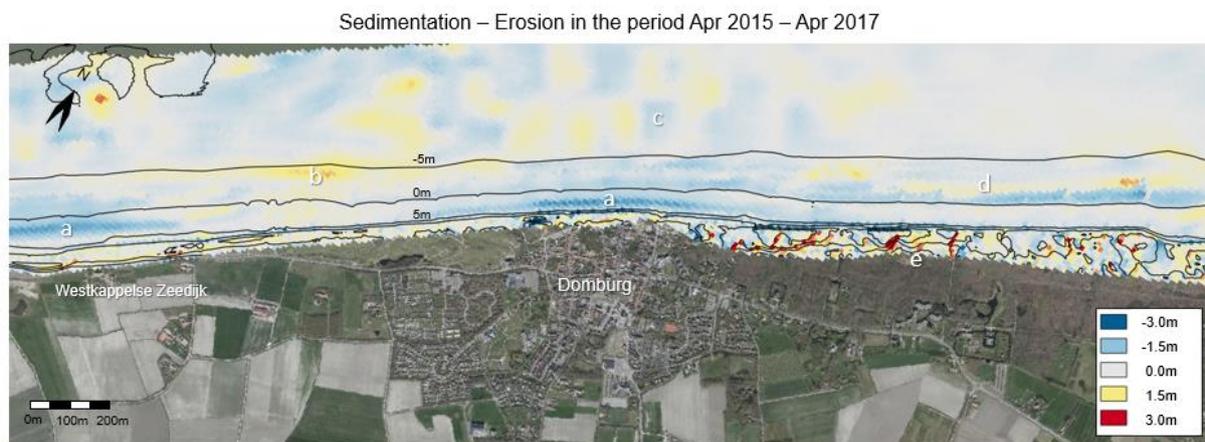
Figure 53: Sedimentation-erosion map between Apr 2015-Apr 2017, showing the morphological changes after a beach nourishment completed in Dec 2014. The contour lines are based on the Apr 2017 survey.

The morphological changes between Mar 2018 – May 2019 are mainly characterized by an onshore migration of the 2017 shoreface nourishment (T_2). Erosion in the order of 1m of the initially nourished area is evident (Figure 54a), while at the landward side accretion is found in the order of 1.5m (Figure 54b). Also, the nourishment spreads alongshore (Figure 54c). Because the accretion is in the order of 1m, the nourishment does not migrate alongshore as a whole but spreads in downdrift direction. Notably, a small portion of the 2019 beach nourishment is already present (Figure 54d).

Sedimentation – Erosion in the period Mar 2018 – Feb 2019
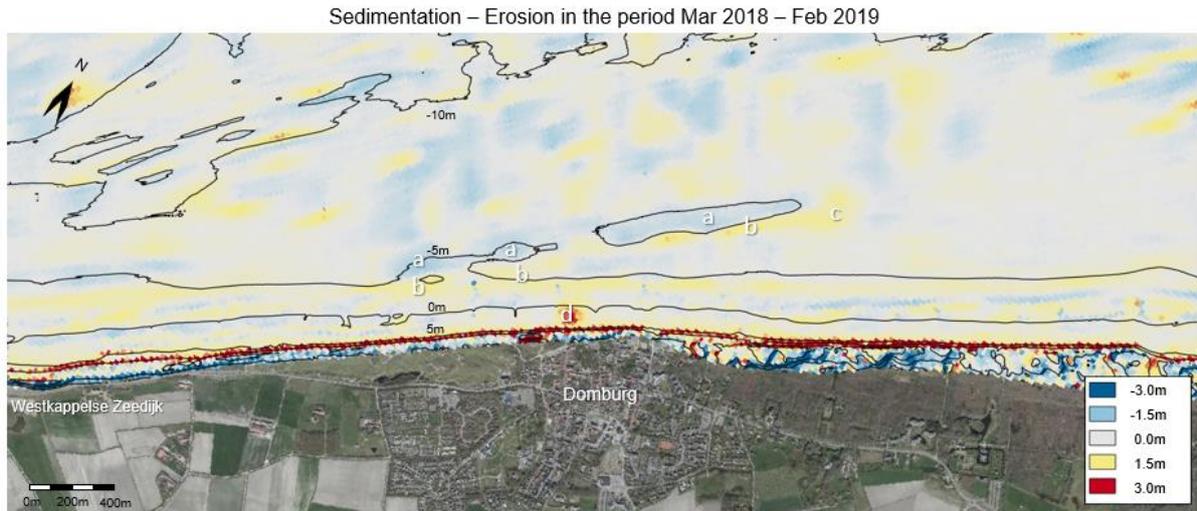
Figure 54: Sedimentation-erosion map between Mar 2018-Feb 2019, showing the morphological changes after a shoreface nourishment. The contour lines are based on the Mar 2018 survey.

Between Feb 2019 – Oct 2020, both a beach and a shoreface nourishment are present near Domburg (T_3). In this period the shoreface nourishment migrates onshore as it erodes (Figure 55a) and accretes at the landward side (Figure 55b). The sedimentation at the Domburg beach is due to the 2019 nourishment (Figure 55c). However, local severe erosion is observed at the beach (Figure 55d). A small stretch was already nourished during the Feb 2019 survey, and this indicates the already occurred erosion from the entire nourished beach. The eroded sediment is distributed between NAP-2m and NAP-5m (Figure 55e). In this way, the eroded sediment starts to fill the trough between the beach and the shoreface nourishment. At the adjacent east shoreline, the intertidal and beach area are eroding in the order of 1m (Figure 55f).

Sedimentation – Erosion in the period Feb 2019 – Oct 2020
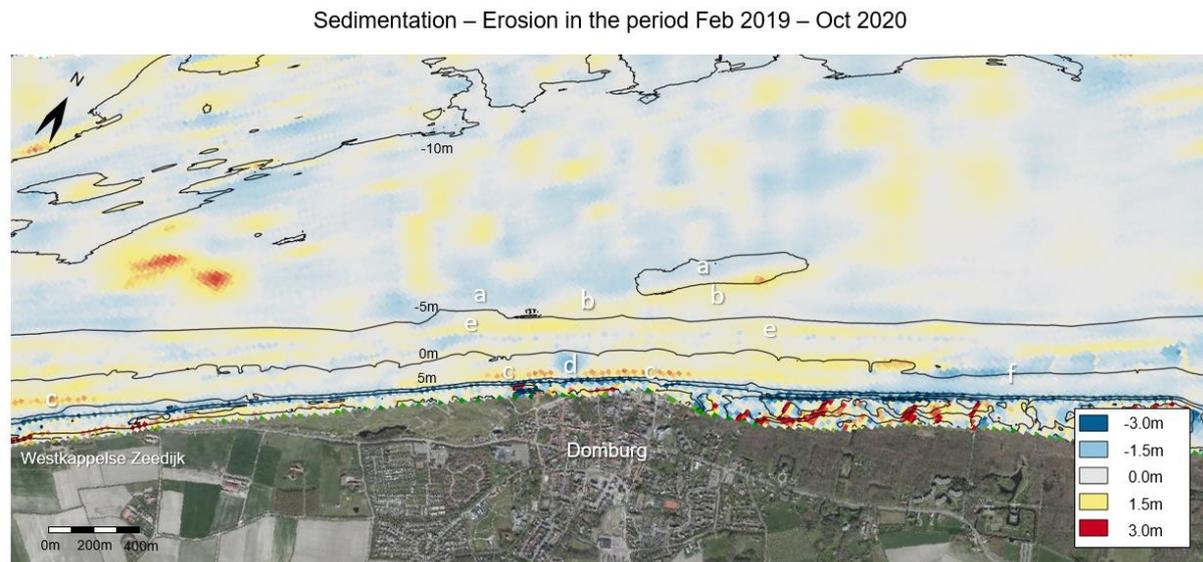
Figure 55: Sedimentation-erosion map between Feb 2019-Oct 2020, showing the morphological changes after a combined beach and shoreface nourishment. The contour lines are based on the Mar 2018 survey.

50

Sedimentation – Erosion in the period Jun 2017 – Oct 2020
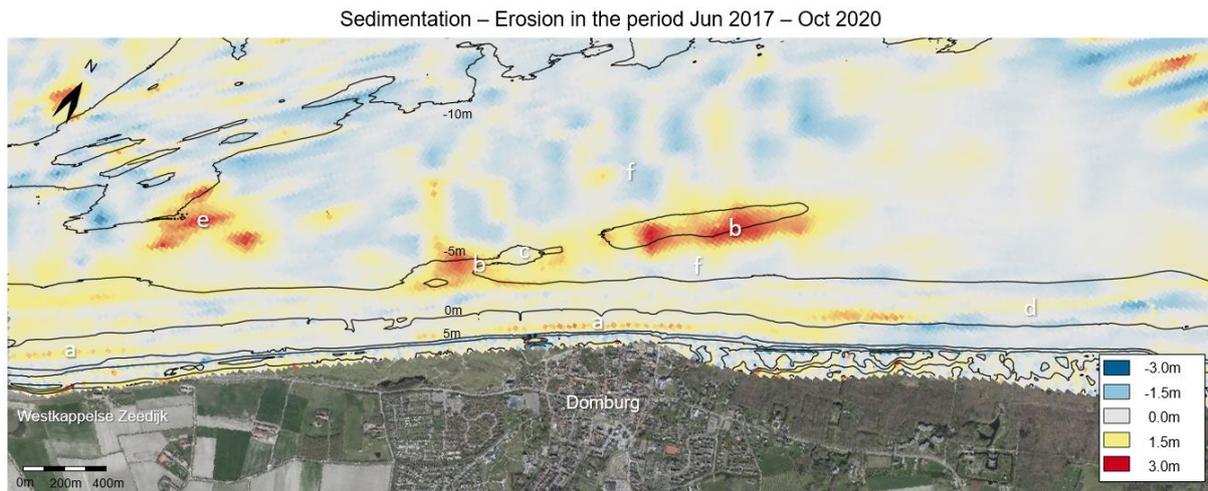
Figure 56: Sedimentation-erosion map between Jun 2017-Oct 2020, showing the morphological changes after a shoreface and beach nourishment. The contour lines are based on the Mar 2018 survey.

To sum up, in the period Jun 2017 – Oct 2020 the following is observed, partly as a result of the 2017 shoreface and 2019 beach nourishment:

- Sedimentation of the beach and intertidal zone at Domburg, which is contributed to the beach nourishment. However, the nourishment quickly erodes. This also holds for the nourishment near West-Kapelle. (Figure 56a)
- Sedimentation in the initial nourished shoreface zone shows that a distinct sandbar is still evident after 2.5 years. Moreover, the sedimentation landward of this zone indicates an onshore migration (Figure 56b). However, the sandbar in the central nourished area is less pronounced, suggesting larger erosion. (Figure 56c)
- At the east adjacent coast between MSL and DF, erosion is observed. The sedimentation near the MLWL suggests the variability of small shore parallel sandbars. (Figure 56d)
- Strong local sedimentation in the western deeper zone might be a result of the ebb-tidal delta dynamics. (Figure 56e)
- Similarly, the tide forces the eastward directed migration of transverse bars, seaward and landward of the shoreface nourishment. (Figure 56f)

Migration of transverse bars

Elongated shore-parallel sand bars, with bar heights in the order of 1m, migrate in alongshore direction to the east (Figure 57). These bars are evident between transects 1673-1406 and are present in the coastal profile between depths of NAP-5m to Nap-10m. The migration rate increases from west to east, with 30m/yr to 50m/yr. Contradictory, the bar height decreases from west to east, from approximately 1.5m to 0.8m. (Figure 58)

The 2017 shoreface nourishment forms a local obstruction for the transverse bars, however no evidence was found that the nourishment disturbs the transverse bar migration.

Sedimentation – Erosion in the period Apr 2017 – Dec 2017
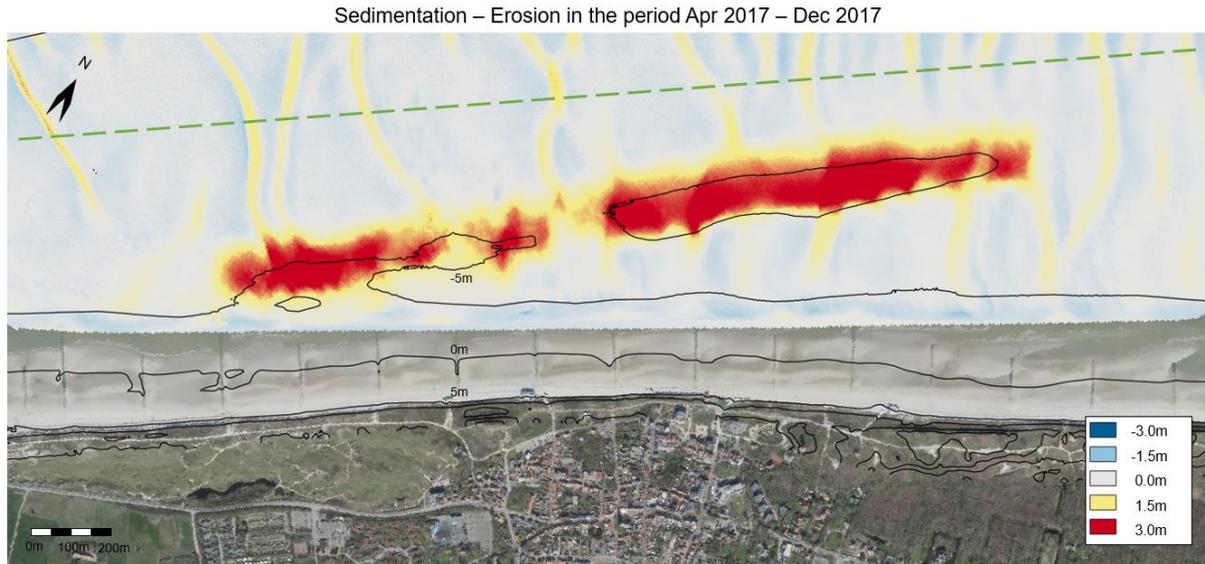
Figure 57: Sedimentation-erosion map between the in- and outsurvey, measured with multibeam, of the 2017 shoreface nourishment. The contour lines are based on the 2018 spring survey. The red area represents the nourished area. The dashed green transect shows the location of the cross-section of Figure 58.
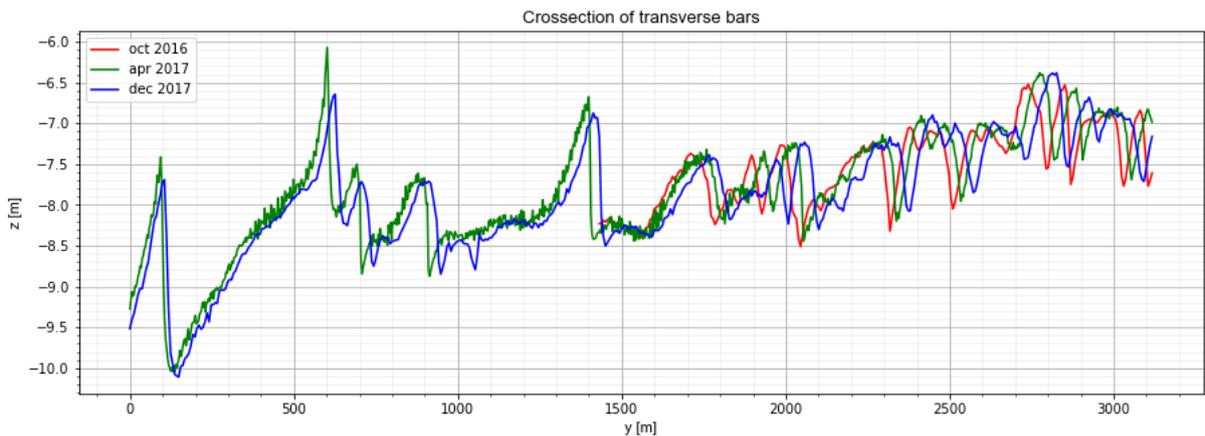
Figure 58: Cross-section of migrating transverse bars at the shoreface near Domburg, at the dashed green transect in Figure 57.

Alongshore migration of the shoreface nourishment

The alongshore migration of the shoreface bar is analysed through the 5m and 6m contour plots (Figure 59). The west end of the shoreface bar migrates alongshore in both the -5m and -6m contours. Contradictory, the east end remains stationary at the 5m contour while it displaces in alongshore direction in the 6m contour. It can be seen that this displacement takes place in the period shortly after construction, because the Oct 2019 and Oct 2020 6m contours are at the same alongshore position. Therefore, the shoreface bar diffuses in downstream direction but a clear migration of the bar as a whole is not observed.

Additionally, erosion in the central part of the nourishment is evident as the area enclosed by the 5m contours decreases in time. Furthermore, the landward side of the nourishment becomes shallower as the 6m contour lines disappear in this zone.
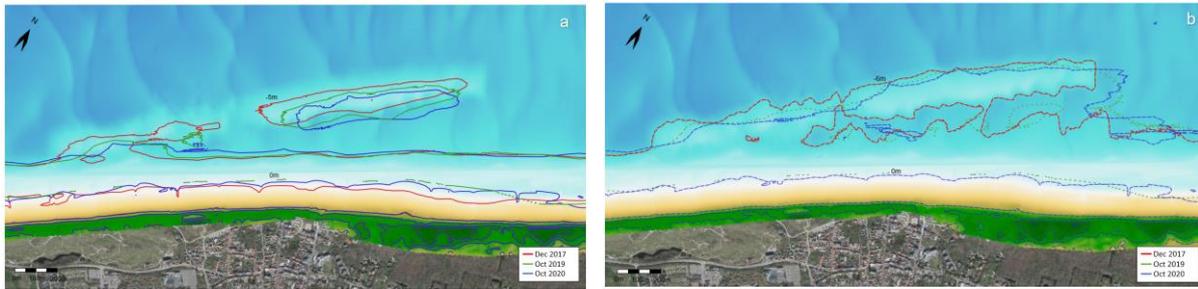
Figure 59: Migration of the shoreface bar in Dec 2017 - Oct 2020. a) The 5m contours. b) The 6m contours.

4.1.4   Volume development

This section focuses on the volume development in coastal zones, such as the beach, inner surf zone which are defined in section 3.2.3, and the sediment fluxes between these zones. The results provide insight in the way the sediment is distributed in the nearshore.

Relative volume changes in nearshore zones

To the west of Domburg, between transects 1694-1653, an effect of shoreface and beach nourishments, applied upstream at the Westkappelse Zeedijk and downstream at Domburg, is distinguished (Figure 60). The beach volume shows a variability in the order of 50m^3/m, being explained by the occurrence of small intertidal bars between NAP+1m – NAP-2m. Meanwhile, the deep coastal zone erodes posterior to the 2017 shoreface nourishment with 100m^3/m and recovers slightly after the 2019 beach nourishment. Likewise, the total volume in the coastal cell decreases and recovers to a total volume equal to the situation before the 2017 shoreface nourishment. It is expected that this effect is largely due to the updrift nourishments near the Westkappelse Zeedijk.
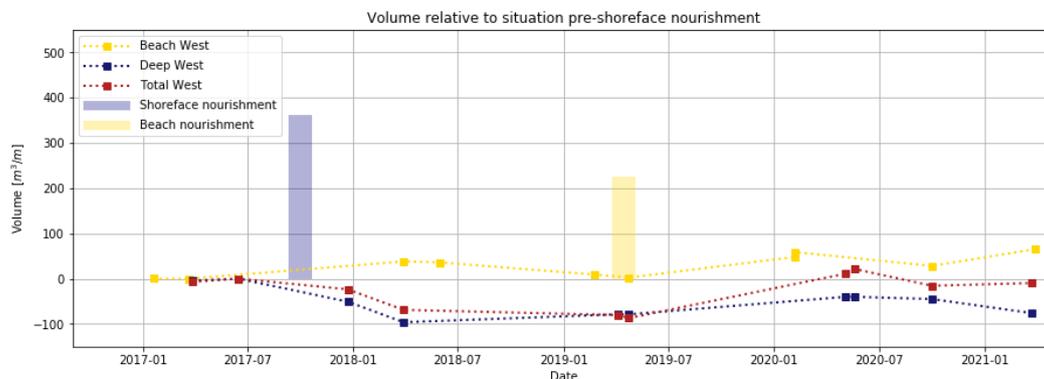
Figure 60: The volume change of coastal zones in transects 1694-1653, to the west of Domburg. No nourishment was placed on these transects, but upstream and downstream a shoreface nourishment and beach nourishment were constructed simultaneously.

The central coast, spanning transects 1632-1448, is divided into more coastal zones. On the shoreface, the initial nourishment zone, trough zone and the inner surf zone are added to more closely distinguish the development of sediment volumes (Figure 61).

The 2014 beach nourishment, T$_1$, shows an exponential decay after construction. Almost the complete nourished volume has eroded from the beach within 2 years. Meanwhile, the deep shoreface and the inner surf zone show accretion, while the initial and trough zones show no significant volume changes. Likely, some of the nourished beach volume accretes in the surf zone. The total volume in the central coast also increases mainly due to the accreting deep shoreface.

After the 2017 shoreface nourishment, T$_2$, the total volume of the coastal cell rapidly increases in the same order as the nourished volume and decreases slightly hereafter with

$20m^3/m$. In Apr 2019, another step in total volume is present due to the implemented beach nourishment. Notably, the total volume shows a large decrease of $175m^3/m$ in the following two years.

The beach volume remains stable after the 2017 shoreface nourishment and is enlarged with $200m^3/m$ due to the 2019 beach nourishment. Afterwards, a quick decline in beach volume is observed which, remarkably, is halted and increases again slightly with $18m^3/m$ in the period Oct 2020 – Mar 2021.

The inner surf zone volume decreases to $-40m^3/m$ between Jun 2017 – Apr 2019, where it increases gradually after the 2019 beach nourishment. The sediment is primarily supplied by eroding sand from the beach which settles in the inner surf zone.

The trough zone, just landward of the nourishment, accretes steadily to $130m^3/m$. Meanwhile, the initial nourishment zone shows a consistent erosion of $190m^3/m$. Both observations indicate the landward migration of the shoreface bar without the formation of a trough. Therefore, the shoreface nourishment is successful at providing sediment to the subtidal nearshore. However, even though the trough and beach zone border each other near transects 1632-1550, it must be noted that the trough zone shows no increased accretion rate after the 2019 beach nourishment.

The zone seaward of the nourishment shows an increased erosion rate in May 2020 – Mar 2021, which is also evident in the total volume. In the same period, the erosion in the trough, initial and seaward zones indicate that the subtidal bar is not sustained in the coastal profile and will eventually be eroded.
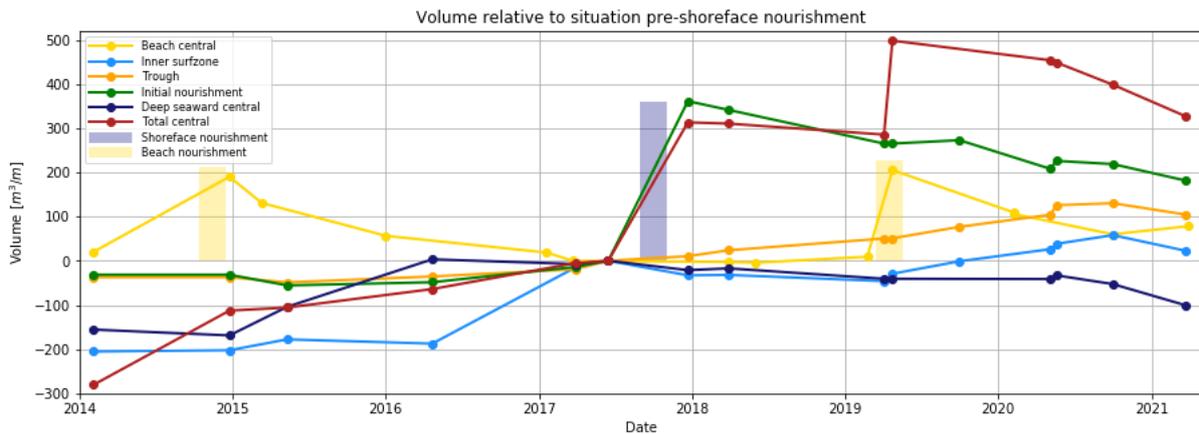
Figure 61: The relative volume change of coastal zones in the nourished transects 1632-1448, at Domburg for T_1, T_2, and T_3.

Downdrift of the nourished zone, in transects 1428-1306, initially strong erosion of the deeper coastal zone is observed, which accretes again hereafter (Figure 62). Concurrently, the beach volume shows very little variation.
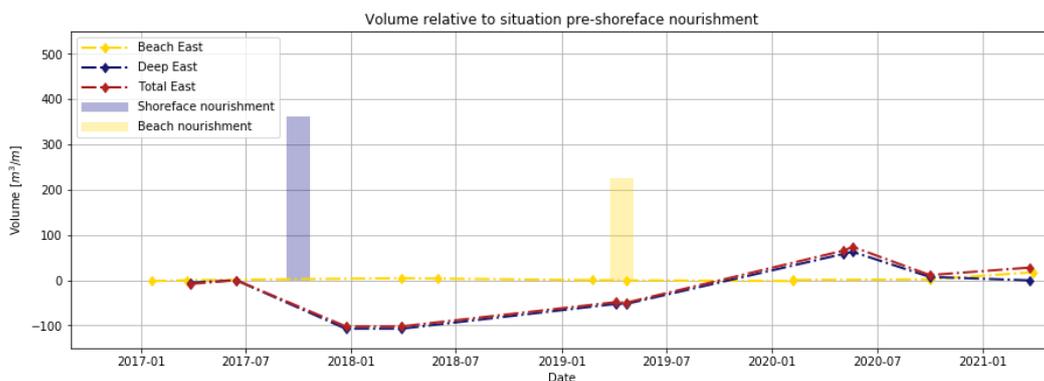
Figure 62: The volume change of coastal zones in transects 1428-1306, to the east of Domburg.

Net sediment fluxes

Based on the volume changes of coastal zones, net sediment fluxes can be estimated as prescribed in sub section 3.2.3, where Figure 19 gives an overview of the defined coastal zones. However, the estimated net sediment fluxes are found to be not entirely realistic. Therefore, the focus is shifted to the volume development of coastal zones where the fluxes provide a rough indication on how sediment is moved.

In the period prior to a nourishment (T_0), the central beach is losing sediment while the adjacent beaches are slightly accreting (Figure 63-yellow). The eroded sediment does not end up just seaward of the beach, as the surf zone and trough zones show only little accretion or erosion (Figure 63-light blue and orange). More likely it is transported in downdrift direction where it is distributed over the beach and shoreface. Moreover, accretion on the shoreface is observed (Figure 63-blue and green), which can be either due to sediment transported over the seaward boundary or variability on the shoreface due to migrating transverse bars. Furthermore, a positive alongshore sediment transport gradient is seen for the central polygons, as 40.000m³ enters and 96.000 m³ leaves the domain.
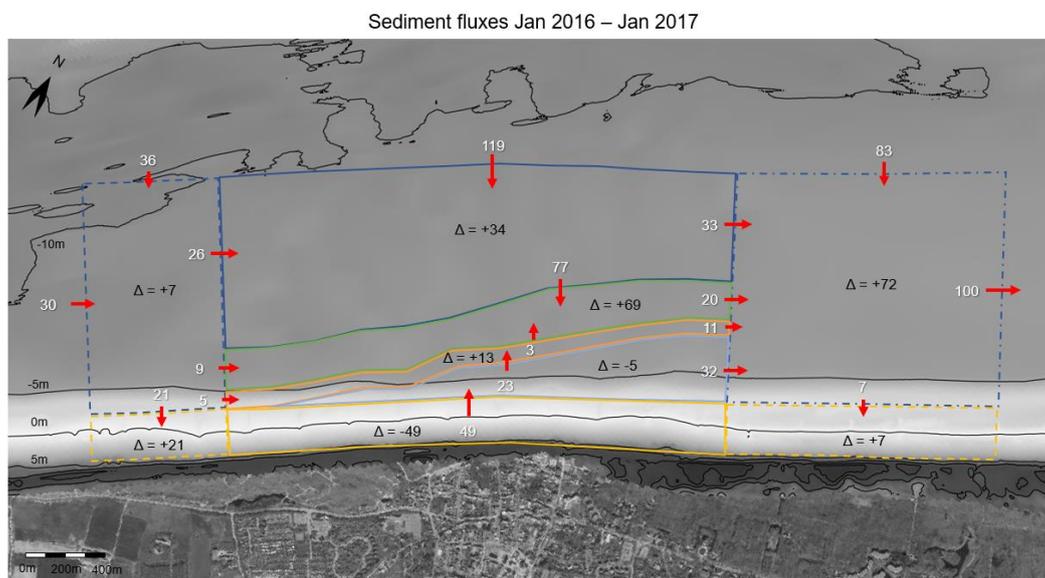
Figure 63: Sediment fluxes and volume changes near Domburg in Jan 2016 - Jan 2017 in 10³ m³ estimated from measurement data. The sediment fluxes are represented by red arrows and the volume change for the individual polygons are given by the black deltas. A beach nourishment was completed in Dec 2014 in the yellow solid polygon.

In the period shortly after a beach nourishment (T_1), the beach loses 105.000m³ of the 304.000m³ nourished material within the first year (Figure 64-yellow solid). The material does not end up solely in the zone just seaward of the beach, as there is about 38.000m³ erosion and sedimentation in these zones (Figure 64-light blue and orange). Striking is the large sedimentation in the deeper zones (Figure 64-dark blue and green), which add up to 537.000m³. This sediment partly originates from the nourishments at Domburg or the Westkappelse Zeedijk, however another source might be responsible for the bulk of the accretion. Meanwhile, the adjacent west beach accretes considerably and the adjacent east beach erodes (Figure 64-yellow dashed and dashed-dotted). So, the nourishment does not directly feed the downdrift beach relative to the autonomous trend.

Sediment fluxes Mar 2015 – Jan 2016
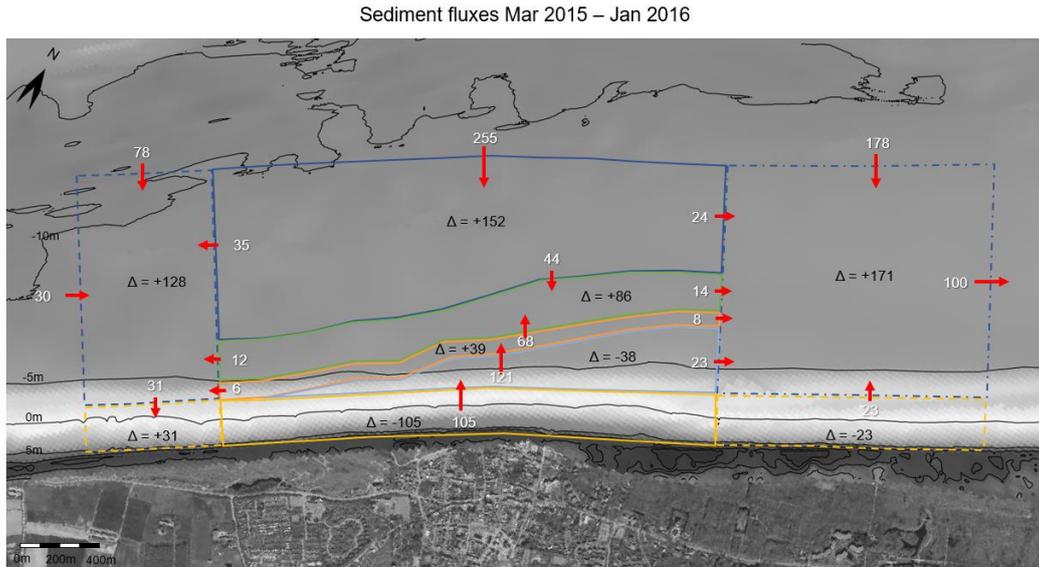
*Figure 64: Sediment fluxes and volume changes near Domburg in Mar 2015 - Jan 2016 in 10^3 m^3 estimated from measurement data. A beach nourishment was completed in Dec 2014 in the yellow solid polygon.*

After the implementation of the shoreface nourishment (T_2), the nourished zone loses a fifth of the supplied volume (Figure 65-green). This sediment is primarily brought landward to the trough area (Figure 65-orange). As observed for T_0, a positive transport gradient prevails at the central coastal zones as 35.000m³ enters and 177.000 m³ leaves the domain.

Sediment fluxes Mar 2018 – Apr 2019
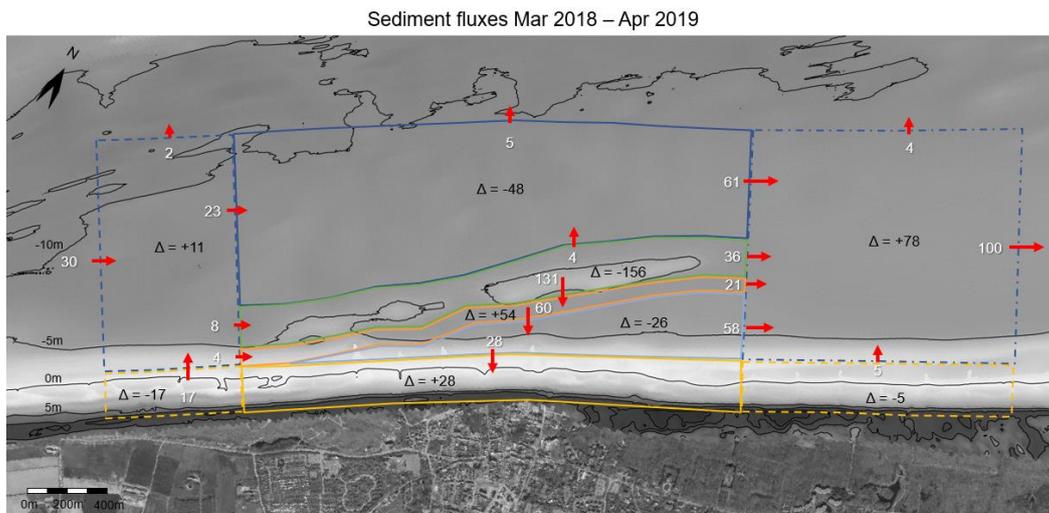
Figure 65: Sediment fluxes and volume changes near Domburg in Mar 2018 – Apr 2019 in 10^3 m^3 estimated from measurement data. A shoreface nourishment was completed in Dec 2017 in the solid green polygon.

Additionally, a beach nourishment was implemented (T_3), which was quickly redistributed as half of the nourished volume was eroded (Figure 66-yellow). The sediment was mainly dispersed in offshore and downstream direction. The shoreface nourishment hinders the seaward redistribution of the beach nourishment, causing accretion in the trough and surf zone polygons (Figure 66-light blue and orange). Meanwhile the shoreface nourishment erodes and causes extra sedimentation in the trough zone (Figure 66-green and orange). Again, a positive alongshore transport gradient is observed for the central zones as 30.000m³ enters and 152.000 m³ leaves the domain. Contrarily, a negative gradient is found in the east sections. The east shoreface accretes as a result of the disposal of nourished sediments.

56
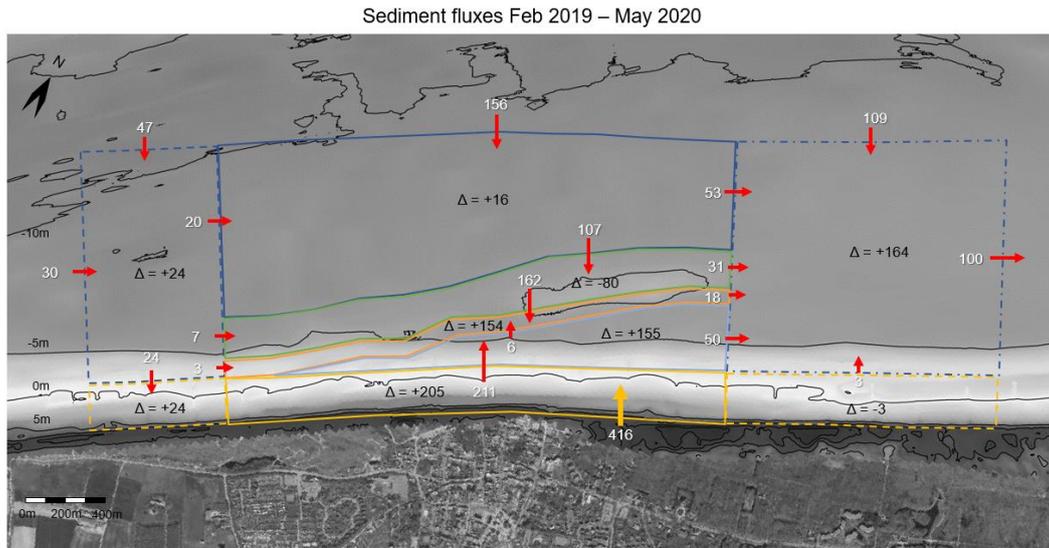
Figure 66: Sediment fluxes and volume changes near Domburg in Feb 2019 – May 2020 in 10^3 m^3 estimated from measurement data. A beach nourishment was completed in May 2019 in the solid yellow polygon, while the 2017 shoreface nourishment is still present.

4.1.5 Longevity of beach nourishments

Nourishing the beach is the conventional strategy at Domburg. Because the lifetime of applied beach nourishments was rather short, it was tried to prolong its longevity by implementing a shoreface nourishment. The longevity is defined as the period of time that the beach volume posterior to a nourishment is greater than before, where the half-life is specified as the estimated time to erode half of the nourished volume from the beach.

The beach nourishments between 1994-2014 had an average lifetime of 3.3 years, half-life of 0.8 years and an average erosion rate of -61m^3/m/yr (Table 12). The annual incoming wave energy, determined at the Schouwenbank wave buoy, indicates small annual differences in the order of 10%. Also note that the nourished beach volume varies considerably in the order of 30%.

*Table 12: Recent beach nourishments at Domburg with their nourished volume, erosion rate, estimated lifetime, and the incoming wave energy measured at the Schouwenbank 2 wavebuoy. *in 2019 the beach nourishment was placed while a shoreface nourishment was already present.*

Beach nourishment	Nourished volume [m³/m]	Mean erosion rate [m³/m/yr]	Estimated longevity [yr]	Estimated half-life [yr]	Annual mean wave energy [MW/m/yr]
Dec 1994	263	-58	4.5	n/a	n/a
Apr 2000	186	-46	4.0	n/a	n/a
Nov 2004	185	-76	2.4	1.0	101.985
Jul 2008	163	-54	3.0	0.6	107.113
May 2012	175	-60	2.9	n/a	108.684
Nov 2014	212	-69	3.1	0.8	120.794
Apr 2019*	226	-70	3.2	1.0	123.729

Taking a closer look at the 2014 beach nourishment, for which a post-construction survey was available, an erosion rate of -69.4m^3/m/yr is found. This is 14% higher than the average erosion rate of beach nourishments at Domburg. The half-life and longevity are 0.8 and 3.1

years respectively. The nourished transects show a similar trend: the exponential decline in beach volume in the first two years (Figure 67).
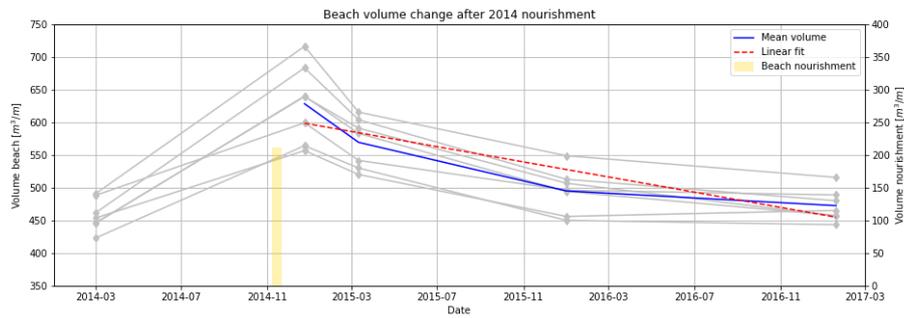
Figure 67: Beach volume change after the 2014 beach nourishment. An average erosion rate of -69.4m³/m/yr and a lifetime of 3.1 years is estimated based on four surveys in the two years post-construction.

The 2019 beach nourishment is combined with a shoreface nourishment, already implemented in Dec 2017. It shows an erosion rate of -70.8m³/m/yr and respectively a half-time and longevity of 1.0 and 3.2 years. Where the erosion first shows a linear decrease, the beach volume increases with 18.5m³/m between Oct 2020 – Mar 2021.
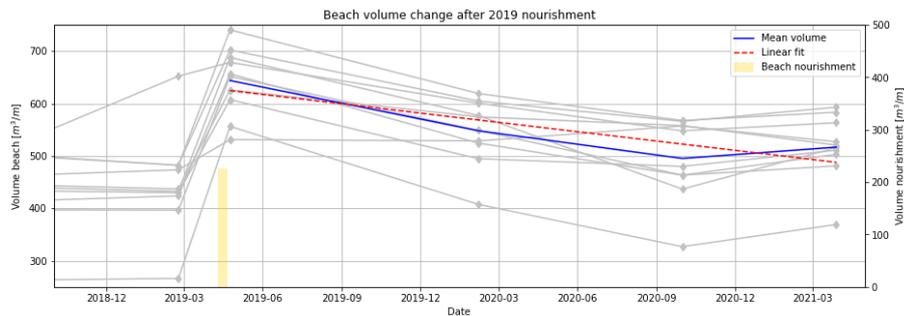
Figure 68: Beach volume change after the combined 2017 shoreface and 2019 beach nourishment. An average erosion rate of -70.8m³/m/yr and a lifetime of 3.2 years is estimated based on four surveys in the two years post-construction.

In conclusion, the 2014 and 2019 nourishments show very similar erosion rates, half-lives and longevities. Although these are comparable to previous beach nourishments, the erosion rates are higher. This may be due to the availability of post-construction surveys, which capture the initially large eroding volumes.

Contrarily, it is observed that the initial eroded volume is lower and the beach volume increases significant after 1.5 years for the 2019 nourishment. To sum up, the 2017 shoreface nourishment has no visible influence on prolonging the lifetime of the 2019 beach nourishment. However, the significant beach volume increase might indicate a positive effect of the shoreface nourishment.

4.1.6 Momentary coastline evolution

The momentary coastline (MKL), defined in subsection 3.2.2, gives insight in the advance and retreat of the coastline. Figure 69 indicates that the implemented nourishment scheme was successful at maintaining the coastline in the past three decades. The central coastline of Domburg and the west and east stretches advance. It is seen that the MKL position at Domburg, between transects 1612-1489 shows a seaward protrusion. The west coast advances faster relative to the central and east stretches as a consequence of periodic nourishments. Thereupon, the seaward protrusion at Domburg and consequently the transport gradients are reduced.
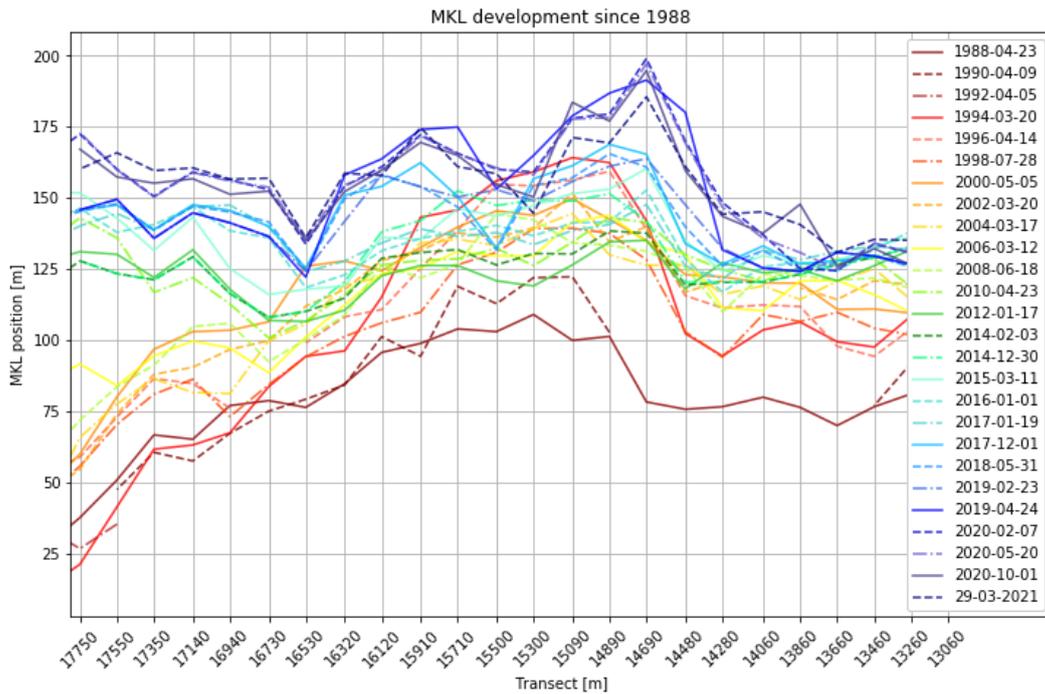
Figure 69: The MKL development between transects 1775-1306 in the period 1988-2020. Domburg is located near transects 1632-1448.

Momentary coastline T_0

Considering the MKL without the influence of nourishments, the period 1982-1988 is regarded. Before the coast was subject to large frequent nourishments, the MKL positions show fluctuations in the order of 10m with, on average, a slowly retreating trend of 0.4m/yr at the central section while the west and east stretches show no visible trend (Figure 70).
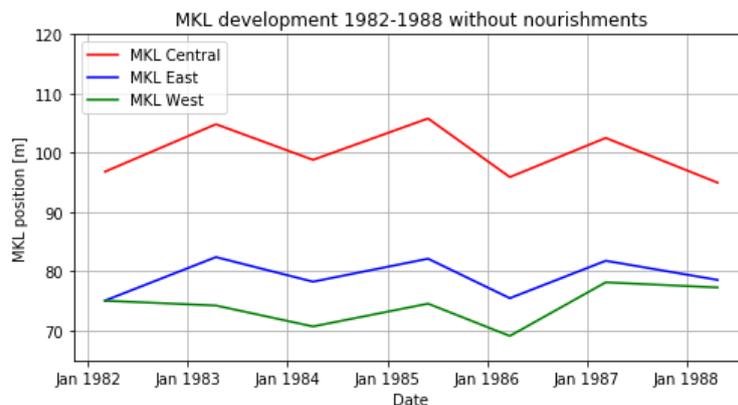
Figure 70: Average momentary coastline development in the period 1982-1988, before large scale sand nourishments were applied. The average MKL development of the central transects 1632-1448 is given in [red]. The adjacent coastlines, transects 1428-1306 to the east and 1694-1653 to the west are portrayed in [blue] and [green] respectively.

Momentary coastline T_1

The momentary coastline response after the 2014 beach nourishment (T_0) is depicted in Figure 71. The nourishment effectively increases the MKL position with 14.6m on average. However, the nourished transects quickly retreat 6.7m in the first year and the year thereafter shows a more gradual retreat of 1.2m. Simultaneously, the eastern coastline shows a rapid advance shortly after construction but remains stationary in the period hereafter. Likely, this is a consequence of the spreading of the nourished sand in downdrift direction. Looking at

the west adjacent coastline, a remarkable increase of 22.5m is observed in 2 years' time. It is likely that this increase is mainly caused by the large beach nourishment at the Westkappelse Zeedijk in Jan 2015 which distributes sand in downstream direction.
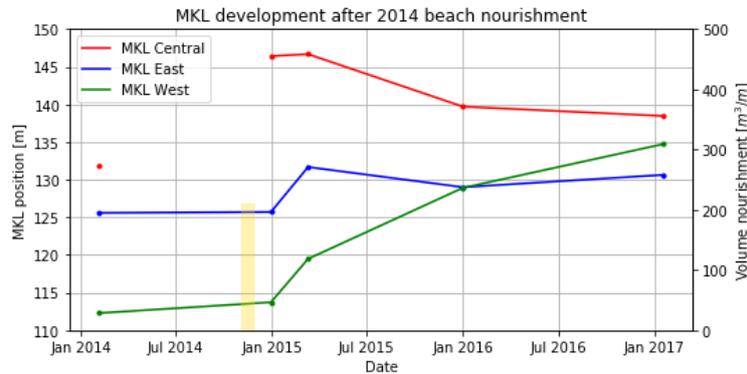
Figure 71: Momentary coastline development after the 2014 beach nourishment.

The MKL retreats with a rate of 4.0m/yr, 3.8 m/yr, 4.0 m/yr for respectively the 2004, 2008 and 2014 beach nourishments, based on 2.5-3 years of data after construction. On average, the MKL retreats with 3.9m/yr for beach nourishments.

Momentary coastline T_2

As a consequence of the 2017 shoreface nourishment(T_2), the MKL position increases with 17.5m on average (Figure 72). Remarkably, in the first year, the MKL shows little variation and remains at the same position on average. Meanwhile, a slight retreat of 3m of the adjacent west coastline is observed. The east downdrift coastline remains stationary.
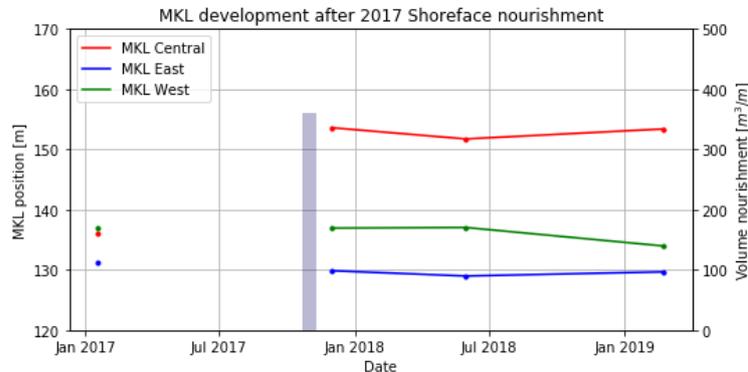
Figure 72: Momentary coastline development after the 2017 shoreface nourishment and before the 2019 beach nourishment is placed.

Momentary coastline T_3

Succeeding the shoreface nourishment, a beach nourishment was implemented (T_3), which advances the central coastline with 19.2m. Hereafter, the MKL decreases gradually with 4.3m/yr. The downdrift east coastline slowly advances after the 2019 nourishment with 3.7m/yr, which can mainly be contributed to the spreading of the beach and to some extent to the shoreface nourishment. The west adjacent coastline shows a stronger initial advance of 14.4m. Contemporary, a nourishment conducted at the Westkappelse Zeedijk contributes to the advance. Thereafter, the western coastline shows some variation but remains stationary.
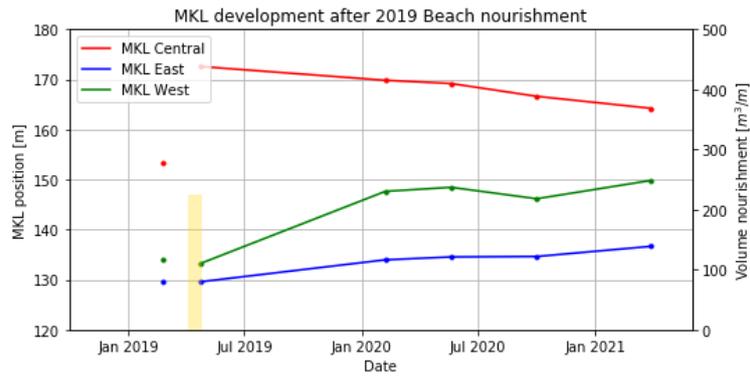
Figure 73: Momentary coastline development after the 2019 shoreface nourishment while the 2017 shoreface nourishment is still evident in the coastal profile.

In conclusion, Table 13 provides an overview of MKL rate of change for different nourishment scenarios. Notably, the presence of a shoreface nourishment does not decrease the MKL retreat after a beach nourishment (T_3) and it can be argued that it is slightly accelerated.

Table 13: Average rate of MKL change for different nourishment scenarios.

Nourishment strategy	MKL change [m/yr]
T_0	-0.4
T_1	-3.9
T_2	0
T_3	-4.3

4.2 Modelled hydrodynamic and morphological changes

This section focusses on the morphostatic numerical model output, which was described in chapter 3.3. The effects of three nourishment strategies on the hydrodynamics and sediment transport patterns are compared to a base case without a nourishment. The nourishment strategies are a beach, a shoreface and a combined beach and shoreface nourishment. The wave height and direction, currents, dissipation, and sediment transports are analysed in respective order. The results per wave condition are averaged in time over one tidal cycle, while the year-averaged results are an ensemble of weighted output per wave condition.

4.2.1 Wave height and direction

Waves are one of the main drivers of sediment transport, and so this subsection deals with the influence of different nourishment strategies on the significant wave height. The effect under a selection of mild and storm conditions is examined, including normal and oblique incoming waves. Thereupon, the influence on the year averaged wave height is examined.

Wave transformation under different wave conditions

The presence of a shoreface bar influences the wave height reaching the Domburg coast for both mild and storm conditions. For near-normally incident non-breaking waves, the wave height is increased over and behind the shoreface bar with 0.05m (Figure 74 c2, c5). Whereas the shoreface bar is less pronounced, at transect 1550, the wave height is reduced by 0.05m. For wave heights of 1.99m and 2.80m during storm conditions, the wave height is reduced by 0.08m and 0.25m respectively (Figure 74 c8, c10). It must be noted that to the east of transect 1448, the wave height is reduced for daily and storm conditions in the order of 0.03-0.10m. This effect is not observed to the west of the nourishment.

| c2) H_s=0.64m, Θ=342°, T_p=5.8s | c5) H_s=1.33m, Θ=328°, T_p=6.5s | c8) H_s=1.99m, Θ=334°, T_p=7.2s | c10) H_s=2.80m, Θ=335°, T_p=8.0s |
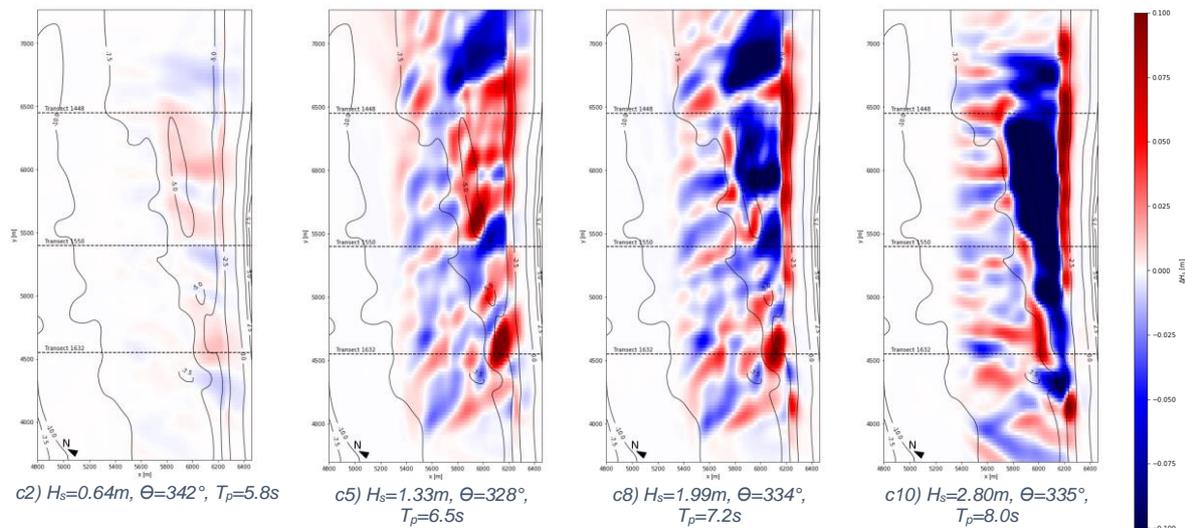
Figure 74: Difference in wave height for T_2-T_0 for four near-normally incident wave classes to examine the effect of a shore parallel bar. The shore normal is at 330° and the depth contours are given with 2.5m intervals.

Similarly, for oblique non-breaking waves, a wave height increment in the order of 0.05m is observed at the bar's leeside (Figure 75 c1, c4). During storm conditions, shoaling increases the wave height at the seaward side of the shoreface bar while the breaking of waves creates a shadow zone at the leeside (Figure 75 c7, c9). The reduction of storm waves in the leeside is 0.15m for an offshore significant wave height of 2.46m. Again, the wave height is reduced to the east of the nourishment but to a lesser extent. On the contrary, this effect can now also be observed at the west side of the nourishment.

Hence, the shoreface nourishment slightly increases wave heights during daily conditions on and at the leeside of the shoreface bar. During storm conditions, the wave height is reduced to a small extent at the leeside. Meanwhile, wave heights are reduced at the adjacent shorelines.


c1) H_s=0.62m, Θ=267°, T_p=4.7s   c4) H_s=1.24m, Θ=284°, T_p=5.8s   c7) H_s=1.76m, Θ=272°, T_p=6.5s   c9) H_s=2.46m, Θ=283°, T_p=7.2s
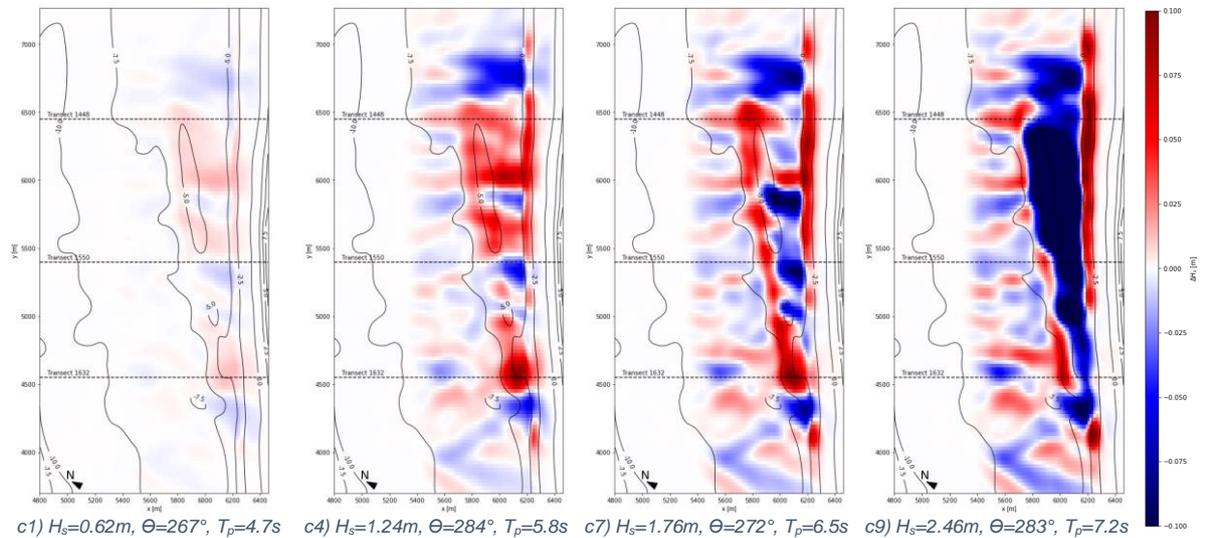
Figure 75: Difference in wave height for T_2-T_0 for four obliquely incident wave classes to examine the effect of a shore parallel bar.

Remarkably, a red zone between the -5m and -2.5m contour lines is visible in all figures. This is a local deviation in the modelled bathymetries and not an increment of the nearshore wave height due to the shoreface nourishment. Additionally, the model bathymetries are based on different surveys in time, and so the variability seaward of the nourishment is caused by the passage of transverse bars.

Annual wave height

The mean annual cross-shore wave height is marginally influenced by the presence of a shoreface nourishment. Transect 1591 shows small deviations at the bar crest in the order of 0.01m, but the breaking wave height at the edge of the surf zone (6250m) is not affected for all nourishment strategies (Figure 76a). Likewise, transect 1530 portrays identical breaking wave heights at the edge of the surf zone (6250m), but an increase of 0.03m is observed at the bar crest which decreases again due to breaking of the largest waves (Figure 76b). On the
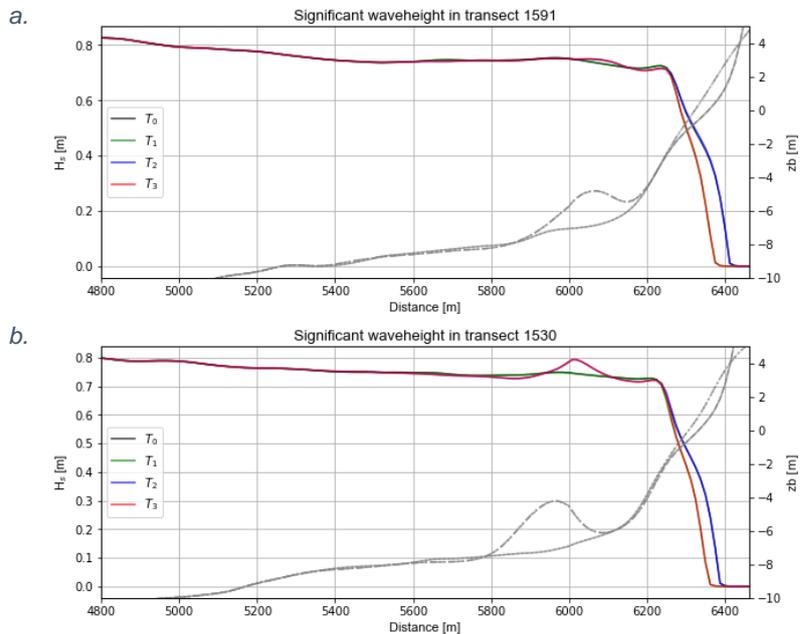
contrary, the breaking wave height for transect 1489 at 6300m is increased due to the presence of the shoreface bar (Figure 76c). Furthermore, if a beach nourishment is present (T_1 and T_3), it is observed that the wave energy is dissipated over a shorter stretch as the wave height decreases more gradual for T_0 and T_2.
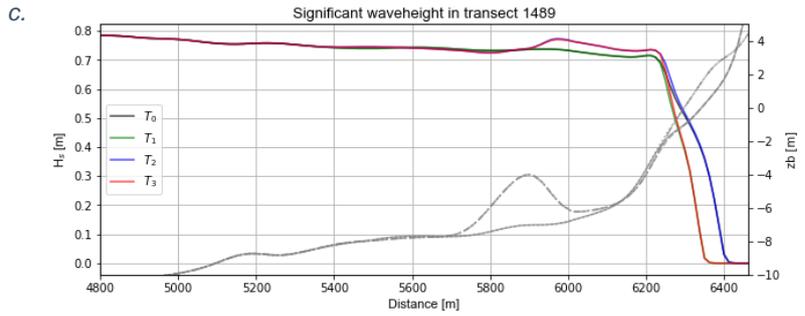
Figure 76: Annual cross-shore significant wave height for transects a) 1673, b) 1591, c) 1550, d) 1489, and e) 1406. On the secondary y-axis, the depth profiles are depicted with or without the beach and shoreface nourishments.

Figure 77 shows the influence of nourishments on the average annual significant wave height. The construction of a beach nourishment does not influence the wave height outside the nourished area (Figure 77a). The differences to the east and west of the nourishment are due to small differences in model bathymetry. The breaking wave height is not increased due to the nourishment, but the waves are dissipated over a smaller distance as the nourished beach is steeper.

A shoreface nourishment, whether or not combined with a beach nourishment (Figure 77b, c), increases the year averaged wave height in the order of 0.02m in the leeside. Notably, at the tips and at transect 1550 a depression of the wave height is observed.

a) T_1-T_0 b) T_2-T_0 c) T_3-T_1
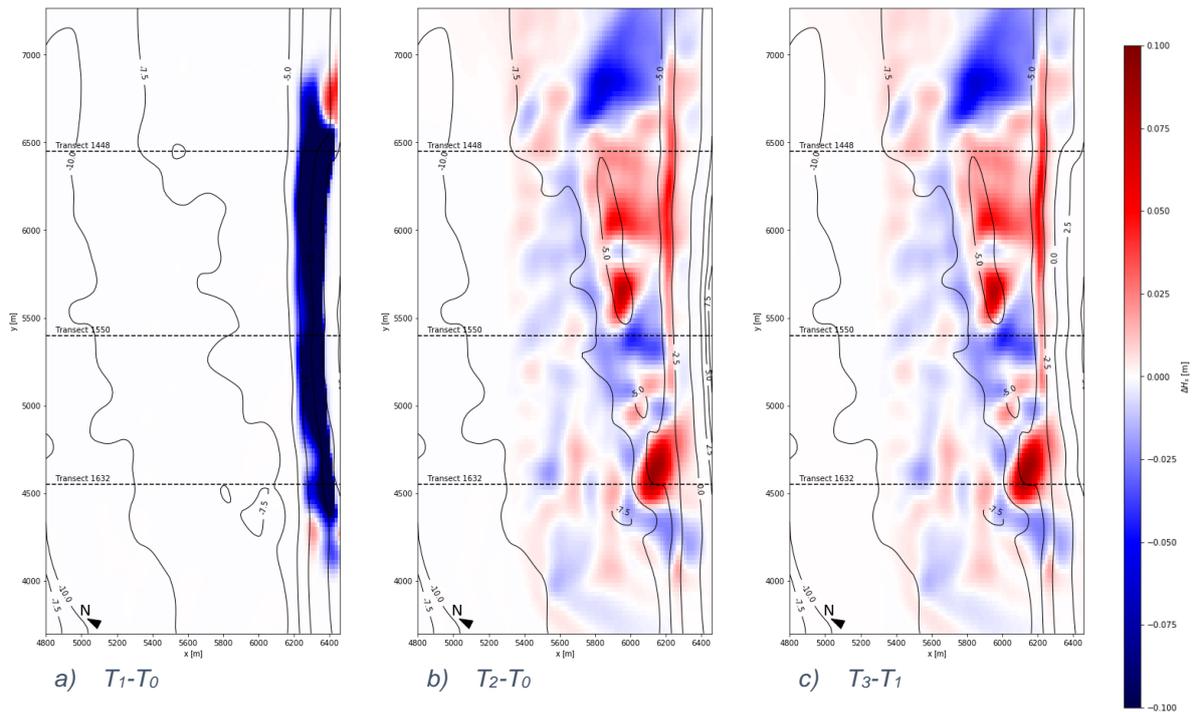
Figure 77: Annual significant wave height changes for the presence of a nourishment. The effect on the wave height due to a: a) beach nourishment: T_1-T_0. b) shoreface nourishment: T_2-T_0. c) combined beach and shoreface nourishment to only a beach nourishment: T_3-T_1.

Wave direction

The presence of the shoreface bar has a marginal local effect on the wave direction.

Considering year-averaged conditions at the west bar segment, the wave direction is changed in shore-normal direction at the bar crest. But as the water depth only slightly decreases hereafter, refraction is limited and no decrease in wave propagation direction is seen (Figure 78a). Therefore, waves reaching the beach at the west segment are relatively more shore normal.

In transect 1530 (Figure 78b), the mean wave direction increases and decreases as waves propagate over the shoreface bar. Remarkably, the wave direction in the trough zone is directed more oblique than further offshore.

At the east bar segment, incoming waves refract over the bar (Figure 78c).

The first transect to the east of the nourishment shows a significant deviation while no bar is present (Figure 78d). The wave direction altered more shore normally at the 5700m, roughly the cross-shore location of the bar crest in transect 1448.

Closer to the shoreline, the wave directions for all nourishment strategies show similar angles, and so the shoreface bar has little influence on the wave direction at the shoreline. Therefore, locally, refraction causes slight wave direction changes, where the mean direction at the coastline is not changed for the east shoreface bar.
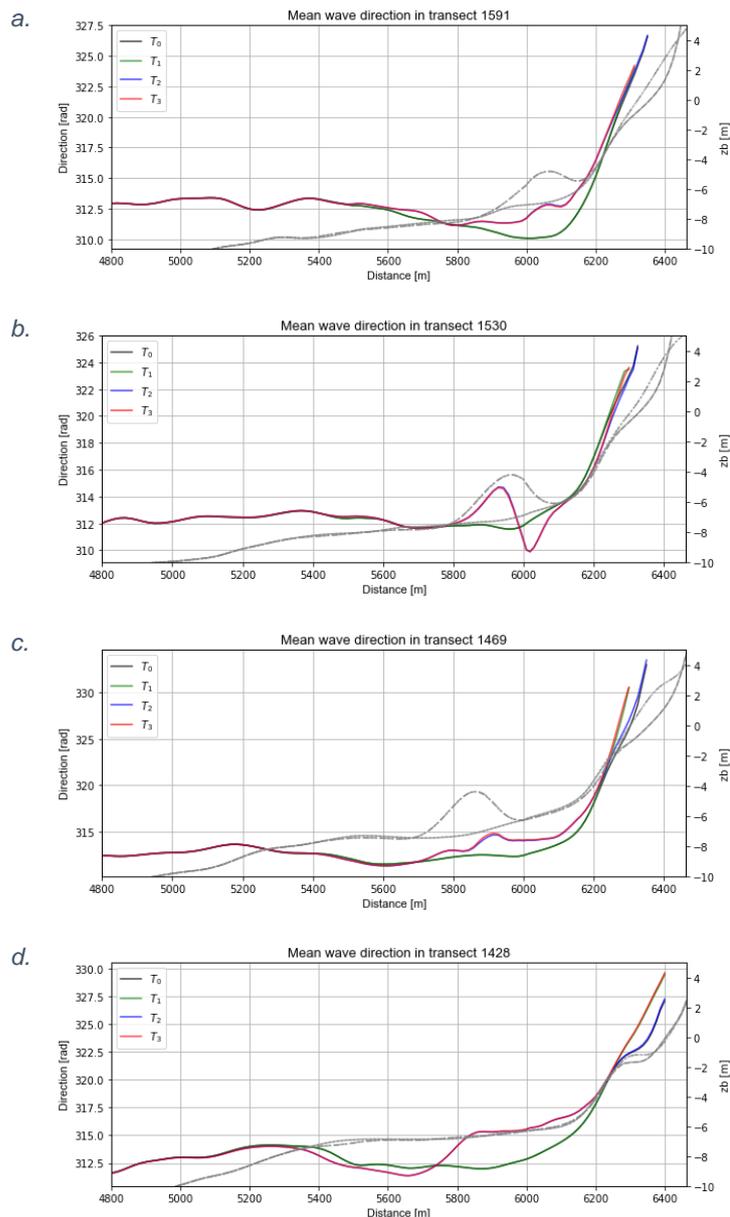
Figure 78: Year averaged wave directions for transects 1591, 1530, 1469, and 1428 [°].

Conclusion wave height and direction

To sum up, it is observed that a beach nourishment has no significant influence on the wave height and direction outside the nourished zone.

On the contrary, a shoreface nourishment causes a small increment of wave heights at the leeside during mild conditions, while the wave height is reduced at the leeside during storm conditions as a result of breaking of larger waves on the shoreface bar. Year averaged, non-breaking conditions have a larger impact on the wave height and thus no reduction in leeside wave height is found. Notably, a wave height reduction is found at the adjacent east coastline. The wave direction is altered on the shoreface bar, but no significant change in wave propagation direction at the beach is found.

4.2.2 Currents

This subsection starts with an overview of currents around the shoreface bar for near-normal and oblique incident waves for a range of mild to storm wave conditions. Next, the year-averaged currents for different bathymetries are highlighted. Then, the cross-shore and alongshore currents are presented for five transects. Last, the main observations are summed up.

Oblique and normally incident waves on a shoreface nourishment

First, the currents under oblique incoming waves of approximately 55° from the SWW are considered (Figure 79). For energetic non-breaking waves, c4 and c7, the cross-shore velocity at the leeside is decreased. Also, at the downdrift end of the shoreface bar, a decrease in alongshore velocity is seen between y= 6400-7000. Contrarily, the alongshore velocity is increased at the seaward side of the shoreface bar. In storm conditions, c9, onshore flow over the bar crest at transects 1509-1469 which is deflected in alongshore direction. At transect 1550, a decrease in cross-shore velocity is observed, indicating a return flow over the shallower part of the shoreface bar.
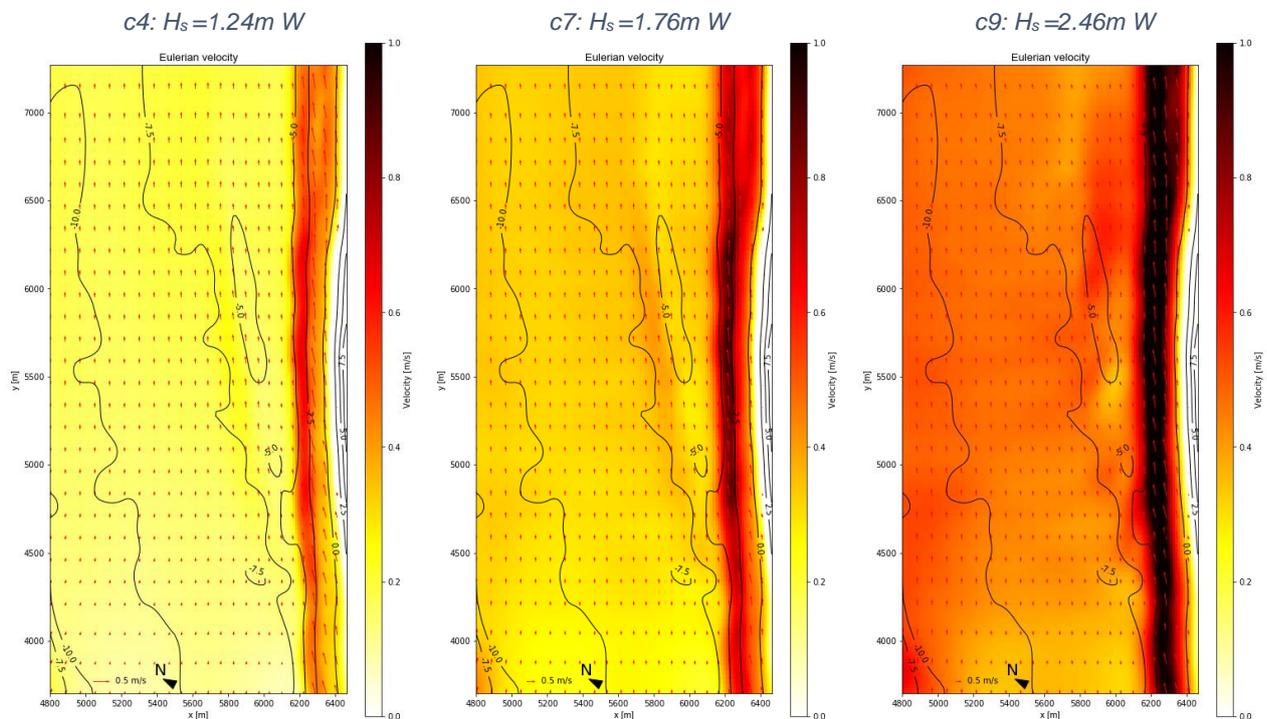
Figure 79: Magnitude of the currents under oblique (272-284°) wave conditions around a shoreface nourishment (T_2).

Second, the currents for normally incident waves from the NW are treated (Figure 80). For energetic non-breaking waves, c5 and c8, the alongshore velocity seaward of the shoreface bar is increased. In the leeside, an eastward current is formed which is directed offshore near transects 1550-1632. For storm conditions, c10, return flows near transect 1448 and on the west bar segment, transects 1550-1632, are observed.
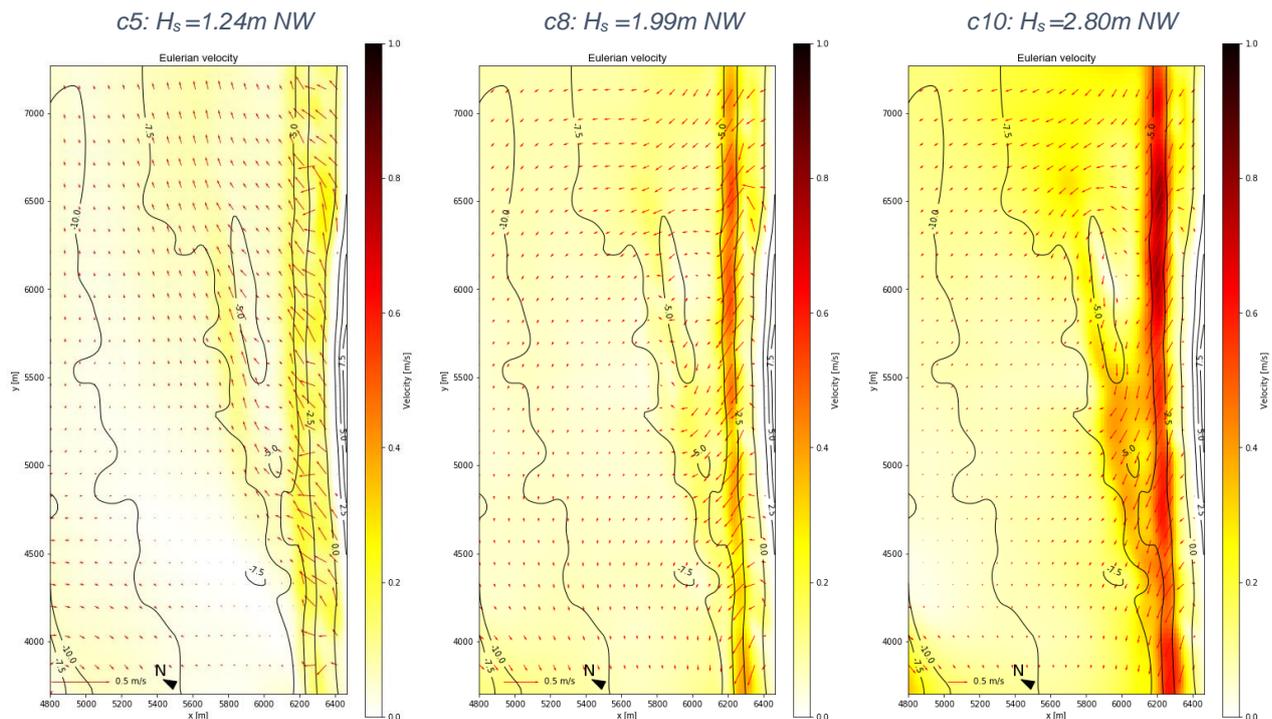
Figure 80:Currents under normally incident (328-335°) wave conditions around a shoreface nourishment (T2).

Year averaged currents

The year averaged currents, a combination of mild to more energetic storm conditions for normally and oblique waves with their probability of occurrence, provide insight in the alternation of stream patterns due to a nourishment. Appendix D.2 presents the difference plots for year-averaged currents between nourishment strategies.

For a shore without a nourishment, T_0, an increasing velocity is observed from the west to the east at both deeper water and near the shore (Figure 81). At the -10m depth contour, the net velocity increases from 0m/s to 0.1m/s. The wave-driven alongshore current in the surf zone causes a nearshore increment, being two to three times larger than the tidal net velocity at the -10m contour.

The influence of a beach nourishment, T_1, on current patterns limits itself to the nourished zone (Figure 82). At the west of the nourishment, the alongshore velocity in the surf zone has slightly decreased while an increase is observed in the east.
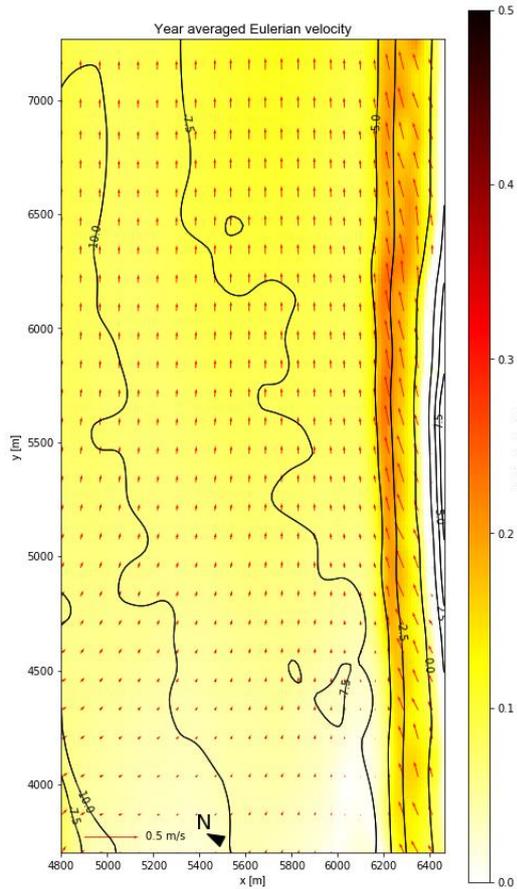
Figure 81: The year averaged Eulerian velocity for T_0, without a nourishment.
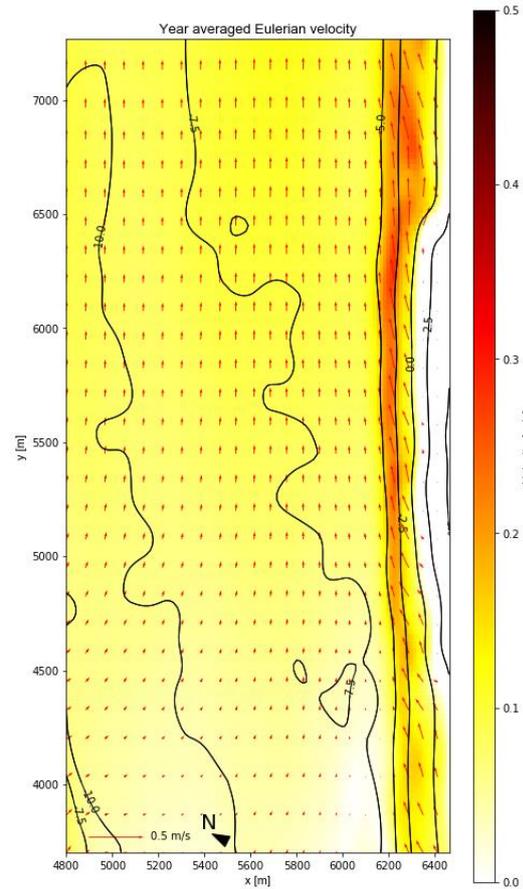
Figure 82: The year averaged Eulerian velocity for T_1, with a beach nourishment.

As a result of a shoreface nourishment, T_2, mainly the alongshore velocity seaward of the shoreface bar increases, while this decreases at the crest and in the leeside (Figure 83). Also, the velocity is increased at transect 1632 where the tidal flow encounters the shoreface bar. At the downdrift shoreline where the shoreface bar ends, a reduction in alongshore velocity is seen that is still evident 800m eastward.

The year averaged velocities for a combined shoreface and beach nourishment, T_3, are similar to T_2 (Figure 84).
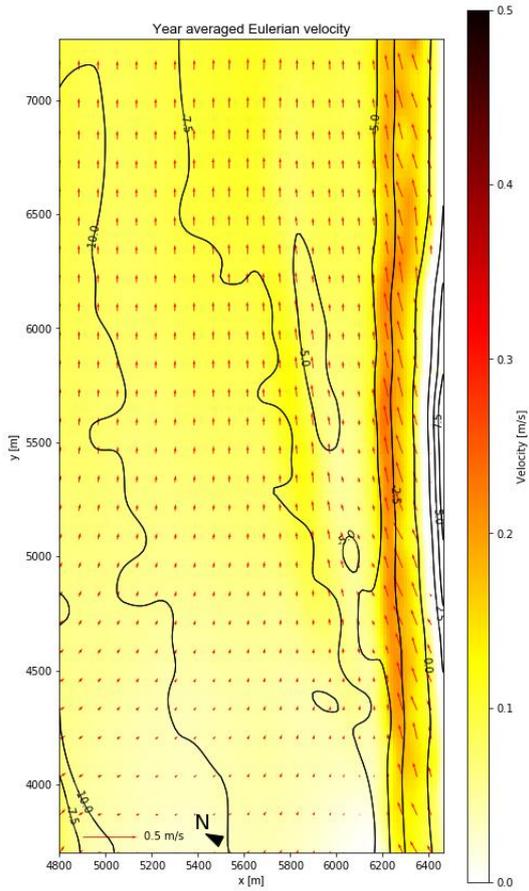
Figure 83: The year averaged Eulerian velocity for T_2, with a shoreface nourishment.
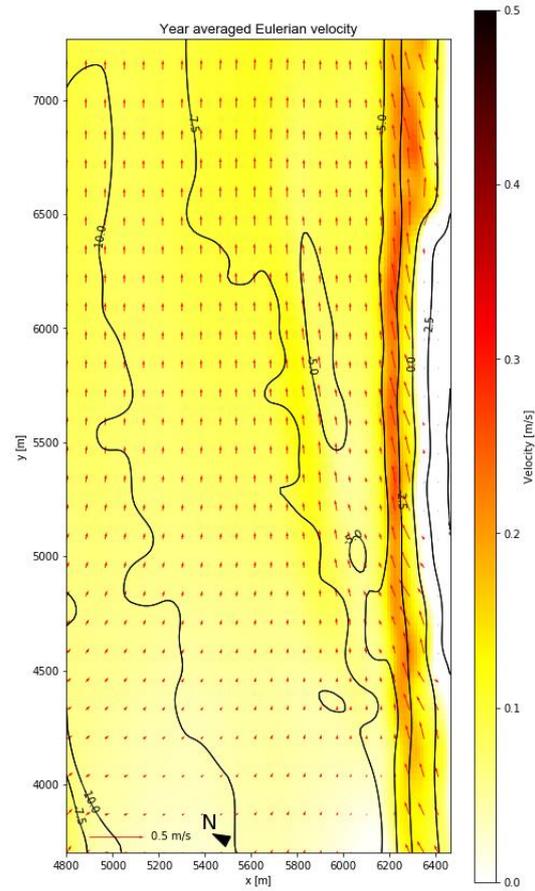
Figure 84: The year averaged Eulerian velocity for T_3, with a combined beach and shoreface nourishment.

Cross-shore currents

The year-averaged cross-shore currents are altered mainly due to the presence of a shoreface nourishment.

At the west adjacent coastline, a higher landward directed velocity is observed close to the coastline if a shoreface nourishment is present (Figure 85a).

The presence of a shoreface bar causes an increased offshore directed flow at the seaward side of the shoreface bar (Figure 85b, c, d). In the leeside, the magnitude of the offshore directed velocity decreases again. The influence of a beach nourishment is limited at the shoreface while, on the beach, it varies per transect.

At the east adjacent coastline, no effect of the shoreface bar on the cross-shore velocities are observed (Figure 85e). However, an offshore directed current of 0.25m/s arises for energetic normally incident wave conditions near transect 1448, at the east end of the shoreface bar. This indicates the formation of a return current. Similarly, an offshore directed current of 0.2m/s is found near transect 1550 for storm conditions.

a.

b.

c.

d.

e.
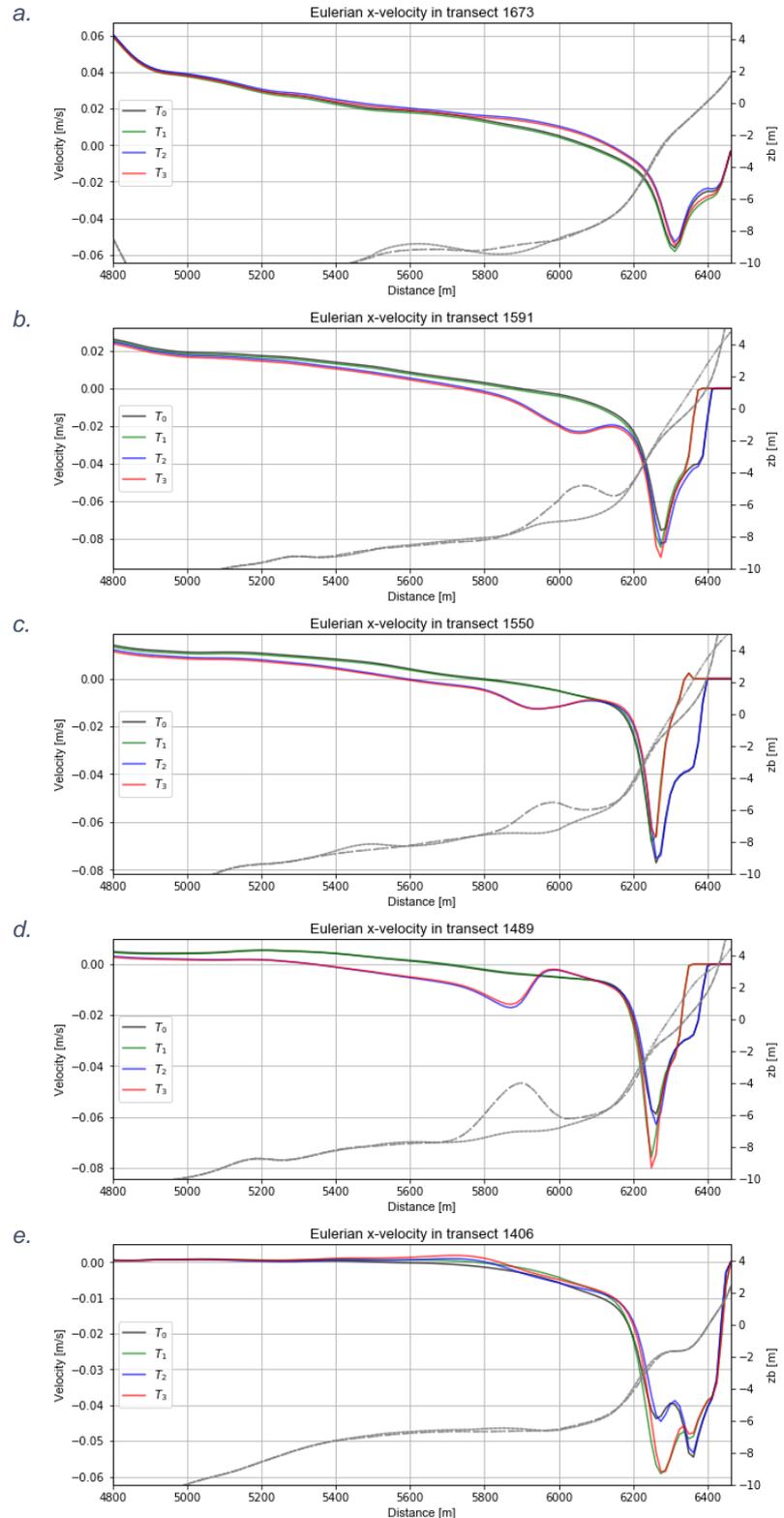
Figure 85: Cross-shore profiles of year-averaged cross-shore current velocities at transects 1673, 1591, 1550, 1489, 1406 under four different nourishment strategies.

Alongshore currents

The year-averaged alongshore currents are altered under the influence of nourishments. Upstream of the nourishments, the nearshore velocity is higher due to the presence of a shoreface nourishment (Figure 86a). At transect 1632, where the shoreface bar starts, the average velocity increases with 0.025m/s in the nearshore. Corresponding, at the seaward side of the shoreface bar, an increment in alongshore velocity is observed (Figure 86b, c, d). Differently, landward of the shoreface bar, a reduction in alongshore velocity is found. Meanwhile, a beach nourishment, increases the year-averaged maximum velocity near the beach for transects 1632-1448.
Up to 800m in downstream direction, a reduction at the cross-shore position of the bar is found even though no shoreface bar is present in the profile (Figure 86e).

Comparing the alongshore velocity of T_0 and T_2 in Figure 87 and Figure 88, it is revealed that a shoreface nourishment increases the velocity at the adjacent west coast and the west side of the nourishment (4500-5700m) for daily conditions c1 and c2. The same holds for T_1 and T_3. Contrarily, a shoreface nourishment decreases the velocity at the adjacent west coast (3800-4500m) and the east nourishment (5700-6500m). Remarkably, a beach nourishment reduces the current at the nourished transects for c1 (Figure 87). For wave conditions c2, the influence of a beach nourishment is marginal (Figure 88).

a.

b.

c.

d.

e.
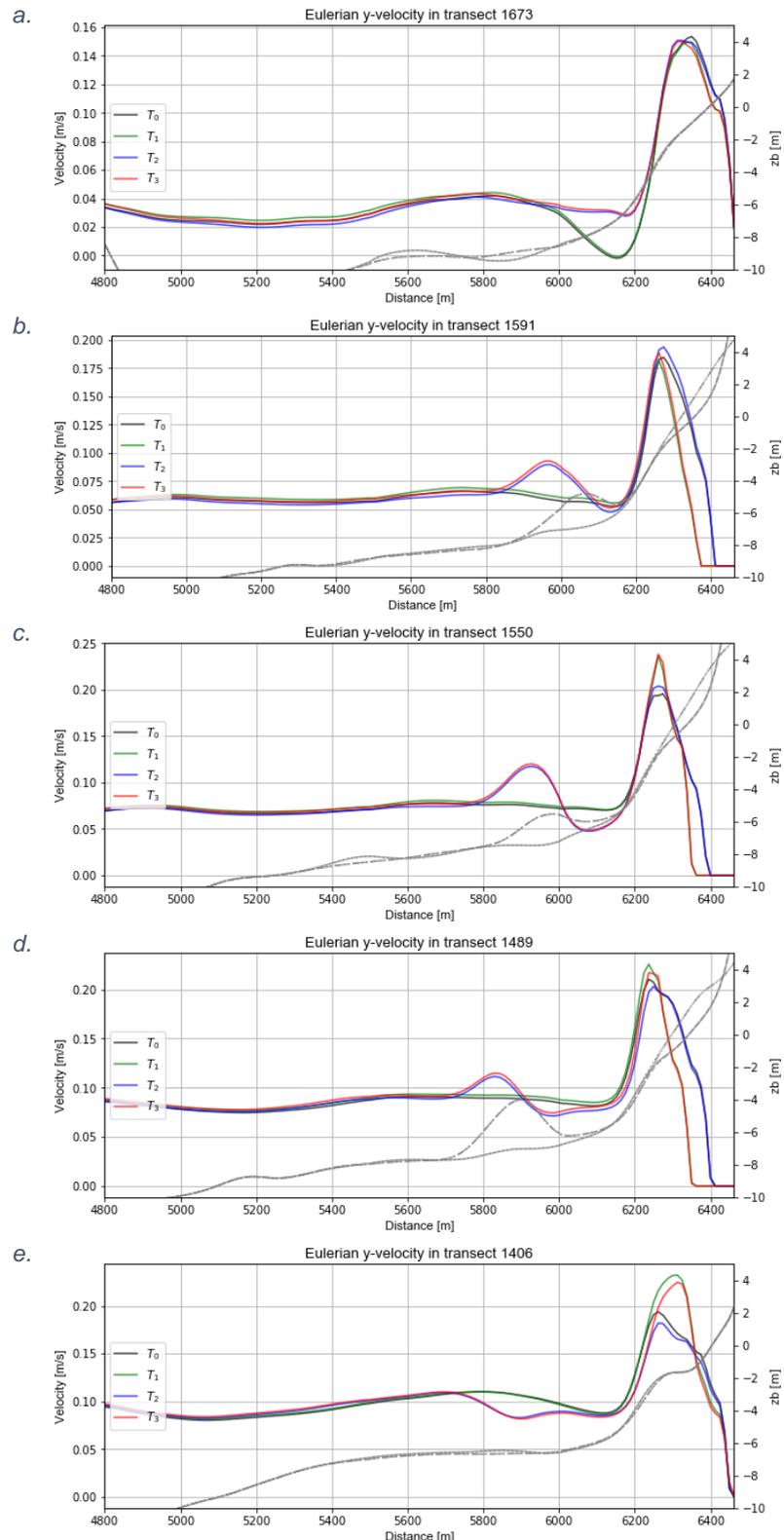
d. Figure 86: Cross-shore profiles of year-averaged alongshore current velocities at transects 1673, 1591, 1550, 1489, 1406 under four different nourishment strategies.
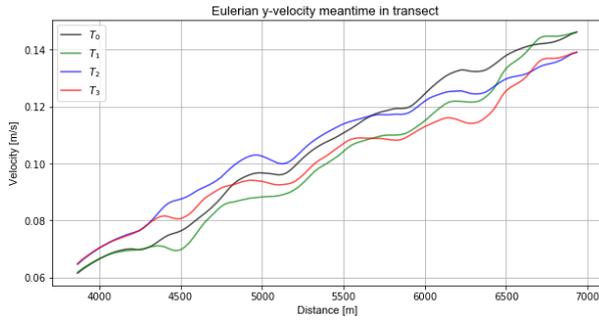
Figure 87: Mean alongshore current for wave condition c1: H_s=0.62m, Θ=267°, T_p=4.7s in the zone from the dune foot to 1000m offshore.
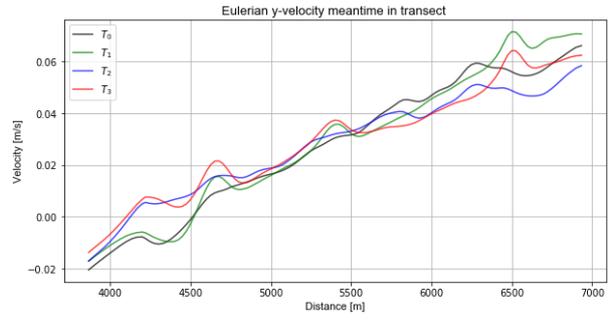
Figure 88: Mean alongshore current for wave condition c2: Hs=0.64m, Θ=342°, Tp=5.8s in the zone from the dune foot to 1000m offshore.

4.2.3 Dissipation

This subsection first describes the dissipation on the shoreface bar and the total dissipation under storm conditions. Then, a look at year-averaged cross-sections is taken.

Dissipation in storm conditions

Looking at storm wave conditions c9 and c10, with significant wave heights of 2.46m and 2.80m and from the SWW and NNW respectively, the shoreface bar dissipates a significant part of the incoming wave energy (Appendix D.1).

For the oblique incoming storm waves from the west, 8.5% of the incoming energy is dissipated on the bar. Meanwhile, the total dissipated energy is 2.3% higher if a shoreface bar is present. For normally incident storm waves, 19.6% of the incoming energy is dissipated at the bar. These conditions show an increment of 3.1% in total dissipated energy for T_2 and T_3 compared to T_0 and T_1. Remarkably, the increment in total dissipated energy is not observed in every transect. Around transect 1550, where the shoreface bar is less pronounced, the dissipated energy is higher for T_0 and T_1 than for T_2 and T_3.

Year-averaged dissipation

The year averaged dissipation on the shoreface bar is limited (Figure 89). It can be seen that a small portion of the wave energy is dissipated on the shoreface bar. Remarkably, even though a part of the wave energy is dissipated at the bar, the pattern of wave dissipation at the beach(6200-6400m) is not reduced due to shoreface bar.
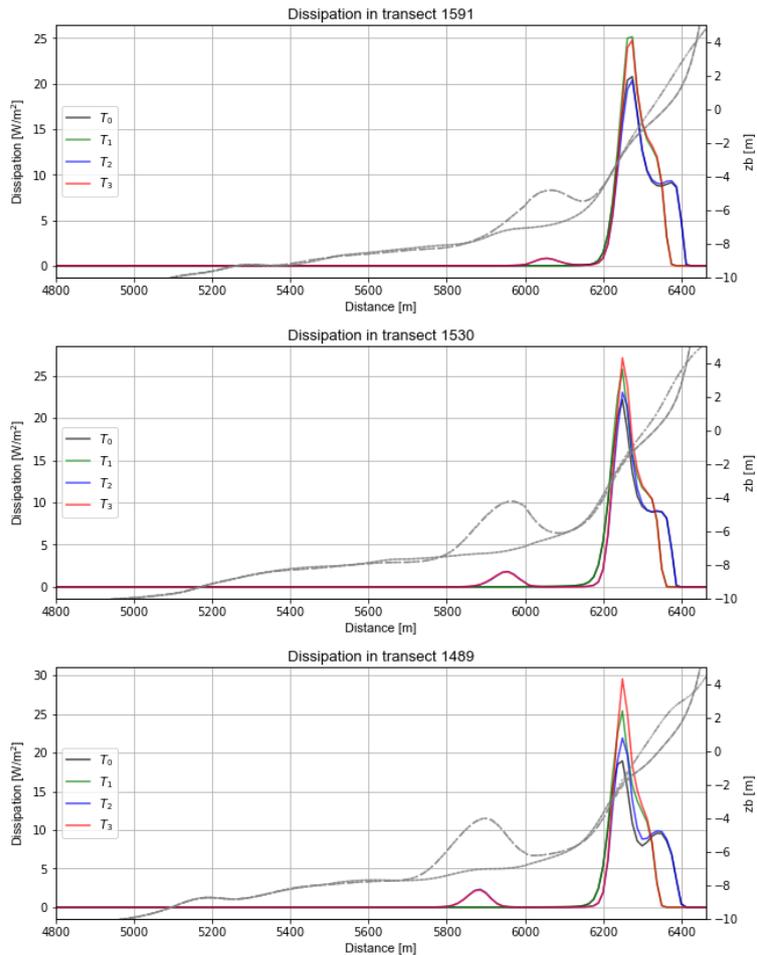

Figure 89: Average annual dissipation of energy at transects 1591, 1530, and 1489.

72

4.2.4   Sediment transport

This subsection elaborates on the year-averaged cross-shore transport, the year-averaged alongshore transport, the alongshore transport gradients and an overview of the sediment transport patterns per nourishment strategy.

Year-averaged cross-shore sediment transport

The following is observed on the shoreface.

At the tip of the shoreface bar, in transect 1632, an increase in offshore sediment transport is found seaward and at the shoreface bar compared to T_0 and T_1 (Figure 90a). A return current at the shoreface bar enhances the offshore sediment transport at the tip of the nourishment.

Also, offshore directed transport is enhanced at the seaward side of the bar (Figure 90b, c, d). At the crest and landward of the bar's west segment, the offshore directed transport is relatively lower compared to bathymetries without shoreface bar (Figure 90b-6000-6200m). In transect 1550, with a low-lying bar crest, the offshore directed sediment transport is higher than in alongside transects (Figure 90c). On the east bar segment, the sediment transport is in landward direction (Figure 90d).

Seaward of the east end of the shoreface bar, the offshore directed transport is relatively lower (Figure 90e). Contrarily, at the landward side, the offshore directed transport is relatively higher.

While at the beach, less sediment is transported in landward direction on transects 1612-1571 and 1530-1469 as a result of a beach nourishment, T_1 and T_3, (Figure 90b, d). Near transects 1632, 1550, and 1448 this is observed.

a.

b.

c.

d.

e.
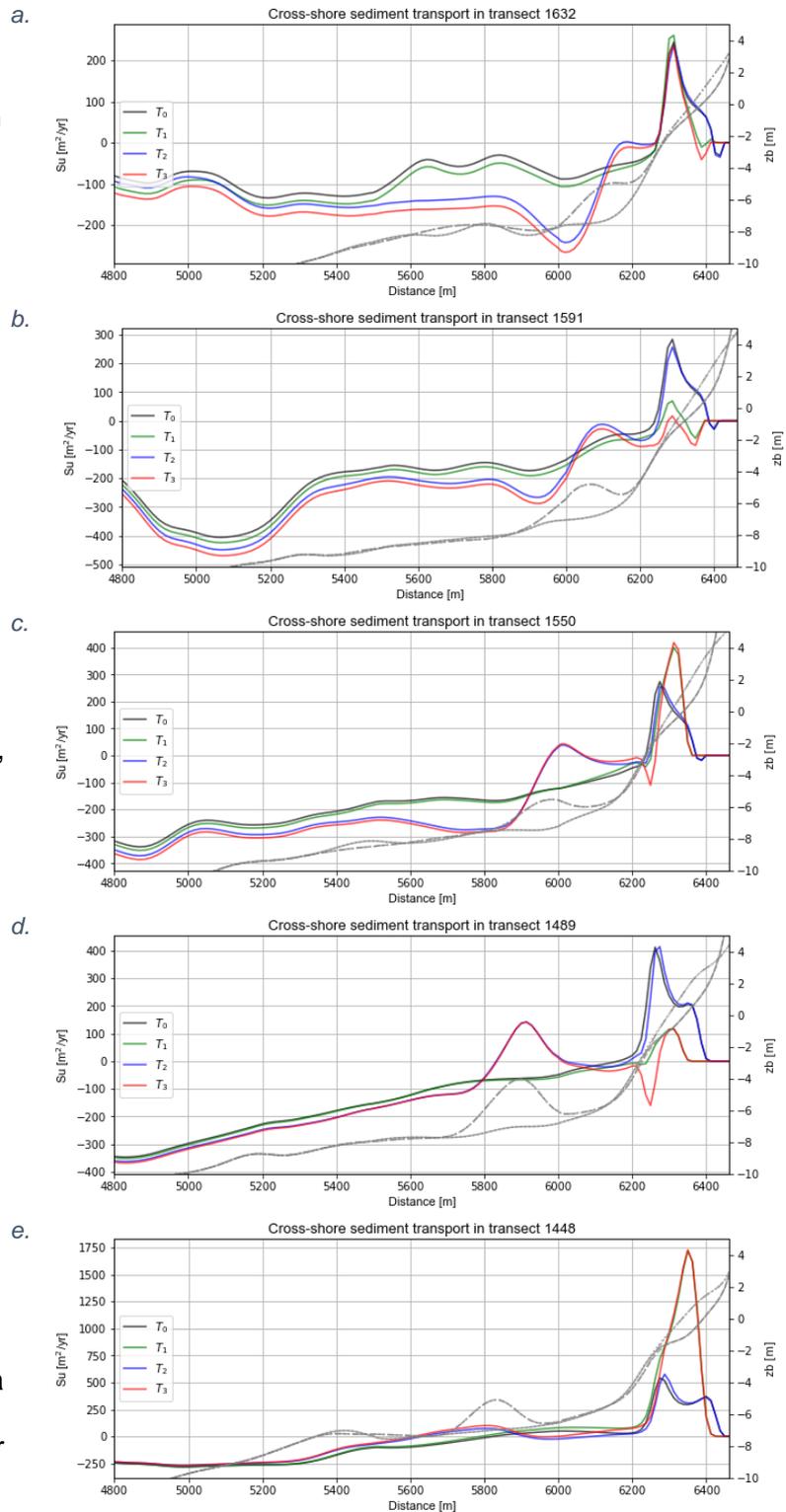
Figure 90: Year-averaged cross-shore sediment transport at the nourished transects 1632, 1591, 1550, 1489, 1448.

73

Alongshore sediment transport

The year-averaged alongshore sediment transport is significantly altered due to a shoreface bar, whereas the influence of a beach nourishment is marginal.

To the west of the nourished zone, the year averaged sediment transport is reduced on the shoreface due to the presence of a shoreface nourishment, while it is enhanced closer to the shoreline (Figure 91a).

At the west end of the shoreface bar, the sediment transport is enhanced on the bar. Moving further alongshore, the sediment transport at the seaward side of the bar and close to the beach is increased (Figure 91b, c, d). The increment reaches relatively far offshore as can be seen in transect 1489. Contrarily, the alongshore sediment transport is reduced in the trough zone in transects 1571-1448, (Figure 91c, d). Moreover, a combined nourishment, T_3, results in the largest alongshore sediment transport.

To the east of the nourishments, the alongshore sediment transport is reduced on the shoreface (Figure 91e).

Closer to the shoreline, the alongshore sediment transport is enhanced for transects 1571-1448 if a beach nourishment is present. (Figure 91c, d). The influence of a beach nourishment is marginal on the adjacent alongshore transport patterns (Figure 91a, e).
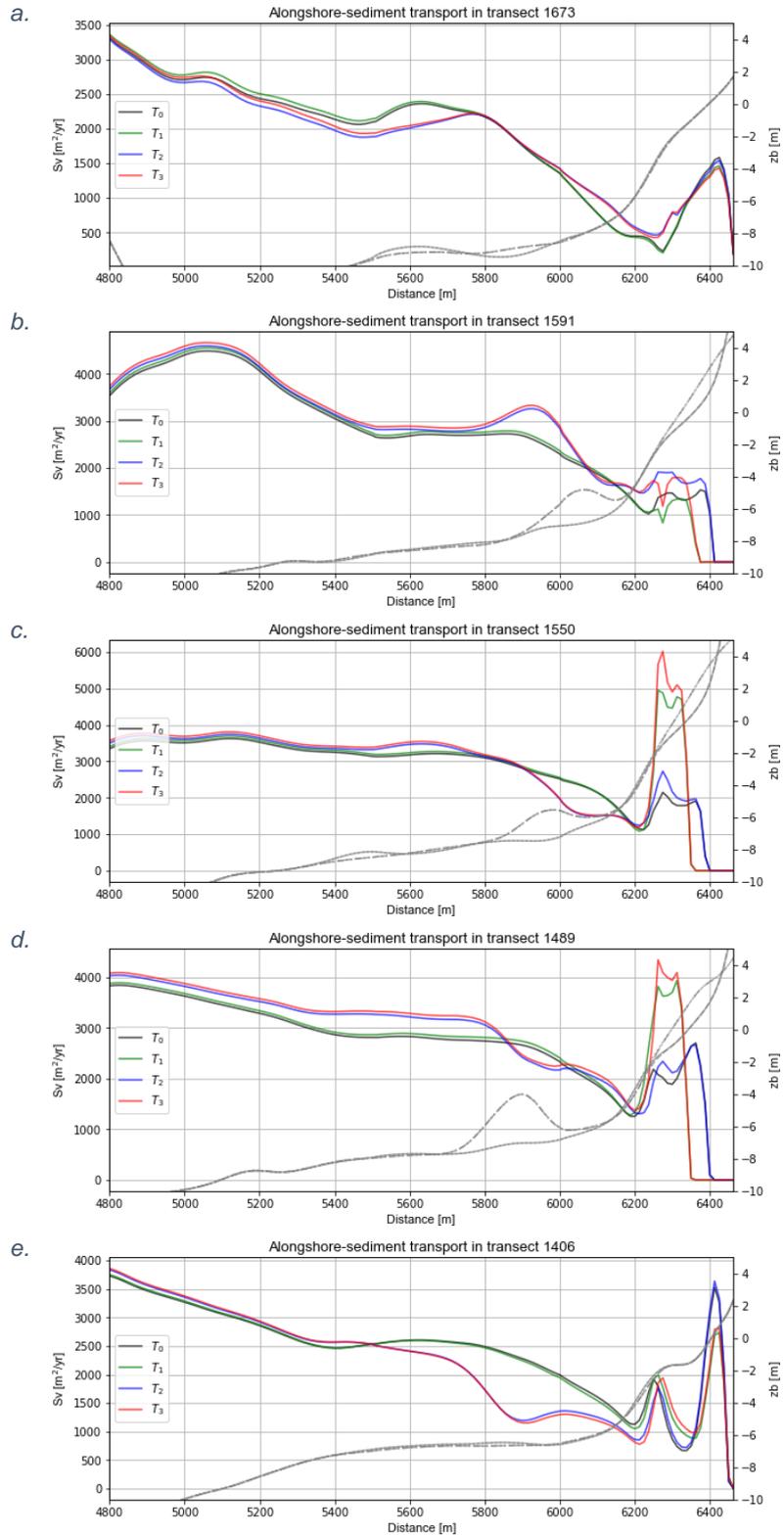
Figure 91: Year-averaged alongshore sediment transport at transects 1673, 1591, 1550, 1489, 1406.

74

Alongshore transport gradients

The alongshore mean sediment transport, between the dune foot and 1000m seaward, is presented for individual wave conditions.

For normally incident waves, c5, a positive gradient in sediment transport is observed at the upstream nourishment tip at 4000-4700m (Figure 92). It is seen that the nourishments increase the transport gradients, where the influence of a shoreface nourishment is larger than that of a beach nourishment. A large transport gradient is evident between 4000m and 4700, the start of the nourished section. The alongshore transport is approximately doubled in this transition zone. Between 4700-6300m, the alongshore sediment transport fluctuates around 1600m^3/m/yr. A beach nourishment causes large gradients around 5400m, while a shoreface nourishment causes an increment at 5700m. At the downstream end of the nourishments, at 6300-6800m, a negative gradient is present, indicating the deposition of sediment. A shoreface nourishment lowers the alongshore sediment transport at the downstream end with 30%. No such effect is seen for a beach nourishment.
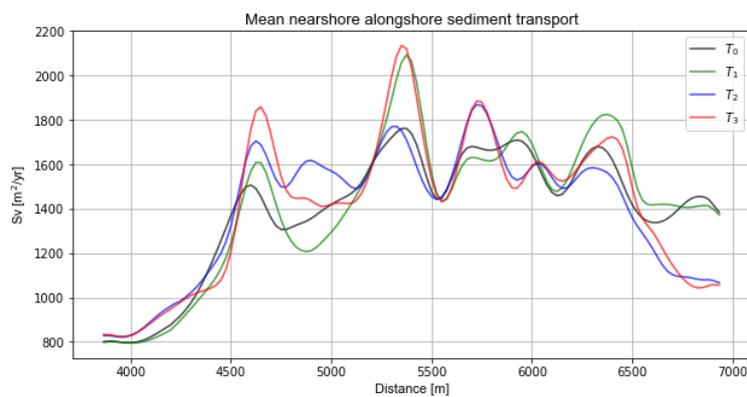
Figure 92: Mean alongshore sediment transport for wave condition c5: H_s=1.33m, Θ=328°, T_P=6.5s in the zone from the dune foot to 1000m offshore. Nourishments are placed between 4500-6500m.

Similarly, a positive gradient in the west and a negative gradient in the east are found for daily wave conditions c1 and c2 (Figure 93 and Figure 94). These gradients are increased due to a shoreface nourishment as the transport rate is increased near 4700m, while it is lowered downdrift (6500-7000m).

A beach nourishment slightly increases the alongshore sediment transport for daily conditions, independent of the presence of a shoreface bar (Figure 93 and Figure 94).
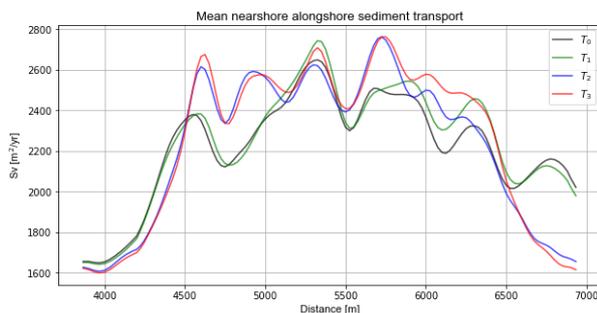

*Figure 93: Mean alongshore sediment transport for wave condition c1: H_s=0.62m, Θ=267°, T_P=4.7s in the zone from the dune foot to 1000m offshore.*
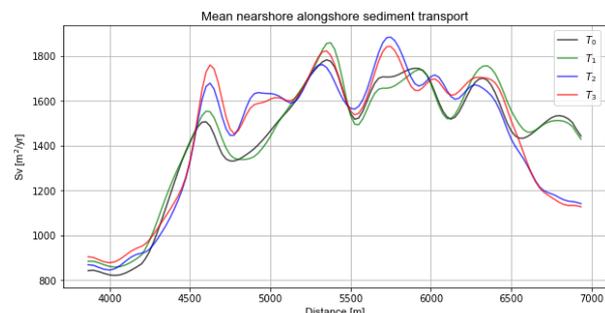
Figure 94: Mean alongshore sediment transport for wave condition c2: Hs=0.64m, Θ=342°, Tp=5.8s in the zone from the dune foot to 1000m offshore.

Year-averaged sediment transport

The transport patterns are altered as a result of nourishments. Appendix D.2 presents the difference plots for year-averaged currents between nourishment strategies.

The construction of a beach nourishment primarily increases the nearshore alongshore sediment transport. Figure 95 and Figure 96 illustrate this between the 0m and -5m contours, where the year averaged transport is approximately 50% higher at the central and east part of the nourishment, 5200-6500m. Notably, the sediment transport in the west nearshore zone is not distinctively increased, 4500-5200m.
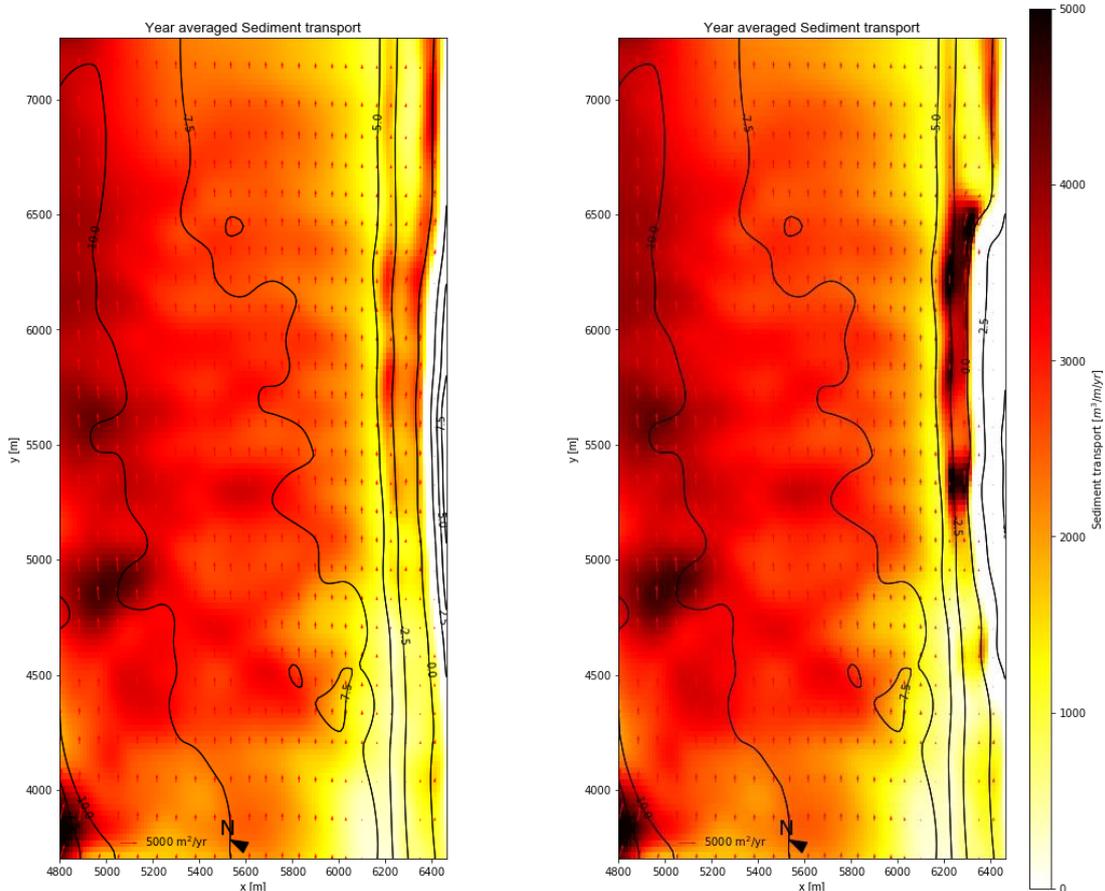

Figure 95: The year averaged sediment transport without a nourishment, T_0.

Figure 96: The year averaged sediment transport with a beach nourishment, T_1.

Contradictory, a shoreface nourishment drastically changes the sediment transport patterns at the shoreface (Figure 97). The alongshore sediment transport on the west adjacent shoreface is reduced. At the west nourishment tip between the shoreface bar and the beach, the alongshore sediment transport is increased. Seaward of the shoreface bar, this is increased significantly up to 1000m offshore from the bar. On the shoreface bar, relatively more landward sediment transport takes place. In the trough zone, the alongshore sediment transport is reduced, but no significant change is observed in the surf zone. At the east shoreface, the alongshore sediment transport is primarily reduced at the cross-shore position of the bar. At a combined beach and shoreface nourishment, T_3, a combination of the transport patterns for T_1 and T_2 are seen (Figure 98).
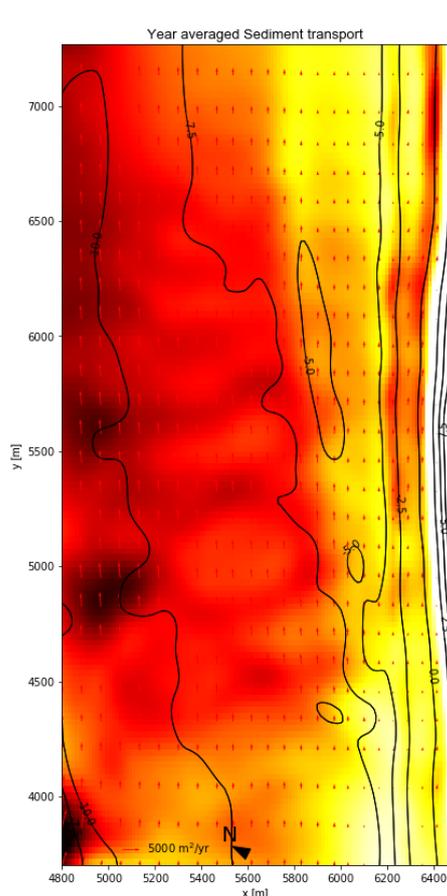
Figure 97: The year averaged sediment transport with a shoreface nourishment, T_2.
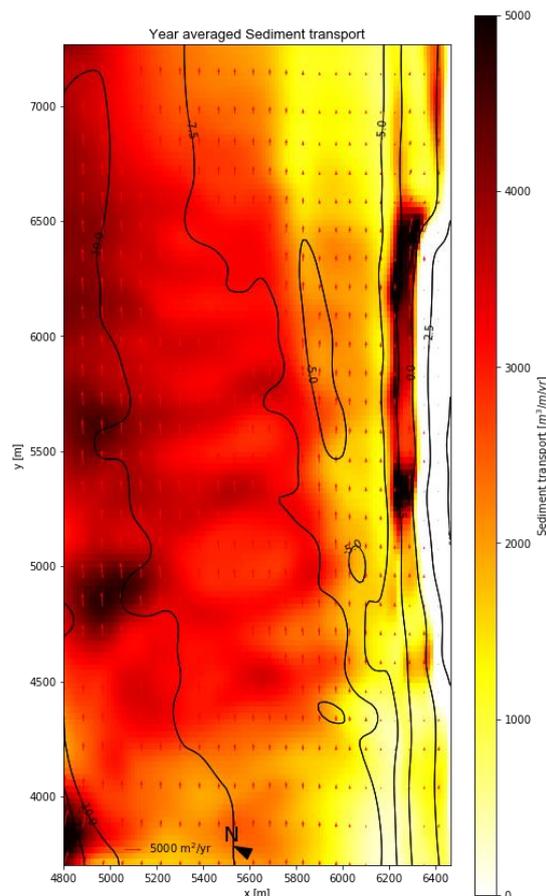
Figure 98: The year averaged sediment transport with a beach and shoreface nourishment, T_3.

4.3 Comparison of observed and modelled volume development

Whereas the previous two sections respectively dealt with observations and with a morphostatic model, this section makes a comparison of the observed and modelled volume changes for T_2 and T_3. To this end, the wave conditions from the Schouwenbank 2 wave buoy were used to assign a wave class for each time instance. According to the timeseries of wave classes, the sediment fluxes are computed over the boundaries of the coastal zones, as defined in Figure 19. Together, the result from the incoming and outgoing sediment fluxes provides the volume change. This modelled volume change is presented together with the volumes calculated from measured bathymetries as earlier presented in subsection 4.1.4.

4.3.1 Comparison T_2

The observed and modelled volume development show no good resemblance for T_2, nor realistic correlations were found (Table 14).

In the west domain (Figure 99), the modelled beach volume increases considerably whereas the observed beach volume remains approximately stationary. On the other hand, total and deep zones show an unrealistic volume decrease, whereas in reality only a considerable initial volume decrease takes places.
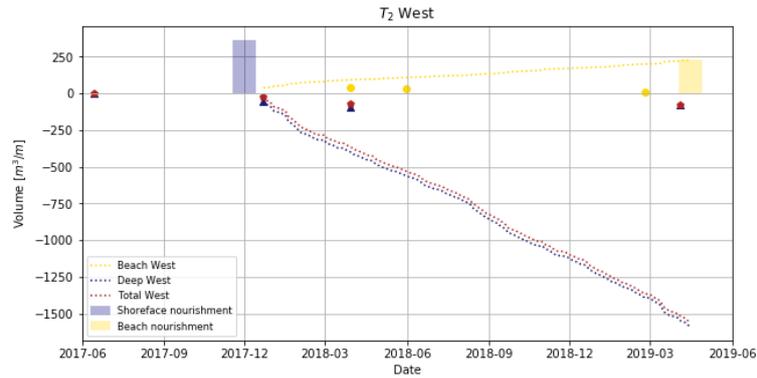
Figure 99: Comparison observed [points] and modelled [dotted lines] volume development west coastal zones for T_2.

The central coastal zones show a somewhat better resemblance (Figure 100). The modelled inner surf zone and the deep seaward zone follow the observations closely. Alike, the total volume shows erosion, however this is overpredicted by the model. Contrarily, the volume development near the shoreface nourishment is incorrect as the initial volume shows an increase while in reality this decreases and the trough shows significant erosion while the observations portray gradual accretion. Meanwhile, the beach accretes significantly according to the model while in reality the beach marginally accretes.
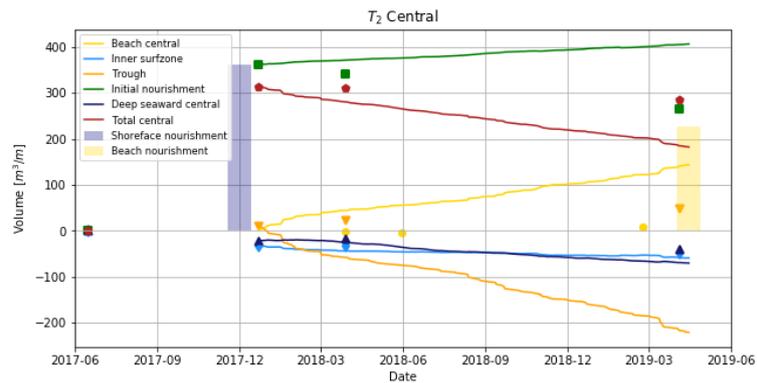

Figure 100: Comparison observed [points] and modelled [lines] volume development central coastal zones for T_2.

In the east of the domain (Figure 101), while the observed beach volume is stable, the model predicts a large volume increase. The development of the deep and total zones shows an unrealistic increase of more than 300m^3/m/yr.
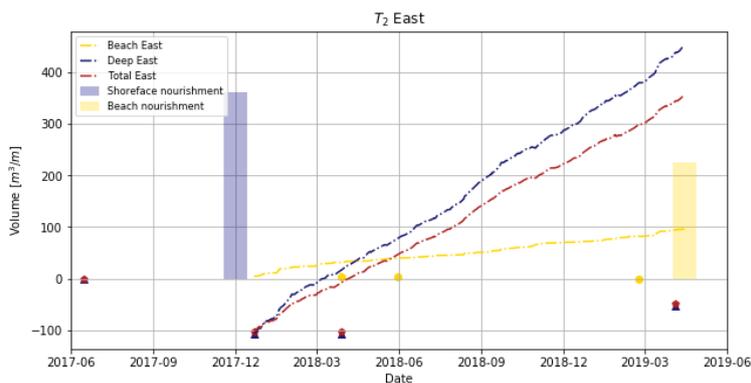
Figure 101: Comparison observed [points] and modelled [dash-dotted lines] volume development of the east coastal zones for T_2.

4.3.2 Comparison T_3

The observed and modelled volume development show no good resemblance for T_3, nor correct correlations were found (Table 15Table 14).

To the west (Figure 102), the total and deep volumes show an unrealistic decrease of 1200m^3/m/yr. Meanwhile, the modelled beach volume increases considerably which was not observed.
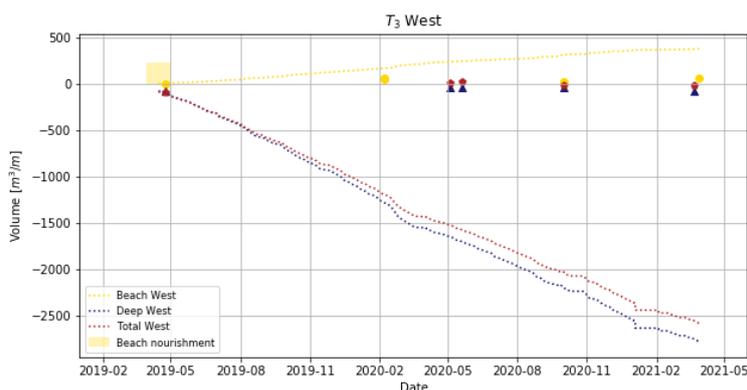

Figure 102: Comparison observed and modelled volume development west coastal zones for T_3.

In the central domain, the development of the deep shoreface shows a good resemblance with the observations (Figure 103). The beach volume shows a very gradual volume decrease after nourishment, while in reality this response was quicker. The total volume portrays an overprediction of the erosion. On the contrary, negative correlations are found for the surf, trough and initial nourishment zones.
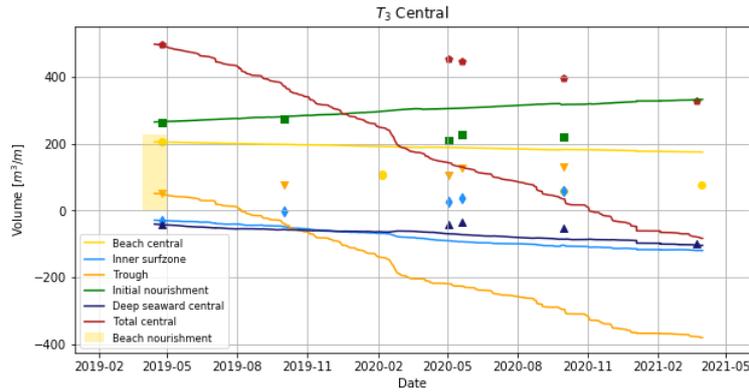
Figure 103: Comparison observed and modelled volume development central coastal zones for T₃.

To the west of the nourishments, some variation of the beach and shoreface volume is measured but the model predicts strong accretion (Figure 104). Moreover, no correlation is distinguished between the measurements and the model predictions.
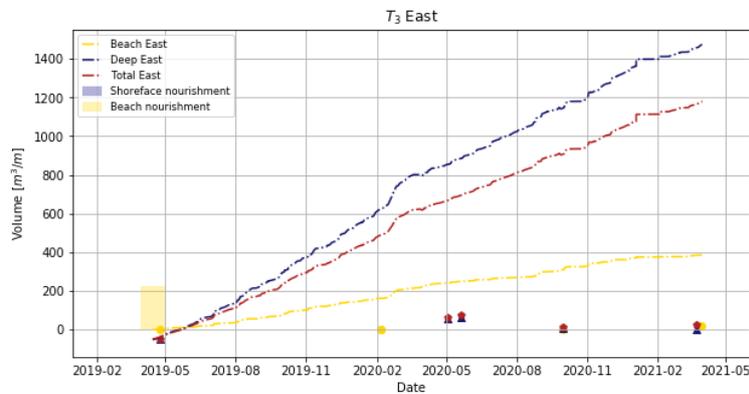

Figure 104: Comparison observed and modelled volume development east coastal zones for T₃.

Table 14: Correlation coefficients and p-values of the observed and modelled development for T₂.			*Table 15: Correlation coefficients and p-values of the observed and modelled development for T₃.*		
Zone	**R²**	**p-value**	**Zone**	**R²**	**p-value**
West			*West*		
Beach	-0.99	0.05	Beach	0.60	0.40
Deep	0.98	0.13	Deep	-0.26	0.67
Total	0.80	0.41	Total	-0.71	0.18
Central			*Central*		
Beach	0.97	0.15	Beach	0.96	0.04
Surf zone	0.89	0.31	Surf zone	-0.85	0.03
Trough	-0.99	0.02	Trough	-0.84	0.03
Initial nourished zone	-0.99	0.05	Initial nourished zone	-0.92	0.01
Deep	0.97	0.15	Deep	0.76	0.14
Total	0.99	0.10	Total	0.89	0.04
East			*East*		
Beach	-0.99	0.04	Beach	0.69	0.31
Deep	0.98	0.14	Deep	0.48	0.41
Total	0.98	0.13	Total	0.59	0.29

5. Discussion

Chapter 5 discusses and evaluates this studies' methodology and the results. First, limitations of the data analysis and the numerical model are explained in Section 5.1. Second, the results are interpreted in Section 5.2. Third, Section 5.3 elaborates upon the performance of the numerical model to predict volume changes.

5.1 Discussion of the methodology

The limitations in the methodology of the data and model analysis are discussed in this section.

5.1.1 Limitations of the data analysis

The results from the data analysis are limited mainly by measurement intervals, both in space and time. Additionally, the passage of transverse bars obscures erosion and accretion trends. Hereafter, it is discussed how this affects the estimation of nourishment longevity. Also, the estimation of sediment fluxes from data and how these can be improved are argued.

Available data

The study side features an extensive timeseries of bathymetric surveys. The study side is additionally surveyed since 2016 with the Verdichte JARKUS survey. This provided a valuable extra data resource. However, some of these measurements cover solely the wet profile, the period between the monitoring of the dry profile and wet profile was rather long, or scheduled measurements were not conducted at all.

First, if only the wet profile or the dry profile was measured, the corresponding part of the profile was added from a previous or following survey. For instance, the 2014 beach nourishment post-construction survey was complemented with the wet profile of the 2014 JARKUS survey. However, this introduces an error as some bathymetric changes are not included and can affect the volume calculation of coastal zones.

Second, a volume might be measured twice due to the large time interval between the wet and dry profile surveys. For instance, the 2020 JARKUS beach measurement was performed in February, whereas the shoreface was measured in May. As a consequence, sediment higher in the profile might be moved to a lower part in the profile and measured again during the wet monitoring. This introduces mainly an error for the volume analysis of beach nourishments, where rapid profile changes can be seen. Moreover, no exact measurement dates for multiple Verdichte JARKUS surveys were available. Hence, the volume development can be represented incorrectly through time.

Thirdly, some Verdichte JARKUS surveys are missing. This decreases the resolution in time which confuses the erosion/sedimentation patterns, profile development, and bar migration rates. Consequently, a larger spatial interval was chosen as multiple Verdichte JARKUS surveys, having a higher spatial resolution, are missing. It is believed that a higher resolution in time with a lower spatial resolution is advantageous over a larger spatial and lower temporal resolution because the coastal profiles show alongshore uniformity. Nevertheless, this introduces a larger error as the measurements are more sensitive to alongshore deviations.

Passage of transverse bars

The passage of transverse bars raises difficulties for the determination of short-term volume trends. Particularly, as transverse bars enter or leave a cross-shore profile, the shoreface

shows considerable erosion or sedimentation in the order of 100m^3/m/yr in a cross-sectional profile. This especially poses issues for calculating the volume changes in the trough zone and the cross-shore migration rate of the shoreface bar. However, this is solved as volumetric changes and migration rates are averaged over multiple transects. This approximately evens out the apparent accretion and erosion by transverse bars but is not accurate as the transverse bar height decreases from west to east.

Estimation of beach nourishment longevity

Dean (2003) stated that the erosion rate of a beach nourishment follows an exponential decay. Nonetheless, it was chosen to approximate the erosion trend with a linear fit due to the limited number of datapoints in time. Shek (2021) found that this leads to a small underestimation of longevity in a study on a large number of beach nourishments.

A larger uncertainty in nourishment longevity is the absence of several post-construction surveys. The beach volume shortly after construction is an important datapoint for calculating the erosion rate. This is overcome by adding an extra datapoint based on a summation of the volume measured prior to construction and the nourished volume as reported by the construction company. However, this method is not very accurate due to uncertainty in nourished volume per transect and the construction period. Several reported construction periods span more than half a year, and so a part of the nourishment can already be present in the survey which used to add the nourishment volume to. Therefore, the spread in erosion rates and longevity can partly be contributed to these uncertainties. Additionally, natural variations such as grain size and wave climate attribute to the spread in results.

Similarly, these uncertainties hold for the MKL change after beach nourishments. However, the spread in MKL change for beach nourishments was small.

Additionally, the annual mean wave energy was compared for each beach nourishment. As the Schouwenbank 2 wave buoy was deployed in 2004, no comparison can be made for the 1994 and 2000 beach nourishments. Also, the annual mean wave energy was based on a crude estimation through linear wave theory for waves in deep to intermediate water. Hence, the estimate is a precise tool for comparison, but the accuracy of the estimation is questionable.

Estimation of sediment fluxes

The estimation of sediment fluxes from volume changes are highly dependent on assumptions and simplifications. McCall et al. (2014) approximated the in- and out-going sediment fluxes in the study area with a single line UNIBEST-CL+ model in the active layer. However, it is unclear how far this active layer extends seaward. As the lower shoreface at Domburg is relatively shallow, the tidal flow is responsible for considerable alongshore sediment transport relatively far seaward. Therefore, the approximated fluxes of 30.000 and 100.000 m^3/year are no reliable boundary conditions. However, changing the magnitude of the boundary conditions did not significantly improve the estimations and so the fluxes found by McCall et al. (2014) were used.

Furthermore, the model was simplified by assuming no sediment exchange between the dunes and the beach. However, it can be expected that the dunes supply sand to the beach during heavy storms and the beach supplies sand to the dunes if a lot of dry sand is available.

Also, the model was simplified by not differentiating in alongshore transport rates in the cross-shore which effectively means that as much sediment is transported alongshore in relatively deep water as close to the shore. It is expected that this leads to considerable errors as more sediment is transported in the surf zone or the sheltering effect of the shoreface nourishment changes transport rates.

Similarly, this is done for the seaward boundary. The cross-shore exchange per meter is assumed to be equal for the west, central and east deep zones. This is not a valid

simplification, hence the offshore bathymetry is highly variable and affects the wave climate and the cross-shore currents. Where the box model estimates large landward fluxes at the seaward boundary, the numerical model predicts year-averaged offshore transport. Although it is argued that the estimated sediment fluxes are unrealistic, it is recommended to further develop this tool.

Effect on the research

Above limitations cause deviations in the estimation of bar migration, erosion/sedimentation rates, nourishment longevity and the rate of coastal retreat. Also, natural variations can cause irregularities in the results. As this research is based on a limited number of nourishments, these deviations can confuse the interpretation of these results. Therefore, conclusions from this research are drawn with caution. However, this can raise new questions and opens up opportunities for future research.

5.1.2 Limitations of the morphostatic numerical model

The morphostatic model is limited mainly due to simplifications of the boundary conditions and in the model itself. These are discussed respectively.

Simplifications of boundary conditions

The simplified hydrodynamic model input limits the performance of the numerical model, nevertheless this was necessary to limit computational times.

The wave and wind input were schematized by 11 wave classes. Although this number of wave classes is useful for the comparison of individual conditions, its use is limited for a year-averaged analysis or hindcast prediction. These wave conditions were determined at a relatively far offshore wave buoy and therefore needed to be transformed to the model boundary. However, the variable morphology of the SW delta influences the alongshore wave climate as presented by McCall et al. (2014). Meanwhile, the morphostatic model does not allow for a varying wave climate along the offshore boundary. This can induce a small error in the numerical model.

In a comparable model study on shoreface nourishments, Huisman (2019) used 100 wave classes with varying wave height and direction, and tidal velocities. To compute hindcast erosion rates, an interpolation of corresponding wave classes is carried out for each time instance. The development of the shoreface nourishment and the surf zone were predicted well by Huisman. It is believed that the number of wave classes and the interpolation step are of importance to accurately describe year-averaged hydrodynamics and sediment transports.

Moreover, this study calculates the sediment transports over the morphological tide. This is the tidal cycle that best represents the average morphological change during a complete spring-neap tide cycle. Small inaccuracies in this procedure can accumulate in the model outcome. The tidal wave is responsible for a relatively large part of the sediment transport on the Domburger Rassen. A source of inaccuracies is the derivation of the water levels at the model boundaries with the zuno4-ASTRO model. It must be noted that a random spring-neap tidal cycle was obtained and that the water level variations can differ from other spring-neap tidal cycles. This can result in too strong or too asymmetric tidal velocities in the model, resulting in unrealistic alongshore transport rates. Nevertheless, the modelled tidal velocities were validated with measurements from the Schouwenbank Stroomgat station. But this station is relatively far from the study site and the tidal current was only validated for the west model boundary.

The applied model makes use of a single tidal signal. At the Domburg coast, where the tide is critical for sediment transport, using only one tidal signal introduces inaccuracies. This can be seen in Appendix C.2.2, where a large spread in sediment transport for different tidal

signals is observed. Contrarily, Huisman (2019) had a timeseries of tidal velocities available at the model boundaries. Accordingly, it is believed that a timeseries of water levels at the model boundaries can force a more realistic tidal current in the model and therefore significantly improve the sediment transport.

Simplifications in the model

The numerical model makes use of depth averaged flows. Therefore, secondary flow patterns with differences in the vertical, e.g. undertow, are not resolved but parameterized. This shortcoming in 2-D depth averaged models is an important reason why bar behaviour is resolved incorrectly. Therefore, it is recommended to look into the parameterization of secondary flows, especially at the secondary flow induced by the tidal current. This curvature-induced secondary flow can be important for the maintenance of shoals due to a sediment flux towards the centre in the lower water column (Bosboom & Stive, 2015).

The model parameters are based on the default values for the safety evaluations of the Dutch primary water defences. The model is not further calibrated and so hydrodynamic and morphological parameters are not adjusted to better represent reality for the Domburg site. Huisman (2019) and Lyu (2019) argue that wave skewness and asymmetry settings dictate to some extent the cross-shore sediment transport. Therefore, it can be looked into calibrating this parameter to better represent the observed volume changes at the shoreface.

5.2   Interpretation of the results

This section elaborates on the effects of nourishments on the coast on short timescales. Also, anthropogenic changes such as the (partial) closure of estuaries affect the coast to some extent, but it is assumed that these processes act in the background on a longer timescale.

5.2.1 Salient effect

According to van Duin et al. (2004), the salient effect can cause leeside accretion as the shoreface nourishment reduces the alongshore sediment transport due to offshore dissipation. However, no evidence was found that supports the significance of a salient effect on the wave driven transport near the Domburg shoreface nourishment.
The wave height was slightly increased at the leeside of the shoreface bar during daily conditions. The reduction of storm waves in the leeside is limited, as these are reduced with 0.15m for an offshore significant wave height of 2.46m. Year averaged, no wave height reduction is observed in the leeside.
This is supported by the dissipated energy on the coast. The year averaged dissipation on the shoreface bar is limited while the total dissipation at the beach is not reduced. In storm conditions, 8-20% of the wave energy is dissipated on the shoreface bar. This indicates that the shoreface bar causes a marginal yearly reduction of wave energy at the leeside.
Moreover, it is seen that the alongshore sediment transport is reduced in the trough zone, but not in the surf and intertidal zones. The bathymetric surveys showed that the leeside and adjacent beach volume remained stable after the construction of the shoreface bar. Additionally, the average wave direction was altered insignificantly in the leeside of the nourishment. In transects 1632-1550, where the shoreface nourishment was constructed close to the beach, the wave direction was altered in a more shore normal direction with 2°. Waves refract on the seaward side of the bar, but not in opposite direction at the leeside. Therefore, inbound waves are directed relatively shore normal which might locally reduce the littoral drift leading to more accretion. A volume increase landward of the shoreface bar is seen, but it is likely that cross-shore wave driven processes are mainly responsible for accretion in the trough zone.
To conclude, no evidence is found for a significant salient effect of the shoreface bar on the

wave-driven transport at the central and adjacent shores. This is supported by the results of van Duin (2004). Although van Duin argued a contribution of the salient effect, the results show erosion updrift and downdrift of the Egmond shoreface nourishment which was larger than the natural autonomous erosion.

Nevertheless, no wave driven salient effect is seen, the numerical model indicates a reduction of alongshore currents to the east of Domburg. The shoreface nourishment shelters the adjacent east shoreface from the strong tidal current. Also, the numerical model indicates that the wave direction is adjusted in this zone. This can be explained by current refraction, whereas the wave direction is altered as a result of a changing wave celerity. Moreover, the wave height at the east adjacent shoreface is reduced. The model output presents a larger negative gradient to the east of Domburg if a shoreface nourishment is present, which predicts accretion of the shoreline. This is supported by observations of a consistent volume increase of the adjacent east shoreface after the 2017 nourishment. Therefore, at Domburg, a salient effect can cause accretion at the downdrift coastline. The relative importance of sediment transported by the tide and the shoreline orientation are responsible for the sheltering effect at the downdrift shoreface. Alternative explanations for the observed accretion are the abundance of updrift sediment or natural variations at the shoreface such as horizontal sand waves.

5.2.2 Feeder effect

According to Huisman (2019), a shoreface nourishment particularly spreads sediment due to water-level setup driven residual circulations and the skewness and the asymmetry of the wave orbital motion. At Domburg, sediment was transported onshore as the bathymetric surveys presented erosion at the initially nourished zone while the trough zone accretes. Although, no trough could be distinguished at the landward side, the seaward migration of the bar in transect 1530 and the quick erosion in transects 1530 and 1632 demonstrate that return currents shape the morphology. This is supported by the modelled cross-shore sediment transport, which predicts more offshore transport for transects 1632 and 1550 and offshore flow under storm conditions near transect 1550 and 1448.

Initially, it was observed that the shoreface bar develops into a triangular landward skewed shape and the steep seaward slope is flattened. The numerical model shows that this is due to larger onshore directed transport at the nourishment crest. The formation of a trough is absent landward of the shoreface nourishment. These findings correspond with Bruins (2016), who found similar morphological bar development and only observed trough formation for coasts with original bar behaviour. The Domburg coast is located on the shallow Domburger Rassen which is partly sheltered by morphological features of the Eastern and Western Scheldt. Therefore, the largest storm waves dissipate energy further offshore. Correspondingly, the limited effect of breaking waves on the shoreface nourishment is a possible explanation for no distinct trough formation, as sediment transport is induced by turbulence (Bosboom & Stive, 2015).

Afterwards, it was seen that the seaward slope continues to flatten, the bar develops into a more rounded bulge, and the crest height reduces. Accordingly, Huisman (2019) observed analogous development for shoreface nourishments at coasts with natural bar cycles.

The initially nourished zone of the Domburg shoreface nourishment shows a gradual decline of 60m^3/m/yr. Likewise, Huisman (2019) found a rather linear decrease of the volume in the initial shoreface nourishment region from measurements. Both Bruins (2016) and Huisman (2019) found an increase of onshore volumes due to the execution of a shoreface nourishment. This is also observed at Domburg, but the volume increase due to the shoreface nourishment is limited to the area directly landward of the bar and not in the inner

surf zone. Concluding, on a short-time scale only a local feeder effect is visible. It is possible that on a longer timescale the shoreface nourishment can feed the nearshore zones.

5.2.3 Contraction of tidal flow

A shoreface nourishment decreases the cross-sectional wet area which leads to a contraction of the tidal flow. The numerical model indicates that this increment is the largest just seaward of the shoreface bar. This induces larger gradients in alongshore sediment transport as supported by modelled alongshore sediment transport, estimated sediment fluxes from data and the volume change of the central deep zone. The estimated sediment fluxes demonstrate that the alongshore transport from the central domain has increased with 50% comparing T_0 to T_2 and T_3. Besides, prior to the shoreface nourishment, the deep central coastal zone shows an accretive trend, whereas it starts to erode afterwards. This indicates an increased alongshore transport gradient on the seaward shoreface.

No definite effect is distinguished at the landward side of the shoreface bar. The inner surf zone erodes for both T_0 and T_2. Contrarily, the surf zone shows little accretion after T_1 while a considerable volume increase is present after T_3. Therefore, the shoreface bar captures the eroded beach nourishment in the inner surf zone.

Also, the model output indicates that the currents and the alongshore sediment transport are enhanced on the west end of the shoreface bar. Cross-sections of transect 1632 show complete erosion of the shoreface bar in the period May 2018-Feb 2020. This is explained as the tidal current forcing a channel through the shore-connected bar, which is evident from the computed transport rates. Although most of the erosion at transect 1632 is after the 2019 beach nourishment, this can be attributed to a transverse bar arising after the 2017 shoreface nourishment.

Consequently, as the alongshore sediment transport seaward of the shoreface bar is enhanced, it is likely that the migration speed of the natural occurring transverse bars is increased. Similarly, the migration rate of the transverse bars in the trough zone is assumably reduced as the alongshore sediment transport in this zone is reduced. Further landward, in the surf zone, no differences in alongshore sediment transport are found, and so the transverse bar migration rate is expected to remain unchanged. Moreover, especially at the downdrift adjacent shoreface, the migration rate of transverse bars is expected to be locally reduced. The region at the bar's end shows a considerable decrease in alongshore transport.

Nevertheless, this cannot be verified from the Verdichte JARKUS surveys, as these are performed as cross-shore transects with intervals of 100m. This obscures the exact location of troughs and crests, and the migration rate cannot be determined accurately.

5.2.4 Residual currents

Residual currents form under normally incident storm waves around the east segment of the shoreface bar (transects 1550-1448). The breaking waves on top of the bar generate a dissipation related wave force, driving an onshore directed flow (Bosboom & Stive, 2015). The numerical model shows that the current is deflected to the west and to the east in the trough. Near the east tip and at the deeper west segment, offshore directed return currents are observed. These return currents can be responsible for the bar erosion observed at transect 1530. For oblique incident storm waves, no pattern of return currents is distinguished. These observations agree with the results of Huisman (2019), who determined stronger residual currents for normally incident storm waves.

Even though erosion at several transects is evident, bathymetric surveys reveal that the average volume decrease of the bar is limited to 2.5m^3/m/yr. A possible explanation for the bar maintenance is a residual current due to the curvature of the tidal flow near shoals. This

secondary flow contributes to the maintenance of shoals (Bosboom & Stive, 2015). Similarly, Zimmerman (1978) showed that residual currents are generated at tidal ridges that are not exactly orientated along the current direction. The upslope current carries more sediment that the downslope current, effectively maintaining the tidal ridge.

These secondary flow mechanisms are not resolved by 2-D depth averaged models such as XBeach. This led for instance to an incorrect prediction of the accretion and erosion at the Eierlandse Dam at Texel (Bosboom & Stive, 2015). As mentioned before, numerical models tend to flatten the bed, and therefore morphodynamic modelling of bars is not yet possible. Hence, resolving secondary flow mechanisms in numerical models can help maintain shoreface bars and improve the morphodynamic modelling of barred coasts.

5.2.5 Longevity of beach nourishments

No evidence is found that the presence of a shoreface bar prolongs the longevity of a beach nourishment at Domburg. The measured erosion rates, half-life and estimated longevity is similar for previous beach nourishments and the 2019 combined beach nourishment. However, it must be noted that the 2021 JARKUS survey indicates an unexpected beach volume increase. This has a large influence on the estimation of the longevity and the erosion rate. This deviation is likely a consequence of the natural variability in the coast. Another explanation can be a contribution of the feeder effect of the shoreface nourishment on the beach.

The measured total incoming wave energy on the 2019 nourishment was similar to previous beach nourishments. The numerical model predicts that the shoreface bar dissipates 10-20% of the incoming storm wave energy. Therefore, less waves are dissipated on the beach and so a relatively lower erosion rate is expected. However, this is not observed and it is argued that the shoreface nourishment does not prolong the lifetime of beach nourishments. Although it is argued by Verhagen (1992) that storms do not cause extra erosion to nourished beaches and Shek (2021) found an insignificance of storm variables for beach nourishment longevity, the total incoming wave energy is likely to have an effect on beach longevity.

Regarding the Momentary Coastline (MKL), the main coastal indicator used to decide upon maintenance, presents that the coastline retreat for T_1 and T_3 is the same order of magnitude. An average retreat of 3.9m/yr is observed for the 2004, 2008 and 2014 beach nourishments while the 2019 beach nourishment presents a retreat of 4.3m/yr. Therefore, maintenance intervals are not extended and it can be argued that the shoreface nourishment causes a larger coastal retreat.

Although susceptible to natural variation, a 7% larger retreat is seen for the combined nourishment (T_3) than for the fastest retreating beach nourishment (T_1:2014). It remains unclear what processes cause this increased erosion rate. Comparing T_1 and T_3 model output, a small increment in alongshore transport in the swash zone is seen. Correspondingly, an increment in year-averaged leeside wave height is computed.

Shek (2021) argues that the implementation of shoreface nourishments on the Holland coast, featuring shore parallel bars, likely increases the longevity of beach nourishments. For Domburg, a transverse barred coast, no such relation is found.

5.2.6 Migration of shoreface bars

The Domburg coast has no original parallel bar behaviour but features shore perpendicular bar between NAP-5m to NAP-10m that migrate from the SW in NE direction. Although these transverse bars show an alongshore migration rate increasing from 30m/yr to 50m/yr, no clear distinct alongshore migration is observed of the shoreface nourishment. Nevertheless, some spreading of sediment in downdrift direction is observed.

Differently, the Domburg shoreface nourishment migrates in landward direction with 18m/yr for T_2 and T_3. It remains unclear if the shoreface bar continues to migrate in landward direction after T_3, or that the eroding sediment from the beach nourishment causes an apparent migration. This sediment likely accretes at the landward side of the bar and is included in the calculation.

The model output shows increased cross-shore transport on the bar crest due to skewed waves. Therefore, sediment is transported towards the trough zone. Moreover, a rotation of the east shoreface bar occurs as the landward migration rate increases from transect 1509 to 1448, and effectively rotates and is more shore parallel oriented.

Bruins (2016) argues that the asymmetry of the tide or the sheltering from the largest waves by the ebb-tidal delta van explain the dominant alongshore migration or no bar migration. However, the Domburg coast is characterized by an asymmetric tide and wave sheltering of the outer deltas of the Scheldt estuaries, but the 2017 shoreface nourishment shows solely onshore migration. A calmer wave climate results in a relative larger importance of the energetic non-breaking waves which are mainly responsible for onshore bar migration.

5.3   Performance of predicting volume changes with a morphostatic model

This section discusses the performance of the predicted volume changes of the numerical model as compared to measured volume changes.

Overall, the applied morphostatic model preforms poorly for a hindcast prediction of volumetric changes for T_2 and T_3. The prediction of volumetric changes on the shoreface at the adjacent shorelines is very poor, as unrealistic high erosion and sedimentation rates in respectively the west and east are predicted. Moreover, the model predicts large accretion in the east beach, central beach, and west beach zones whereas the measurements show that these zones are approximately stable without the influence of a beach nourishment. Remarkably for T_3, the decrease in beach volume is underpredicted by the model.

The model predictions on the central shoreface show better resemblance. The modelled volume change on the seaward shoreface show good resemblance with measured volumes for T_2 and T_3. The inner surf zone is predicted well for T_2 but not for T_3, which is explained by a large amount of nourished beach sediment that settles in the surf zone in reality.

The initial nourishment zone is not represented correctly, as the model predicts a volume increase while a decrease is observed. Likewise, the model predicts significant erosion in the trough zone where in reality a volume increase is seen. Even though, the volume change of the central shoreface is in the correct order of magnitude. The total volume change of the central zone predicts more erosion than observed.

In a similar morphostatic model study, Huisman (2019) found contradictory results. He found a good representation of the erosion of the initial nourishment, trough and inner surf zone. Remarkably, Huisman found an incorrect prediction of seaward erosion while a good resemblance is found in this study.

The limited model performance can be due to multiple simplifications.

First, as the bathymetry is fixed, crucial feedback loops are omitted. For instance, the transport rate near transect 1632 is high as a consequence of the tidal contraction. However, the current is not able to erode a larger channel and reduce the transport rate. These feedback loops are necessary as these are present in reality.

Second, too few wave and tidal conditions were applied to realistically represent sediment transports. The number of directional bins, wave heights and tidal signals was limited to reduce computational times. Huisman (2019) used 100 hydrodynamic conditions and performed an interpolation to derive sediment transports from wave and current

measurements. Contrarily, this study utilizes 11 wave conditions with two main wave directions and no interpolation step is used.

Also, no calibration could be done for the model parameters for the Domburg coast. The relative importance of the tidal current and the characteristics of this specific coast might not be captured in the default model parameters.

6. Evaluation of nourishment strategies

This chapter evaluates the performance of previously applied nourishments and proposes an alternative strategy which is consecutively evaluated through results from the morphostatic model.

6.1 Nourishment strategies for NW Walcheren

This section elaborates on different nourishment strategies for the NW Walcheren coast. These strategies include both previously applied methods and alternative nourishments. Even though the impact on beach recreation, costs and constructability can play a major role in decision making, these socio-economic considerations are not included in this evaluation which focusses on the effect on hydrodynamics and morphodynamics.

6.1.1 T_1: Beach nourishment

A beach nourishment has proven to be very effective in preserving the coastal functions at Domburg. The volume contributes directly to the MKL zone. Although, the lifetime of this nourishment is short while the hindrance and costs are relatively high. The effect on the larger-scale hydrodynamics beyond the nourishment location is limited, as currents and wave heights and wave directions are marginally altered. This nourishment strategy is therefore an effective way to locally maintain the coastline at Domburg. It is expected that the seaward protrusion of Domburg will be reduced as the adjacent coastlines advance on longer timescales.

6.1.2 T_2: Shoreface nourishment

The 2017 shoreface nourishment adds volume to the coastal cell, and thus effectively maintains the coastal system. It is seen that sediment is transported in landward direction and that the bar dissipates little wave energy. However, the contribution to the MKL zone is limited and it is unclear if the shoreface nourishment feeds the nearshore. Also, as the coast features no parallel bars, this nourishment does not interact as effectively with the natural system.

Although the 2017 shoreface nourishment did not have a clear impact on the shoreline, it is worthwhile to consider continuing this nourishment strategy. Repeatedly implementing extra bars in the coastal system might push the existing bar onshore, comparable to the bar behaviour at the Holland coastline. However, as the tide plays a relative import role at this coast, such bar behaviour is questionable. Nevertheless, it is expected that the repeated implementation of shoreface nourishments will feed the nearshore and help maintain the coastline on longer timescales. However, these shoreface bars will cause a larger transport gradient near Domburg.

6.1.3 T_3: Combined beach and shoreface nourishment

The 2017 shoreface nourishment was combined with a beach nourishment in 2019. The erosion rate, longevity, half-life and MKL change of the 2019 beach nourishment were not positively affected by the presence of the shoreface nourishment. Therefore, no evidence was found that the nourishment interval is substantially prolonged for the combined nourishment strategy. However, a variant where sand is supplied on the shoreface in the leeside of the 2017 nourishment and at the beach is deemed more successful. The beach nourishment is expected to reshape to its equilibrium profile, and as the subtidal zone features a gentler slope, this process takes longer and the erosion rate from the beach is expected to be lower. However, this can induce contraction of the tidal flow and likely increases the subtidal erosion rate. The repeated application of this nourishment strategy will

maintain the coastline at Domburg and supply sand to the adjacent coastlines. The application of this strategy will cause a locally larger transport gradient and maintains the seaward protrusion of Domburg.

6.1.4 Mega nourishment

Both the Westkappelse Zeedijk and the Domburg coastline require regular sand nourishments. An alternative strategy is to implement a mega nourishment which is be able to supply both sites with sediment. It is expected that the coastline perturbation is flattened out and the sediment is spread alongshore to the southwest and the northeast. The adjacent coastlines are supplied with sediment for an extended period compared to beach or shoreface nourishments and therefore offers a longer maintenance interval. Furthermore, this strategy will diminish the seaward protrusion of Domburg which is currently partly responsible for the structural erosion. The application of this nourishment strategy on the NW coast of Walcheren is further explained in section 6.2.

6.1.5 Transverse bar nourishment

Another alternative strategy is to apply a shore perpendicular shoreface nourishment. This is more in line with the coastal system which features transverse bars. An effect of migrating transverse bars on wave heights was seen in this study. So, nourishing the bar crests can affect the hydrodynamics. It should be further investigated if accretion in the nearshore can be expected for this strategy. On the other hand, supplying sediment in the troughs is a more practical method of nourishing as larger vessels can navigate there.

It is expected that the nourishment will have an effect on the migration of the natural transverse bars and will likewise migrate alongshore from east to west. This nourishment strategy will most likely contribute to the coastal foundation and attribute little to the volume in the MKL zone. It is questionable if this strategy can maintain the coastline on longer timescales as it is unknown if sand is supplied to the nearshore zones.

6.2 Substantiation for alternative nourishment

This section proposes an alternative nourishment strategy in the form of a mega-nourishment to feed both the Domburg and Westkappelse Zeedijk.

To the North of Domburg, near nature reserve Oranjezon, the coast features a large perturbation with an alongshore length of 1.2km and a seaward protrusion of 200m (Figure 105). This feature has developed strongly in the last 30 years (Figure 106). The cross-sectional profiles show the formation of juvenile dunes which quickly develop into larger dunes. Interestingly, the highly dynamic intertidal and subtidal area shows the formation and offshore migration of breaker bars.

2016:
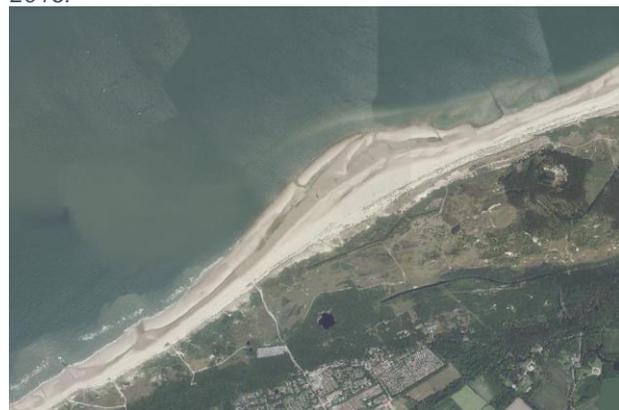
As this naturally formed feature is present at the same coastline as Domburg, applying a mega-nourishment in the same order of magnitude would fit the coastal system. The mega-nourishment is projected between the Westkappelse Zeedijk and Domburg to supply both coastlines with sediment. The design includes an estimated 4 million m³, being applied symmetrically between transects 1775-1612 with a maximum protrusion at transect 1694 (Figure 107). In this transect, the MLWL is moved approximately 300m seaward. The nourishment has a similar morphology as at Oranjezon. It is therefore likely to fit the coastal system in this location.

2019:

Figure 105: Aerial pictures of the natural protrusion near Oranjezon, at the NW coast of Walcheren. [Source: satellietdataportaal.nl]
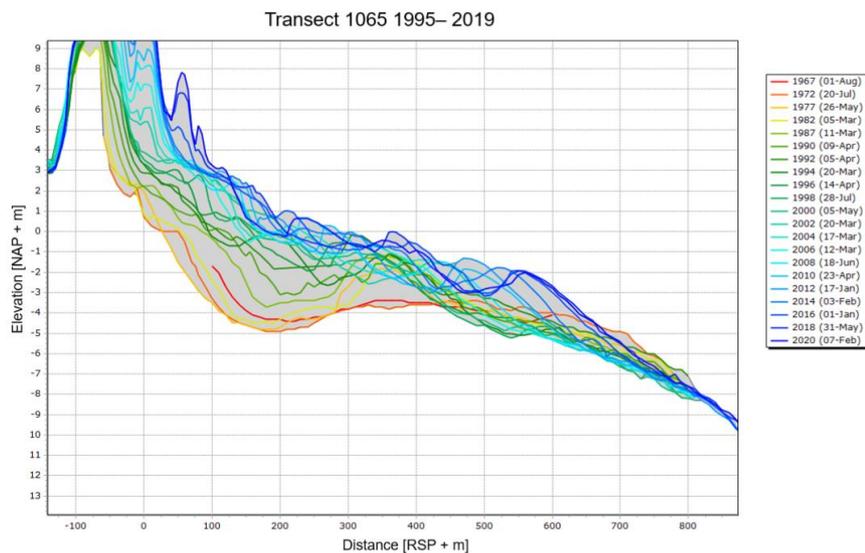
Figure 106: Cross-shore profiles in the period 1967-2020 at transect 1065, near Oranjezon.

Due to the seaward protrusion, gradients in wave driven alongshore sediment transport will arise. The centre of the nourishment will erode and the sediment is likely deposited in upstream and downstream direction as previously explained in Section 2.2.1. Also, sediment transport can be enhanced in upstream and downstream direction due to the contraction of the tidal flow. Both effects result in spreading of the mega nourishment and supplying sediment to the adjacent coasts.

Another benefit is that the protrusion at Domburg is largely neutralized, and so transport gradients at Domburg will be decreased. Presumably, this lowers the need for frequent coastal maintenance.

The mega nourishment might induce the formation of morphological features. For instance, the development of breaker bars, as observed near Oranjezon. Another possibility is the development of growing juvenile dunes. Furthermore, it might increase the alongshore migration of transverse bars due to a local contraction of the tidal flow.

A first evaluation of the mega nourishment design on the local hydrodynamics and transport patterns is performed with the morphostatic model, previously handled to evaluate the effects of beach and shoreface nourishments at Walcheren.
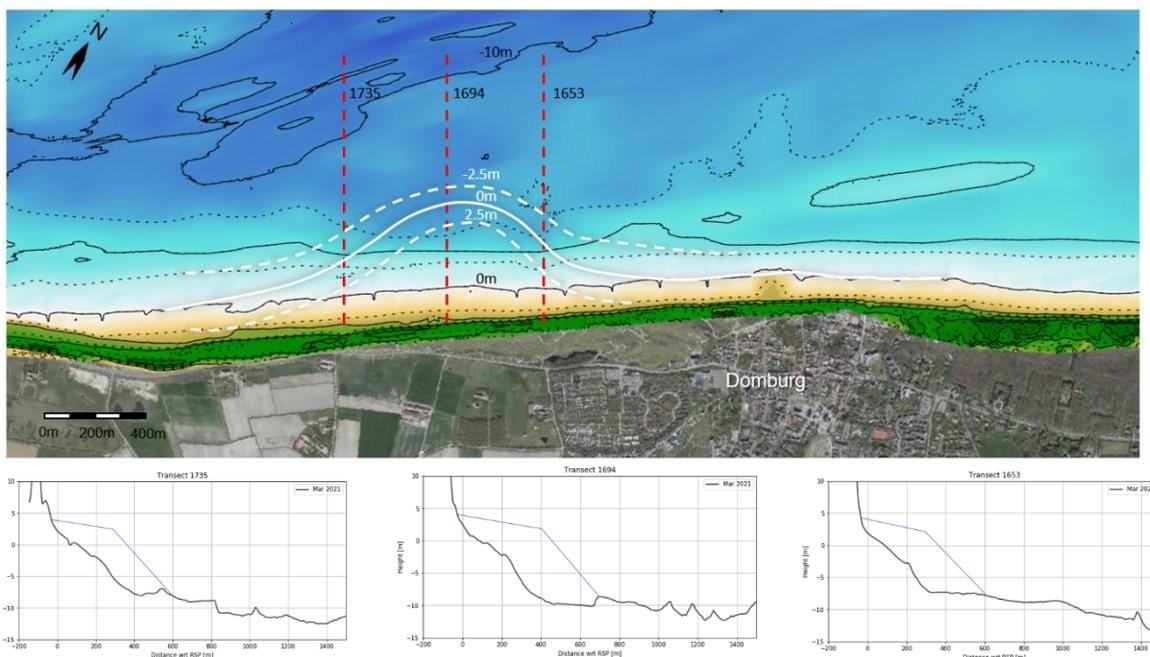
Figure 107: Design of the mega-nourishment, placed to the West of Domburg. The top panel gives a top view of the nourishment with the 2.5m, 0m, and -2.5m contours [white]. The bottom panels provide cross-sections with an indication of the nourished body of sand [dark blue].

6.3 Comparison of hydrodynamics and sediment transport

The numerical model output for a mega nourishment (T_4) are compared to output for an unnourished coast (T_0). This section starts with elaborating on the wave heights and directions. Then, the effect on current patterns is presented. The section is finalized with the sediment transport patterns. It must be noted that this section focusses on the effect near Domburg and not at the Westkappelse Zeedijk as the model boundaries are too close to this coastline to produce correct model output. Furthermore, the model was set-up for the evaluation of shoreface nourishments and not for a large coastline perturbation. For this reason, other process-based or equilibrium models might be more suited to evaluate this nourishment strategy.

6.3.1 Wave height and direction

The effect of a mega nourishment on the wave height and direction are discussed respectively in this subsection.

Annual wave height

The effect on the year-averaged wave height is limited (Figure 108 and Figure 109). To the east of the nourishment at Domburg, little effect on the wave height is observed (Figure 109a, b). The wave heights are reduced at the sides of the nourishment (Figure 109c, e). This was expected as incoming wave energy is spread over a longer coastline. A small increment at the tip is observed (Figure 109d), which can be explained by convergence of wave energy. Although Figure 108 supports these observations, it shows a remarkable area of wave height increase near transect 1612. This is caused by a small difference in model bathymetry.
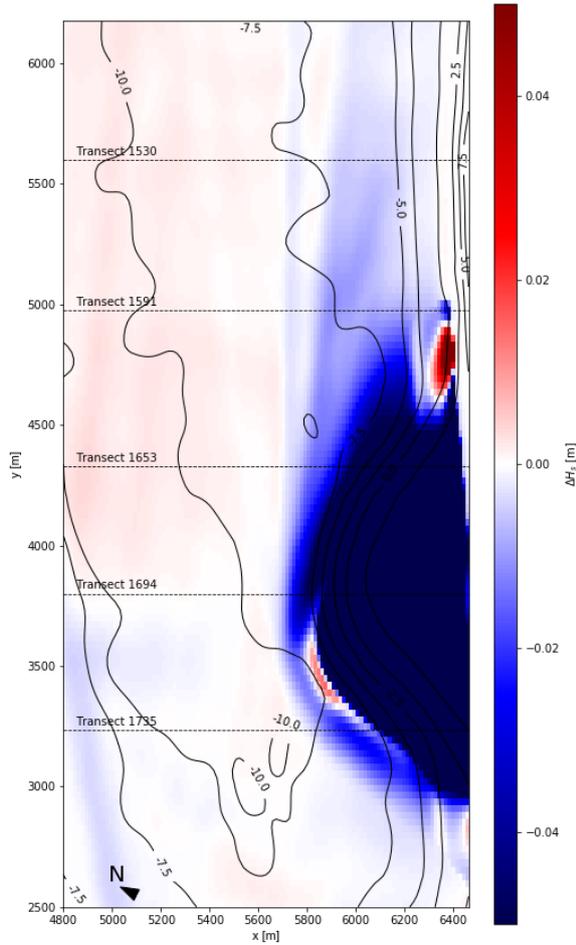
Figure 108: Difference in wave height between T_0 and T_4
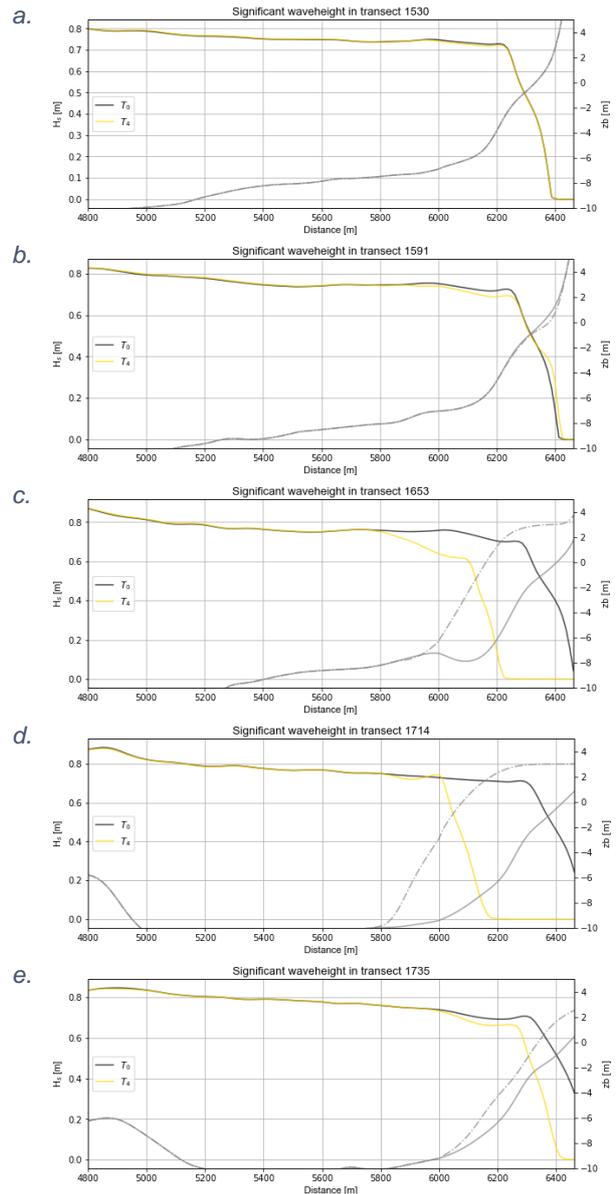
Figure 109: Year-averaged wave heights for T_0 and T_4 for transects a. 1530, b. 1591, c. 1653, d. 1694, e. 1735.

Annual wave direction

The mega nourishment locally influences the nearshore wave direction (Figure 110 and Figure 111). Near the Westkappelse Zeedijk at the west side of the nourishment, the wave direction is reduced as waves are refracted towards the new shoreline orientation (Figure 111d, e). Likewise, the wave direction increases at the east side near Domburg as the wave crests are refracted in shore-normal direction (Figure 111c). Downstream of the nourishment at Domburg, minor differences in wave direction are observed but the orientation in the surf zone is unchanged (Figure 111a, b).
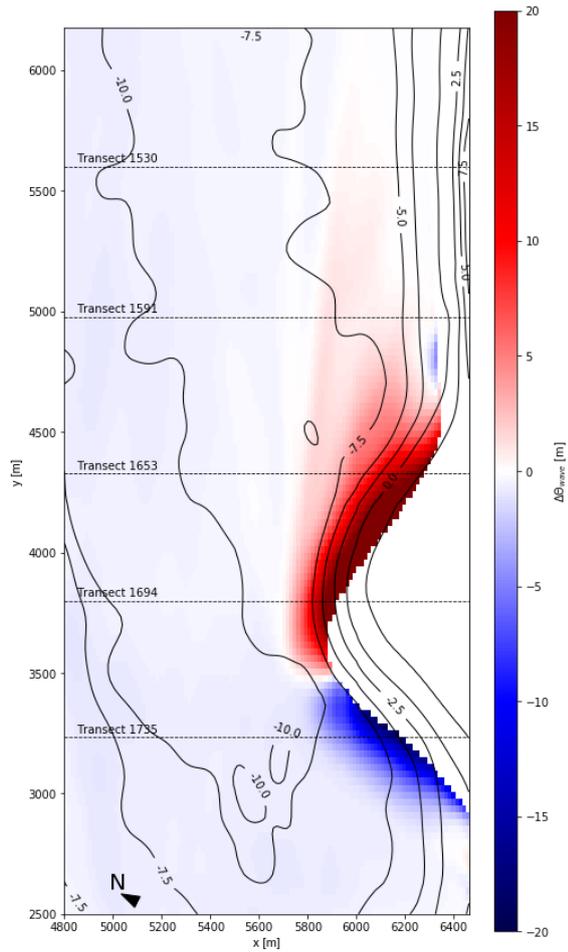
Figure 110: Difference in wave direction between T_0 and T_4
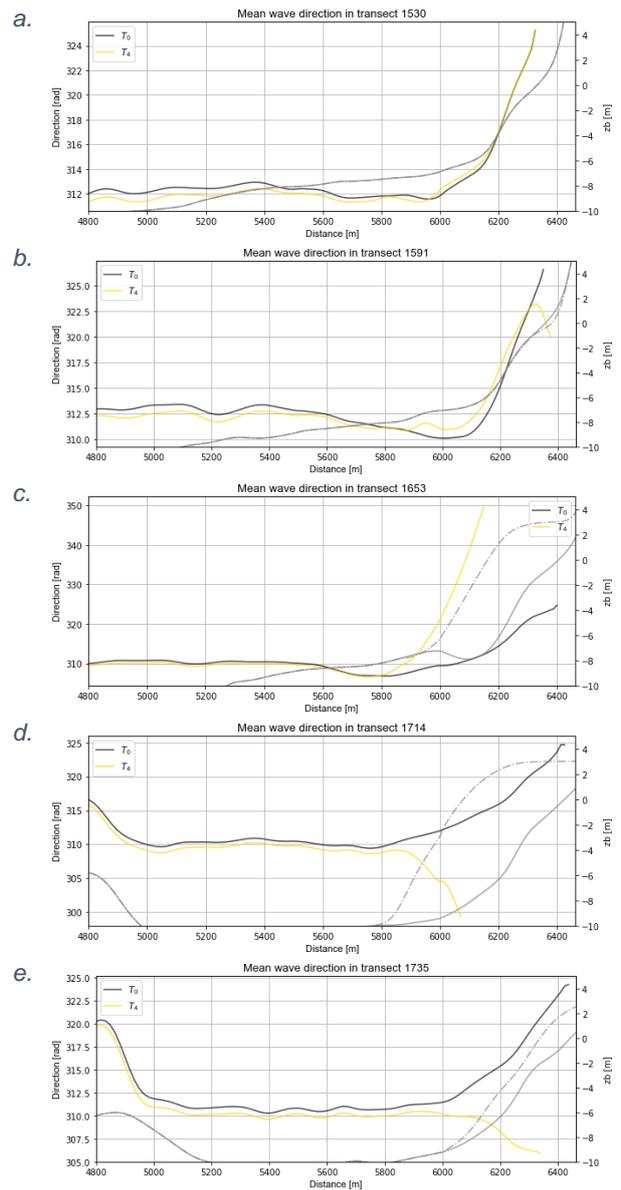
Figure 111: Year-averaged wave directions for T_0 and T_4 for transects a. 1530, b. 1591, c. 1653, d. 1694, e. 1735.

6.3.2 Currents

Two eddies are created due to the shoreline perturbation (Figure 112). The year averaged velocities show that a strong clockwise eddy is formed between transects 1653-1591. Also, a weaker anti-clockwise eddy near transect 1735 forms. Close to the nourishment head, the alongshore current is enhanced in eastward direction.
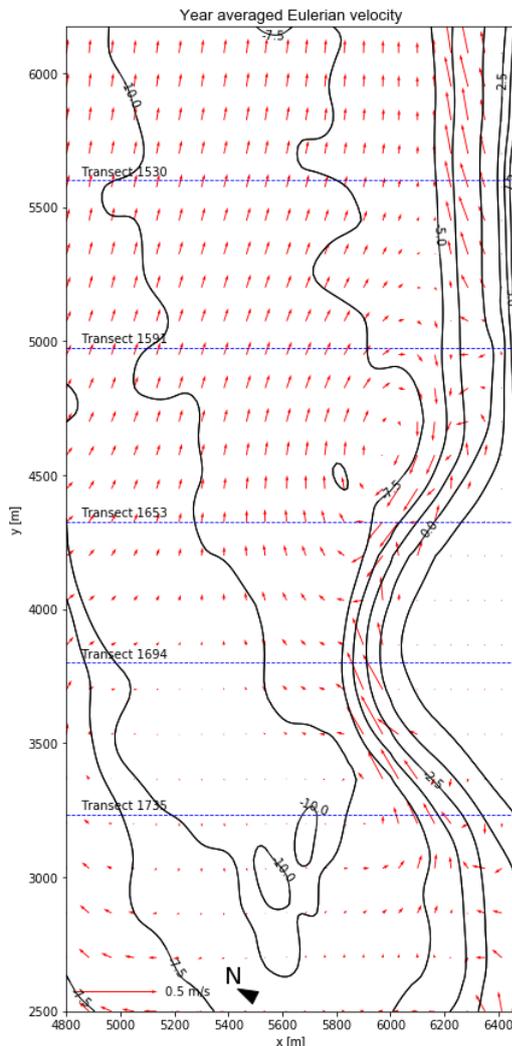
Figure 112: Year-averaged currents for T₄.
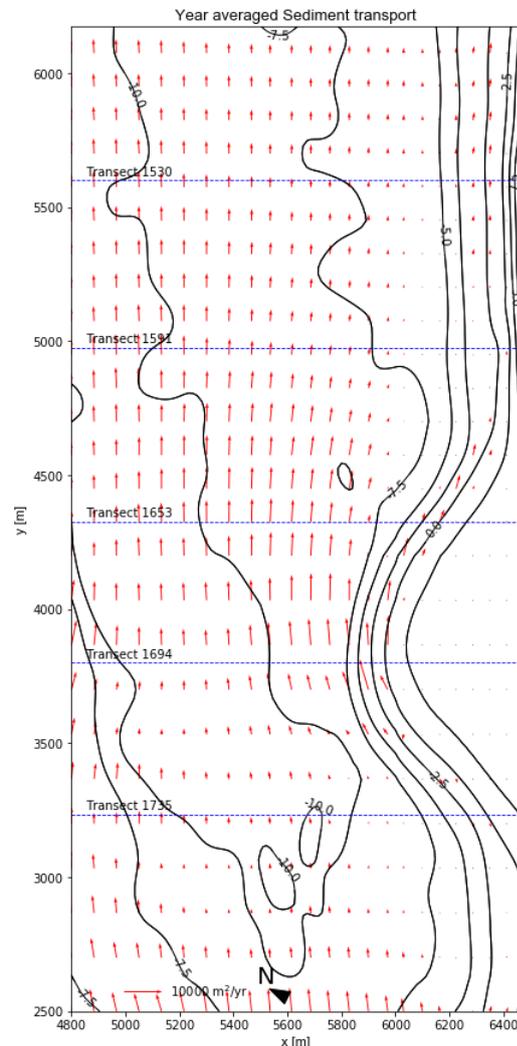
Figure 113: Year-averaged sediment transport for T₄.

6.3.3 Sediment transport

The year averaged sediment transport shows a low transport rate near the Westkappelse Zeedijk, resulting in local accretion (Figure 113). Figure 113 also shows a large positive gradient in alongshore transport at the nourishment tip. Therefore, locally the beach and the shoreface will erode. To the east, the alongshore gradient is negative. In this manner, the eroded sediment will accrete on the shoreface and in the subtidal zone. Therefore, the mega-nourishment will feed the downdrift coastline at Domburg. This is supported by the mean alongshore sediment transport for wave condition c7, with the largest morphological impact (Figure 114). It can be seen that a positive transport gradient causes erosion at the west side of the nourishment (3300-3800m). The gradient changes into a negative gradient at the tip of the nourishment, and therefore accretion to the east is expected. Mainly the Domburg west coast, between 4500-5000m, is therefore supplied with sediment. Then, again a positive gradient is seen. Therefore, a mega nourishment does not solve the erosion near Domburg but supplies enough sediment to the coast.
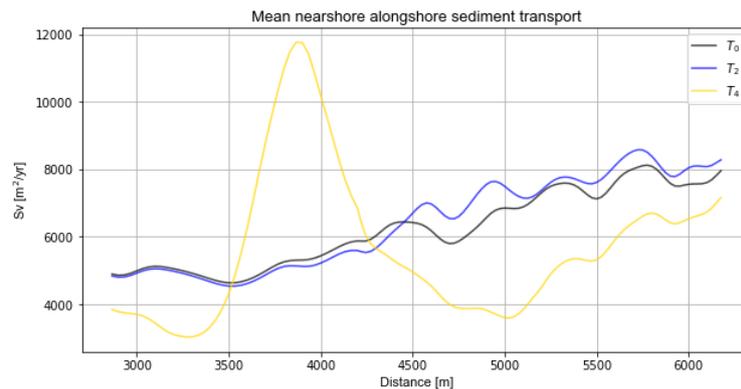
Figure 114: Mean alongshore sediment transport for wave condition c7: Hs=1.76m, Ө=272°, Tp=6.5s in the zone from the dune foot to 1000m offshore. The coast without nourishment (T₀), with a shoreface nourishment (T₂) and a mega-nourishment (T₄) are displayed.

6.3.4 Conclusion

The model results indicate that sediment will spread to both the west and east adjacent coastlines. As the net transport direction is eastward oriented, mainly the Domburg coastline will be fed. It is recommended to further look into this nourishment strategy as these preliminary results are promising. It should be further investigated what the consequences of the changed current and sediment transport patterns are.

7. Conclusions

The research questions from section 1.4 are answered with the observations and model results from a selection of beach and shoreface nourishments at the coast of Domburg, the Netherlands. This coast is located between the outer deltas of the Western- and Eastern Scheldt estuaries and does not feature shore parallel natural bars.

7.1 Observed development of the coast for different nourishment strategies

The first research question and sub-questions are answered with the results from the morphological data analysis.

1. *How does a coast without existing shore-parallel subtidal bars develop for different nourishment strategies?*

Beach nourishment

Beach nourishments at Domburg, T_1, are reshaped within one year after construction from a linear sloping beach of 1:27 to an exponential beach profile with a gentler average slope of 1:35. The beach volume reduction follows an exponential decay with a halftime of 0.8 years. Meanwhile, the inner surf zone accretes to some extent, but a substantial part of the nourished sediment is transported further seaward or alongshore. The average longevity of beach nourishments is estimated as 3.3 years with an erosion rate of -61m^3/m/yr.
A retreat of the momentary coastline (MKL) of -3.9m/yr is found. To sum up, beach nourishments are reshaped and eroded in a short time after construction but are effective at maintaining the MKL on short time scales.

Shoreface nourishment

For the shoreface nourishment at Domburg, T_2, a distinction is made between the western and eastern bar segments. The west segment, positioned close to the steep sub-tidal shoreface, moves onshore, erodes and merges with the shoreface. The east segment migrates onshore and transforms from triangular bar into a more rounded body. Remarkably, no formation of a trough was distinguished. No clear alongshore movement of the bar body was observed, although the sediment is mainly spread in downdrift direction to the adjacent east shoreface.
Meanwhile, the total bar volume remains relatively constant but is highly variable per transect as transects 1632 and 1530 show significant erosion. The alongshore sediment flux shows a larger positive gradient near Domburg for T_2 than for T_0, while the volume development shows that little volume is lost from the central coast. No MKL retreat is observed in the first 1.5 years after nourishment.
The adjacent west coastline shows a varying and stable beach and shoreface whereas the downdrift east shore shows a stable beach and an accreting shoreface.
To conclude, the shoreface nourishment migrates landward and feeds the coast locally on short time scales.

Combined beach and shoreface nourishment

The combined beach and shoreface nourishment at Domburg, T_3, show a rapid eroding beach despite the presence of a shoreface bar. The western shoreface bar portrays accretion in the trough zone due to the eroding beach nourishment, continuous smoothening and merging with the steep shoreface, and the emergence of a small breaker bar. Whereas the east segment shows considerable accretion in the surf zone which likely originates from the eroding beach nourishment. The eastern bar remains evident and the migration rate decreases. The alongshore sediment flux shows a larger positive gradient near Domburg for T_3 than for T_0. No evidence is found that the longevity of the beach nourishment is prolonged

98

due to the shoreface nourishment. Similar erosion rates, longevities and half-lives are computed for the 2019 beach nourishment compared to previous beach nourishments at Domburg. Also, it is observed that sediment is lost from the central coastline and that the MKL retreats with 4.3m/yr. To conclude, the shoreface nourishment shows no evidence for prolonging the lifetime of a beach nourishment, but the shoreface nourishment captures the eroded beach sediment to some extent.

7.2   Processes induced by different nourishment strategies

The second research question and sub-questions are answered with the output from the model analysis.

2. *What processes explain the observed morphological changes of a nourished coast without existing cross-shore subtidal bars?*

Salient effect

Although waves are dissipated further offshore at the shoreface nourishment during storms, the year-averaged wave height and dissipation on the leeside of the bar is not significantly reduced. Therefore, no wave-driven salient effect is evident. Although, a current reduction at the landward side and in downdrift direction of the shoreface nourishment is computed. Evidence is found at the downdrift coastline of accretion at the shoreface from the data analysis.

Contraction of tidal flow

Due to the presence of a shoreface bar, the current velocity seaward of the bar is enhanced. This is mainly caused by the contraction of the tidal flow. As a consequence, larger gradients in alongshore sediment transport are computed. This is supported by the morphological changes at the seaward shoreface, where an accreting trend before the 2017 shoreface nourishment changes into an erosive trend after the implementation of the 2017 shoreface and 2019 beach nourishments.

The influence of a beach nourishment is insignificant on the large-scale nearshore hydrodynamics and alongshore transport rates. Marginal effects on currents and sediment transport rates are computed and therefore no contraction of the tidal flow is found for a beach nourishment.

Migration and residual currents

The landward migration of a shoreface bar is due to sediment transport induced by skewed non-breaking waves. This sediment was deposited in the through zone. The residual current formed at the shoreface bar was not able to erode a trough at the landward side. For shoreface nourishments at coasts with original cross-shore bar behaviour, the landward zone usually erodes whereas considerable accretion is observed at Domburg.

The numerical model output indicates that return currents are formed at the central shoreface bar and at the east bar end. These return currents are responsible for the local erosion at transect 1530.

7.3   Hindcast volume prediction with a morphostatic model

The third research question and sub-questions are answered with a comparison between computed and observed volume changes.

3. *To what extent is a morphostatic numerical model able to represent the volume changes in coastal zones?*

The comparison between modelled and measured volume changes in coastal zones show a poor performance of the model. The modelled erosion and sedimentation at the adjacent coastlines are unrealistically large. Therefore, the alongshore gradients in sediment transports are smaller in reality.

The volume changes at the central coastline are approximately in the right order of magnitude. Additionally, the volume change of the central seaward shoreface was predicted accurately. However, the model predicted accretion in the initial nourishment zone where erosion was observed. Similarly, erosion was predicted in the trough zone while measurements show sedimentation.

The performance of the hindcast prediction for a shoreface nourishment and a combined shoreface and beach nourishment showed no significant differences. Concluding, a morphostatic model with simplified boundary conditions and a single post-construction bathymetry was not able to correctly hindcast volume changes.

8. Recommendations

Chapter 8 starts with the recommended nourishment strategy to maintain the structural eroding coastline near Domburg. Hereafter, suggestions for follow-up studies are done as this research raises multiple questions.

8.1   Recommended nourishment strategy Domburg

Considering the different nourishment strategies from section 6.1, it is recommended to apply an extra shoreface nourishment just seaward of the 2017 shoreface nourishment. This nourishment contributes to the sediment balance of the coastal cell and showed a landward migration while a distinct body of sand remained for more than four years after construction. Therefore, repeated shoreface nourishments are likely to feed the nearshore zones on a longer timescale. On shorter timescales, it is advised to implement a beach nourishment to mitigate the loss of dune and beach areas. Moreover, applying shoreface nourishments is cost-effective and the first experience with this nourishment type at Domburg is good.

Continuing this nourishment strategy allows for more research on remaining knowledge gaps regarding shoreface bars. Subsequent shoreface nourishments at Domburg may create a barred coast with bar behaviour. Moreover, if a barred system can be created, the net migration direction and the existence a bar cycle and a zone of decay are of interest. The cross-shore position of the shoreface nourishment can also be researched, as the implementation on top or landward of the 2017 shoreface nourishment are viable options. Hence, it is advised to continue this nourishment strategy and invest in extra monitoring and research to improve the understanding of the morphodynamic behaviour of shoreface bars.

Alternatively, if this strategy fails to maintain the coastline at Domburg, it is recommended to further investigate the opportunity for a mega nourishment which can supply sediment to both the coastline at the Westkappelse Zeedijk and at Domburg. This nourishment strategy is promising as the results from this study indicate that sediment is spread to the southwest and the northeast. Also, the implementation is cost-effective and the maintenance interval is extended. Furthermore, such an artificial shoreline perturbation would fit the natural character of the coast, as a similar feature is found at Oranjezon, Walcheren.

8.2   Transverse bars

Relatively unknown morphological features are transverse bars. It is recommended to further look into the variety and behaviour of these features. For example, differences in the alongshore migration rate in the surf zone and seaward of the surf zone can be researched. Transverse bars are affected by both the wave-driven alongshore and the tidal current in the surf zone, whereas further offshore, solely a stronger tidal current is present. Additionally, what processes are responsible for the changing alongshore migration rate, bar height and wavelength as observed at Domburg. Also, the sediment supply to the beach by processes such as wave-focussing can be investigated.
Furthermore, this study predicts that the alongshore migration rate is increased and decreased at respectively the seaward and the landward side of the shoreface nourishment. It can be studied whether their behaviour is affected by the presence of the shoreface bar. For this purpose, additional surveys are recommended in a shore parallel manner. This allows for a better determination of crest and trough positions.
Additionally, it is suggested to look into a nourishment strategy considering the transverse bars as elaborated upon in subsection 6.1.5.

8.3   Estimating sediment fluxes from data

It is argued that the estimated sediment fluxes are unrealistic in this study. Nevertheless, it is recommended to further develop this tool. Estimating sediment fluxes from data instead of a numerical model implicitly captures all hydraulic and morphological processes. Therefore, this can be a valuable tool to evaluate sediment transport patterns in hindcast. This technique has been applied in previous studies on longer timescales with large spatial domains. More insight in transport patterns is valuable for our understanding of coastal processes.

It is recommended to improve the level of detail of the box model and apply it for shorter timescales. This can be done by increasing the number of boxes. For instance, every JARKUS transect can be evaluated with 5-10 cross-shore zones.

Nevertheless, reliable boundary conditions need to be provided to eliminate errors from simplifications and assumptions. For instance, a field campaign can provide more information on the sediment flux over the landward boundary, being dependent on the type and amount of vegetation, or the in- and out-going sediment fluxes.

As variations or measurement errors can affect the results of such linear model, the mathematics of linear systems can help to allow more margin for the estimation of sediment fluxes. For example, a Monte Carlo method can be applied for estimating boundary conditions and sediment fluxes to converge to the most realistic estimate. Moreover, a Monte Carlo method can be used to calculate the most probable sediment fluxes for a range of boundary conditions.

8.4   Bar flattening in morphodynamic models

Morphodynamic models are not capable of correctly predicting the volume development of a barred coast. The model-physics have a tendency to flatten out sub-tidal bars and it is not yet clear what mechanisms cause this. To enhance morphodynamic model performance, it is suggested to improve the understanding of mechanisms driving the behaviour of shoreface bars and nourishments. This can help the parameterization of secondary flows in numerical models. Moreover, instead of using 2-D depth averaged models, it is suggested to look into the application of models that resolve vertical flows such as OpenFoam or Unibest TC. However, as these models are computationally expensive, simulating large domains is challenging.

8.5   Performance of morphostatic models with multiple bathymetries

This study shows a limited performance of predicting volume changes with a morphostatic model with a single fixed bathymetry. It is recommended to look into the performance of a morphostatic model with multiple fixed bathymetries. In this manner, the first period can be simulated with the post-construction survey and hereafter the bathymetry can be changed to surveyed JARKUS bathymetries. The realistic bar transformation is captured in the morphostatic model which will likely produce more realistic output. Then, the response of hydrodynamic and morphodynamic parameters to a nourishment can be evaluated. Also, it can be studied whether this method significantly improves the hindcast as compared to one single post-construction bathymetry.

References

Ashton, A., & Murray, A. (2006). High-angle-wave instability and emergent shoreline shapes: 1. Modeling of sandwaves, flying spits and capes.

Bagnold, R. (1966). *An approach to the sediment transport problem.* General Physics Geological Survey.

Benedet, L., Finkl, C., & Hartog, W. (2007). Processes Controlling Development of Erosional Hot Spots on a Beach Nourishment Project. *Journal of Coastal Research*, 33-48.

Bosboom, J., & Stive, M. (2015). *Coastal dynamics 1.* Delft.

Bruins, R. (2016). *Morphological behaviour of shoreface nourishments along the Dutch coast.*

Brutsché, K., McFall, B., Bryant, B., & Wang, P. (2019). *Literature review of Nearshore Berms.* US Army Corps of Engineers.

de Ruig, J. (1998). Coastline management in The Netherlands: human use versus natural dynamics. *Journal of Coastal Conservation*, 127-134.

de Schipper, M., de Vries, S., Ranasinghe, R., Reniers, A., & Stive, M. (2013). *Alongshore topographic variability at a nourished beach.*

de Sonneville, B., & van der Spek, A. (2012). *Sediment- and morphodynamics of the shoreface nourishments along the north-holland coast.*

Dean, R. (2003). Beach nourishment: theory and practice. *World Scientific Publishing Company*, volume 18.

Deltares. (2014). *Ontwikkeling Zwakke-Schakel suppletie Westkapelle - morfologische veranderingen 2008-2013.*

Deltares. (2018). *Beheerbibliotheek Walcheren en Noord-BevelandNeerse Dam.*

Deltares. (2020). *XBeach manual.*

Elias, E., van der Spek, A., & Lazar, M. (2016). *The 'Voordelta', the contiguous ebb-tidal deltas in the SW Netherlands: large-scale morphologcal changes and sediment budget 1965-2013; impacts of large-scale engineering.* Netherlands Journal of Geosciences.

Ende, I. v. (2017). *Onshore sandbar migration, Processing PIV measurements to analyse wave driven sediment transport in the nearshore.*

Fockert, A. d. (2008). *Impact of relative sea level rise on the Amelander inlet morphology.*

Geurts van Kessel, A. (2004). *Verlopend tij; Oosterschelde, een veranderend natuurmonument.*

Giardino, A., den Heijer, K., & Santinelli, G. (2014). *The state of the coast: Case study of the South-Westerly Delta.*

Giardino, A., den Heijer, K., Santinelli, G., & van der Werf, J. (2013). *Tools for medium- and long-term prediction of nourishment effects.*

Grunnet, N., & Ruessink, B. (2005). *Morphodynamic response of nearshore bars to.* Coastal engineering.

Hallermeier, R. (1981). *A profile zonation for seasonal sand beaches from wave climate.* American Society of Civil Engineers.

Hamm, L., Capobianco, M., Dette, H., Lechuga, A., Spanhoff, R., & Stive, M. (2002). *A summary of European experience with shore nourishment.* Coastal Engineering.

Hands, E., & Allison, M. (1991). *Mound migration in deeper water and methods of categorizing active and stable depths.* American society of Civil Engineers.

Henriquez, M. (2019). *Onshore sandbar migration in the nearshore.*

Huisman, B. (2019). *On the redistribution and sorting of sand at nourishments: Field evidence and modelling of transport processes and bed composition change.*

Interreg. (2019). *National analyses of nourishments; coastal state indicators and driving forces for Domburg, the Netherlands.*

Interreg. (2021). *Embracing nature based solutions - Policy Brief The Netherlands.* Retrieved from NorthSeaRegion: https://northsearegion.eu/building-with-nature/output-library/

Kohsiek, L. (1984). *De korrelgrootte karakteristiek van de zeereep (stuifdijk) langs de nederlandse kust.* Rijkswaterstaat.

Kraus, N., Larson, M., & Wise, R. (1998). *Depth of Closure in Beach Fill Design.* Vicksburg.

Larsen, B., Carstensen, R., Carstensen, S., van der A, D., & Fuhrman, D. (2021). Experimental Investigation of Shoreface Nourishment Scenarios. *Coastal Dynamics 2021.* Delft.

Lazar, M., Elias, E., & Spek, A. v. (2017). Coastal maintenance and management of the 'Voordelta', the contiguous ebb-tidal deltas in the SW Netherlands. *Coastal Dynamics.*

Lesser, G. (2009). *An approach to medium-term coastal morphological modelling.*

Levoy, F., Anthony, E., Monfort, O., Robin, N., & Bretel, P. (2013). Formation and migration of transverse bars along a tidal sandy coast deduced from multi-temporal Lidar datasets. *Marine Geology*, 39-52.

Lodder, Q., & Sørensen, P. (2015). *Comparing the morphological behaviour of Dutch-Danish shoreface nourishments.*

Ludka, B., Gallien, T., Crosby, S., & Guza, R. (2016). Mid-El Niño erosion at nourished and unnourished Southern California beaches. *Geophys. Res. Lett.*, 4510–4516.

Lyu, J. (2019). *Examining parameters that control spreading of a concentrated noruishment.*

McCall, R., van Santen, R., & Huisman, B. (2014). *Coastline modelling - Phase III - Investigation of the influence of model schematisation on a hindcast for the coast of Domburg.*

Ojeda, E., Ruessink, B., & Guillen, J. (2008). *Morphodynamic response of a two-barred beach to a shoreface nourishment.* Coastal Engineering.

Onnink, C. (2020). *Dynamic shoreline response to a shallow concentrated nearshore berm nourishment.*

Radermacher, M., de Schipper, M., Price, T., Huisman, B., Aarninkhof, S., & Reniers, A. (2018). *Behaviour of subtidal sandbars in response to nourishments.* Geomorphology.

Ribas, F., & Kroon, A. (2007). Characteristics and dynamics of surfzone transverse finger bars. *GEOPHYSICAL RESEARCH*.

Rijkswaterstaat. (2007). *Richtlijnen onderwatersuppleties.*

Rijkswaterstaat. (2020). *Kustgenese 2.0: kennis voor een veilige kust.*

Rijkswaterstaat. (2020). *Memo uitvoeringskader suppletieprogramma 2020 v2.5.*

Rijkswaterstaat. (2021, june). *Coastviewer*. Retrieved from https://www.openearth.nl/coastviewer-static/

Rijkswaterstaat and Deltares. (2019). *National analyses of nourishments; Coastal state indicators and driving forces for Domburg, the Netherlands.*

Roelvink, D., Reniers, A., van Dongeren, A., van Thiel de Vries, J., McCall, R., & Lecinski, J. (2009). Modelling storm impacts on beaches, dunes and barrier islands. *Coastal engineering*, 1133–1152.

Ruessink, B., & Kroon, A. (1994). *The behaviour of a multiple bar system in the nearshore zone of Terschelling, the Netherlands: 1965-1993.* Marine geology.

Ruessink, B., Kuriyama, Y., Reniers, A., Roelvink, J., & Walstra, D. (2007). *Modeling cross-shore sandbar behavior on the timescale of weeks.* Journal of geophysical research.

Ruessink, B., van der Grinten, R., Vonhögen-Peeters, L., Ramaekers, G., & Lodder, Q. (2012). *Nearshore evolution at Noordwijk (NL) in response to nourishments, as inferred from Argus video imagery.*

Schiereck, G., & Verhagen, H. (2019). *Introduction to bed, bank and shore protection.* Delft.

Shek, K.-W. (2021). Relationship Analysis between Beach Nourishment Longevity and Design Aspects using a Multiple Linear Regression Model.

Spanhoff, R., & van de Graaff, J. (2007). Towards a better understanding and design of shoreface nourishments. *Proceedings of the 30th international conference coastal engineering 2006*, 4141-4153.

Sündermann, J., & Pohlmann, T. (2011). A brief analysis of North Sea Physics. *Oceanologia*, 663-689.

Tonnon, P., Huisman, B., Stam, G., & van Rijn, L. (2018). *Numerical modelling of erosion rates, life span and maintenance volumes of mega nourishments.* Coastal Engineering.

van der Spek, A., & Lodder, Q. (2015). *A new sediment budget for the Netherlands; the effects of 15 years of nourishing (1991-2005).*

van Duin, M., Wiersma, N., Walstra, D., van Rijn, L., & Stive, M. (2004). *Nourishing the shoreface: observations and hindcasting of the.* Coastal engineering.

van Rijn, L. (2011). *Coastal erosion and control.* Ocean and Coastal management.

Verhagen, H. (1989). *Sand waves along the Dutch coast.* Delft: Coastal engineering.

Verhagen, H. (1992). Method for Artificial Beach Nourishment. *International Conference on Coastal Engineering*.

Vos, P., Bazelmans, J., Weets, H., & van der Meulen, M. (2011). *Atlas van Nederland in het Holoceen; Landschap en bewoning vanaf de laatste ijstijd to nu.*

Walstra, D. (2016). *On the anatomy of nearshore sandbars: A systematic expostion of inter-annual sandbar dynamics.*

Walstra, D., Hoyng, C., Tonnon, P., & van Rijn, L. (2011). *Experimental study investigating various shoreface nourishment designs.*

Walstra, D., van Ormondt, M., & Roelvink, J. (2004). *Shoreface nourishment scenarios.*

Zimmerman, J. (1978). Topographic generation of residual circulation by oscillatory (tidal) currents. *Geophys. Astrophys. Fluid Dyn. 11*, 35-47. Retrieved from http://www.coastalwiki.org/wiki/Sand_ridges_in_shelf_seas#cite_note-12

Appendix A

A.1 Wave climate

Figure 115: Significant wave height Schouwenbank. Wave height measurements above 2m have been indicated in orange to stress the high energy level of the waves.

Waverose Hs 2008

Waverose Hs 2012

Waverose Hs 2014

Waverose Hs 2017
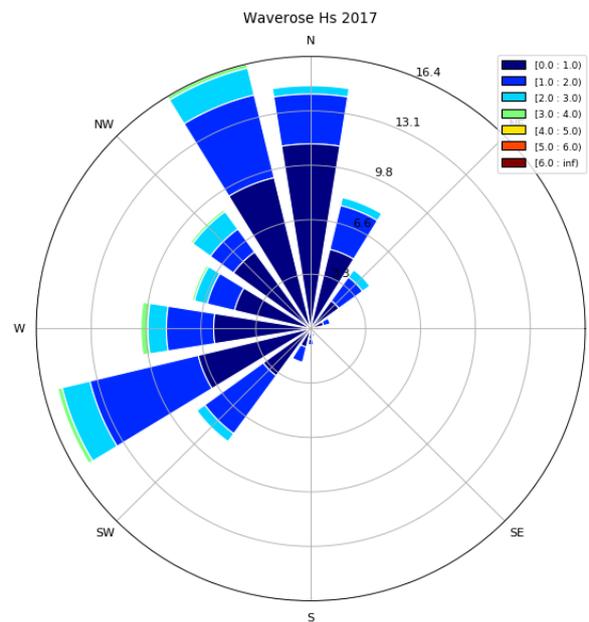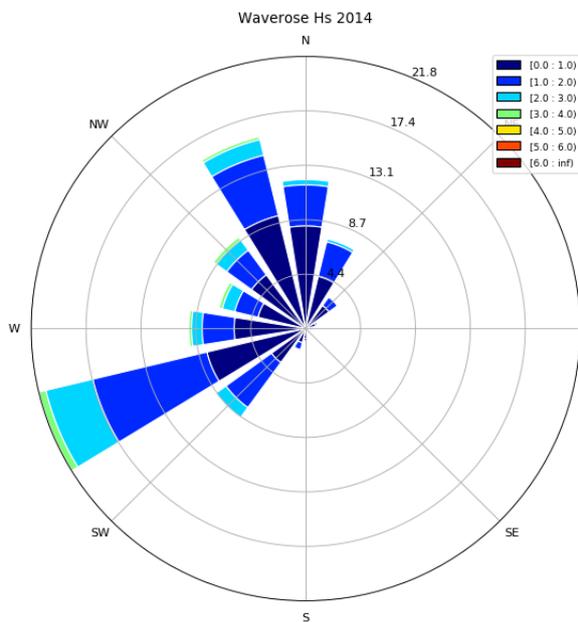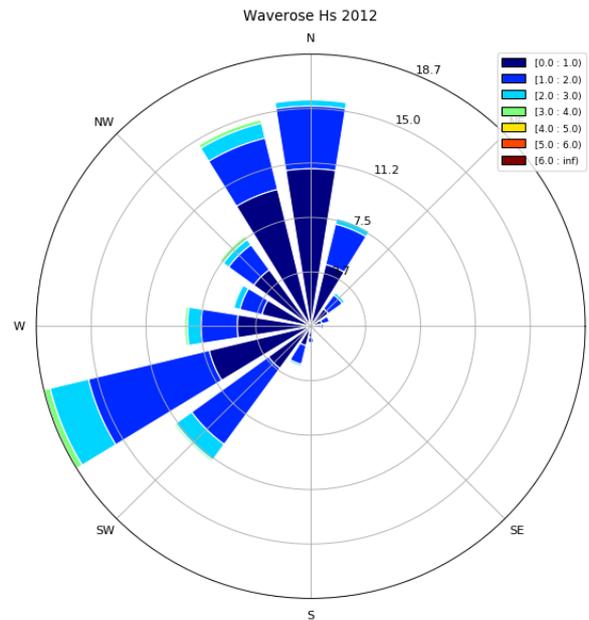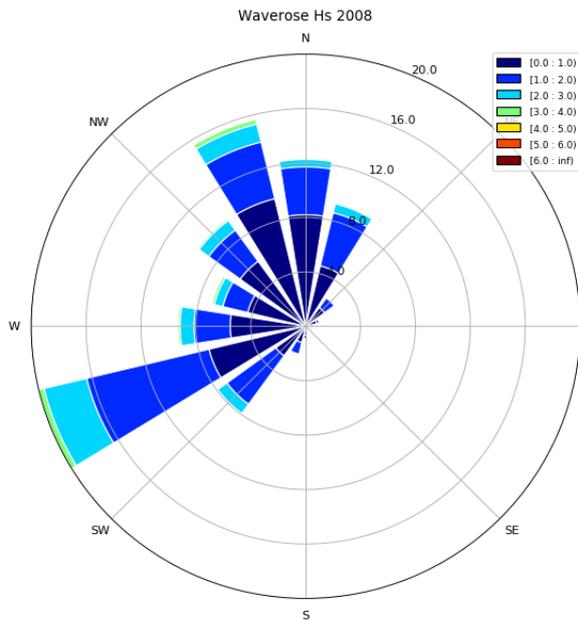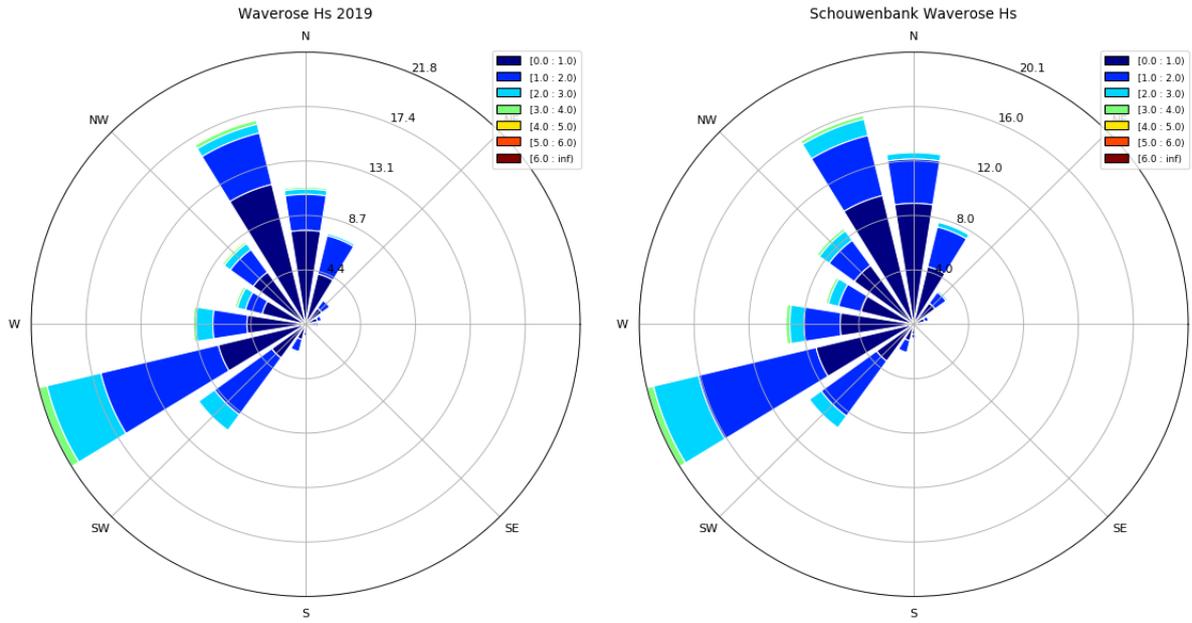
Figure 116: Wave roses after the 2008, 2012, 2014, 2017,2019 nourishments and the wave rose over the period Jan 2008-Jan 2021. Based on wave data from the Schouwenbank wave buoy [m].
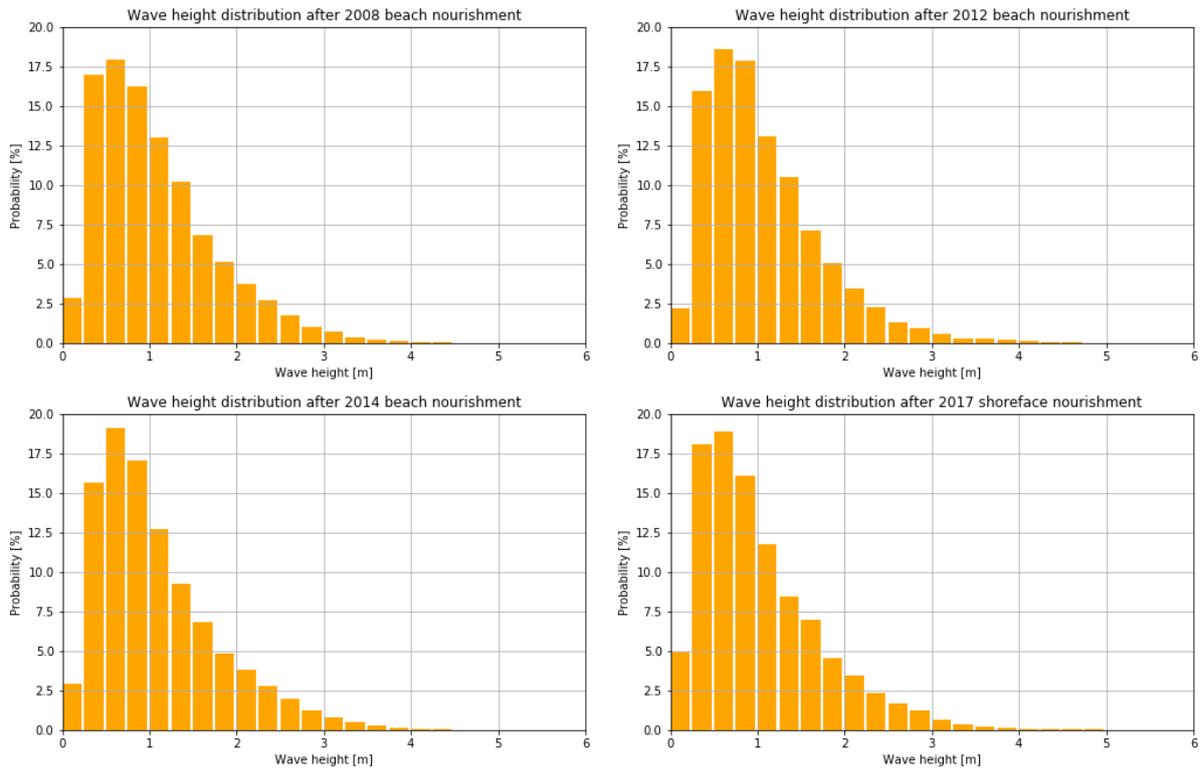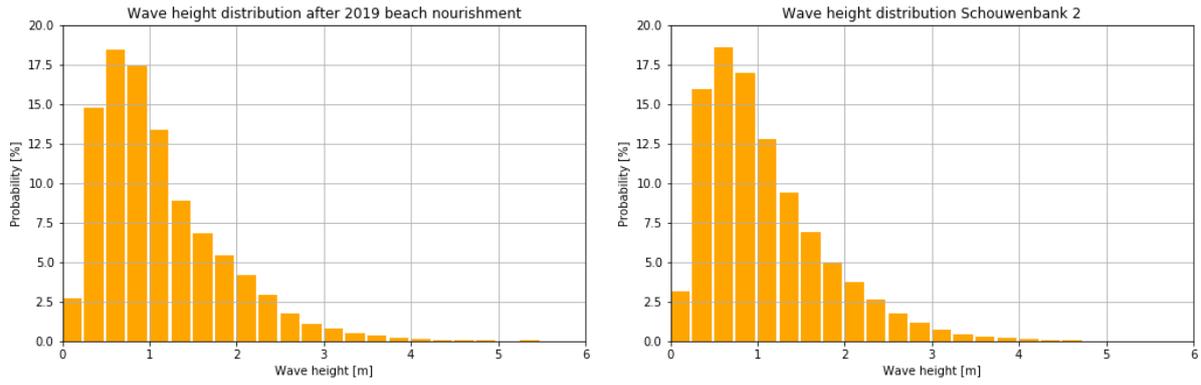
Figure 117: Wave height distribution between the 2008, 2012, 2014, 2017,2019 nourishments and the general wave height distribution over the period Jan 2008-Jan 2021. Based on wave data from the Schouwenbank wave buoy.

A.2 Wind climate
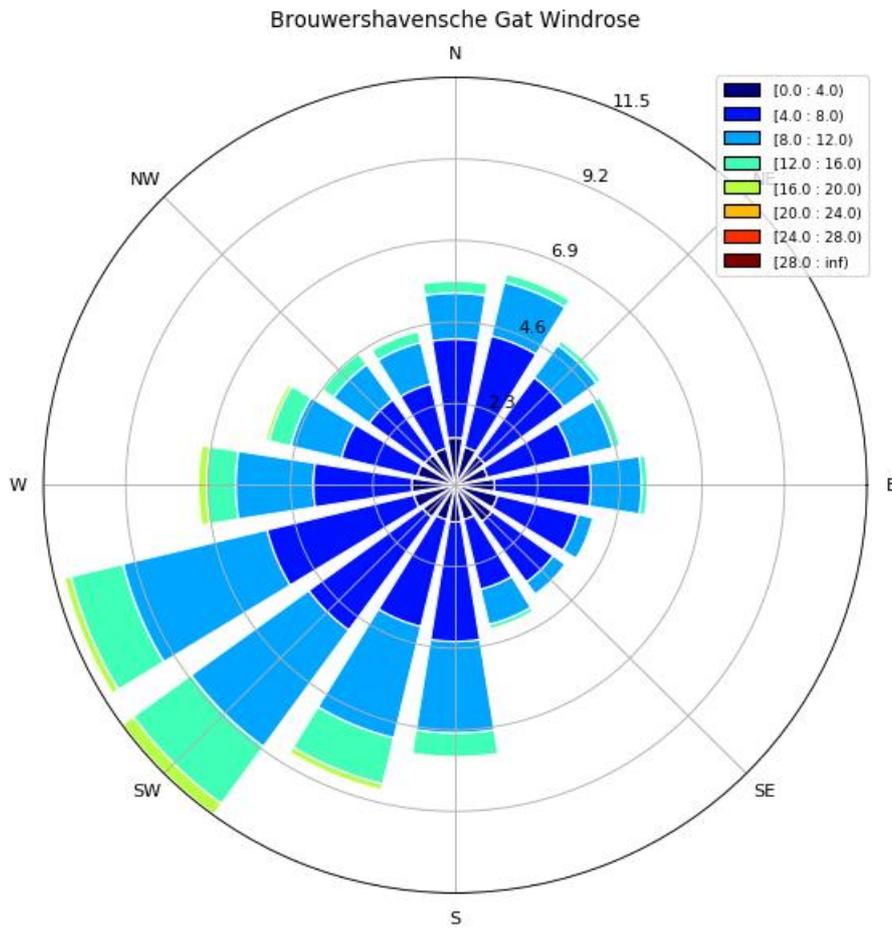
Figure 118: Wind rose at the Brouwershavensche Gat in the period Jan 2016 - Jan 2021 [m/s].

Appendix B

Appendix B presents the cross-shore profiles of the NW Walcheren coast in the period Jun 2017 - Mar 2021. The transects start in the west at the Westkappelse Zeedijk, to the nourished coast near Domburg in the Centre, and to the East with an interspacing of approximately 200m.

B.1 West: transects 1735-1653

The transects 1694-1653 are used for the analysis of the west coastline, as nourishments are implemented in the same period in transects 1948-1735.

Transect 1694

Transect 1673

Transect 1653
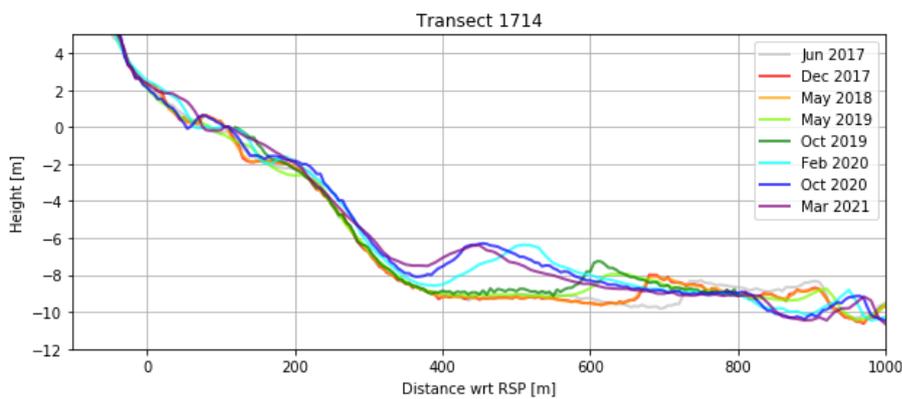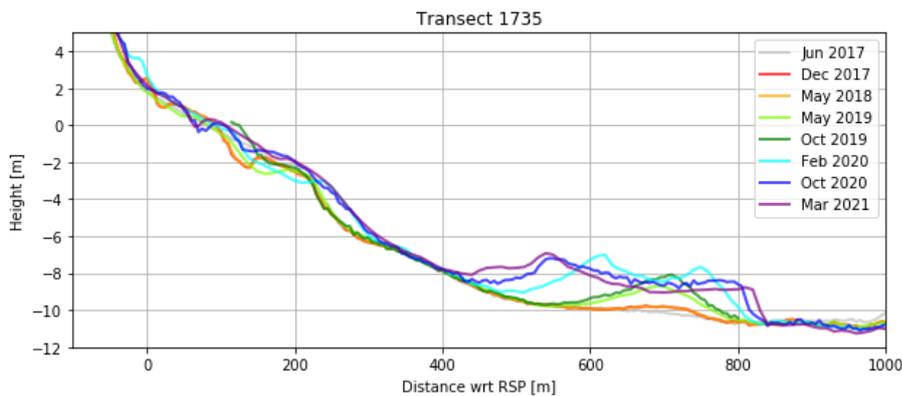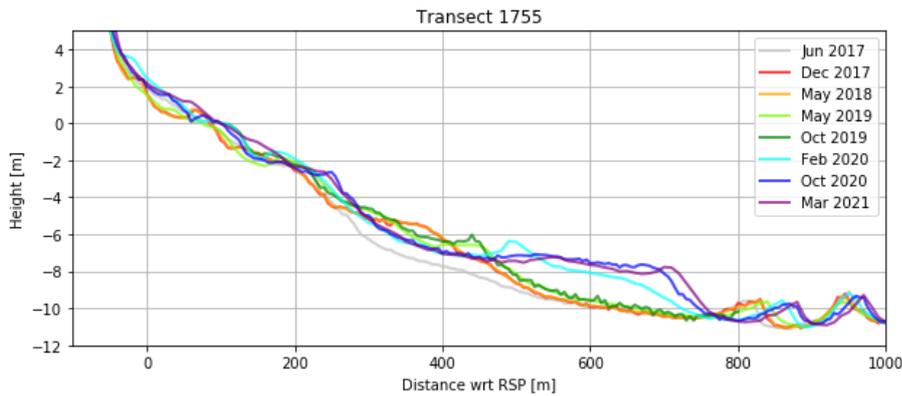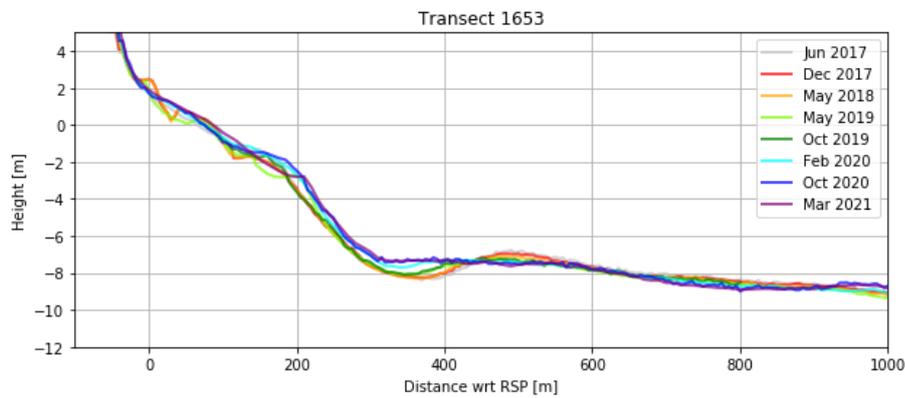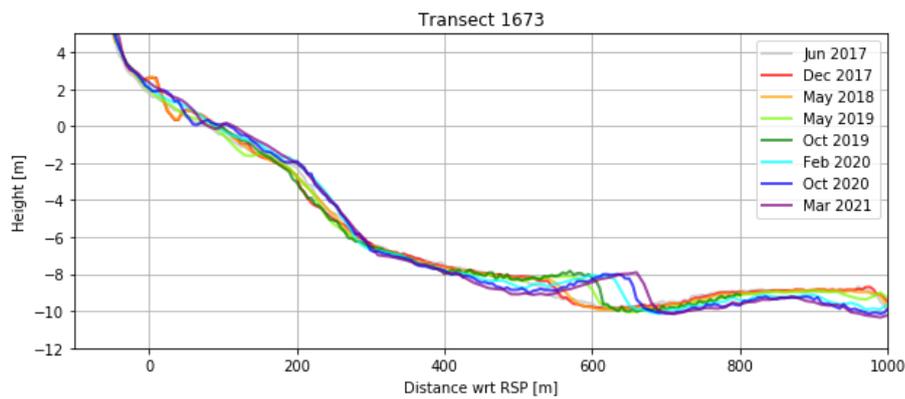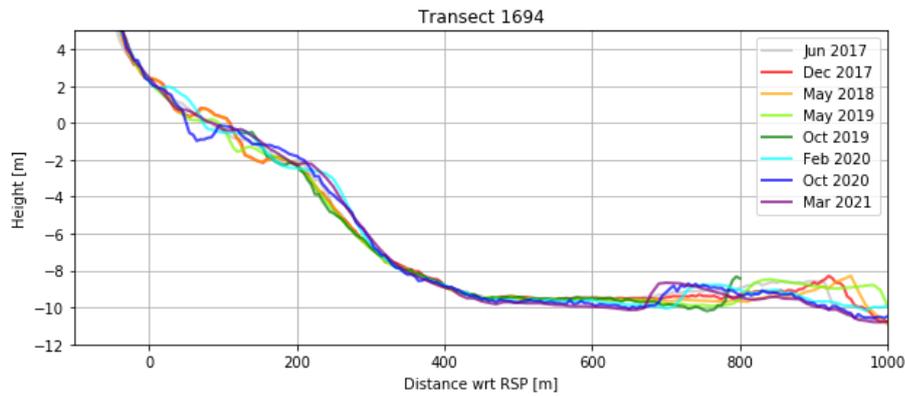
B.2 Central: transects 1632-1448

The central transects are supplied with a shoreface nourishment in Dec 2017 and a beach nourishment in Apr 2019.


Transect 1632

Transect 1612

Transect 1591

Transect 1571

Transect 1550

Transect 1530

Transect 1509

Transect 1489

Transect 1469
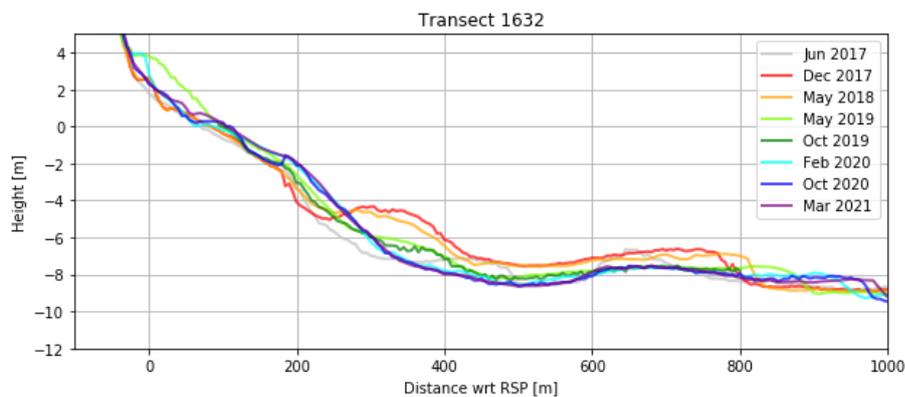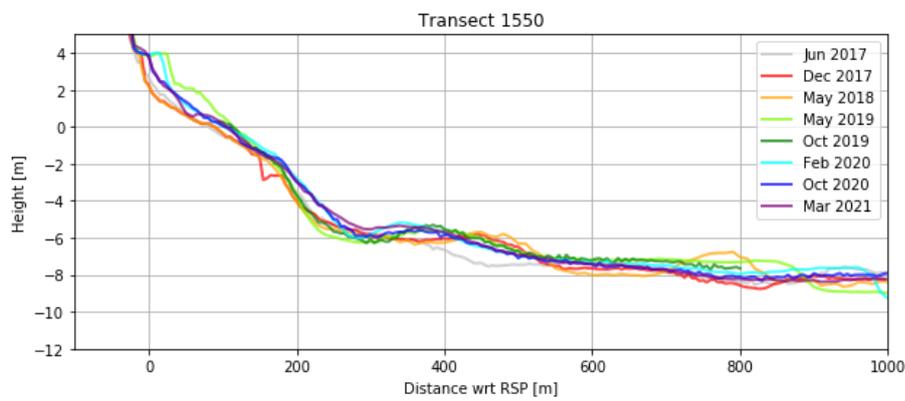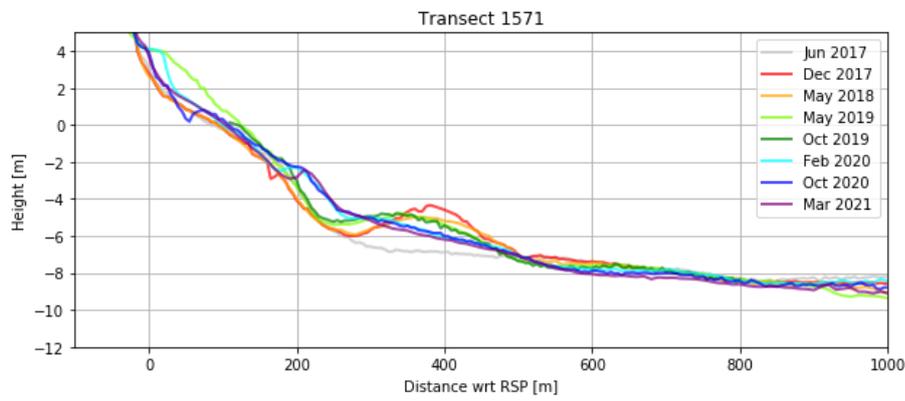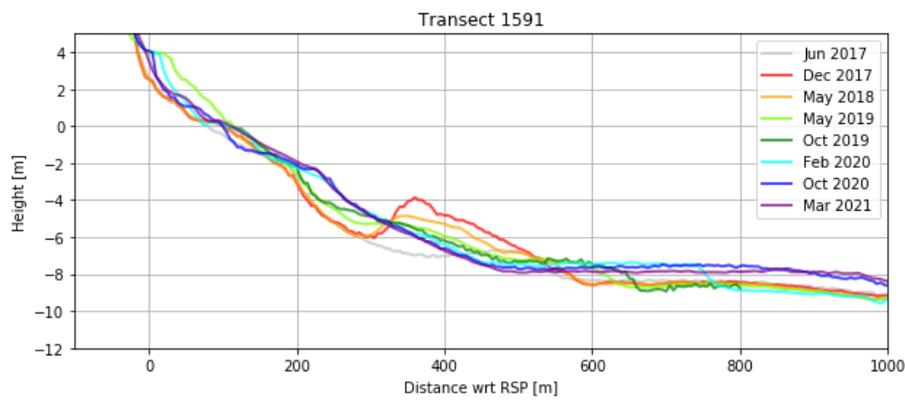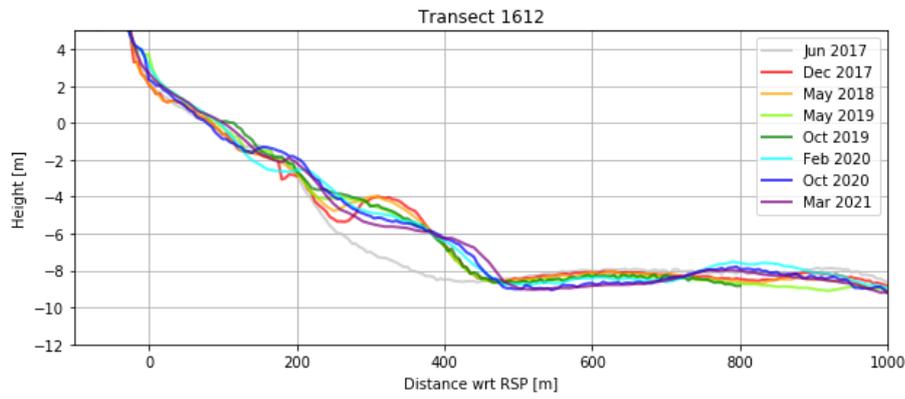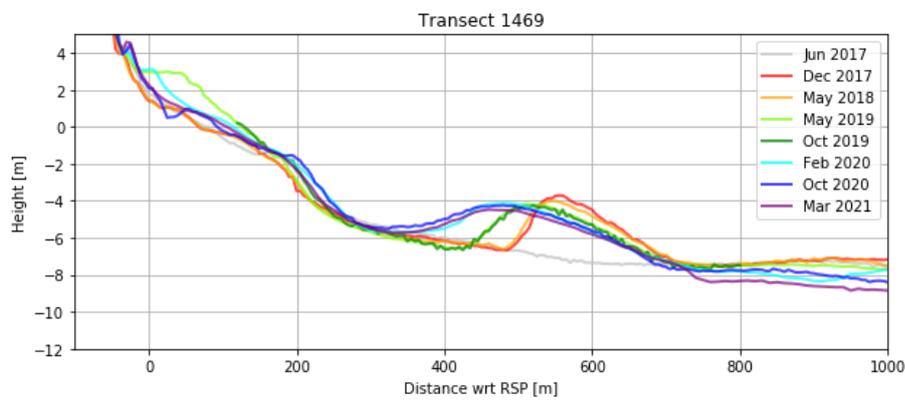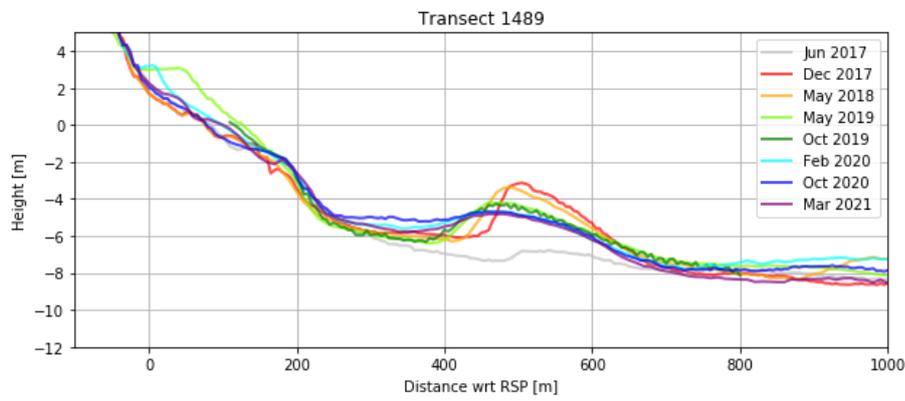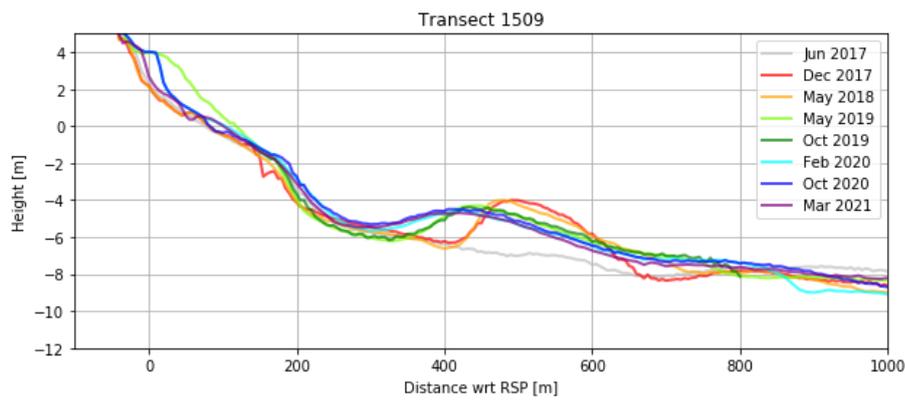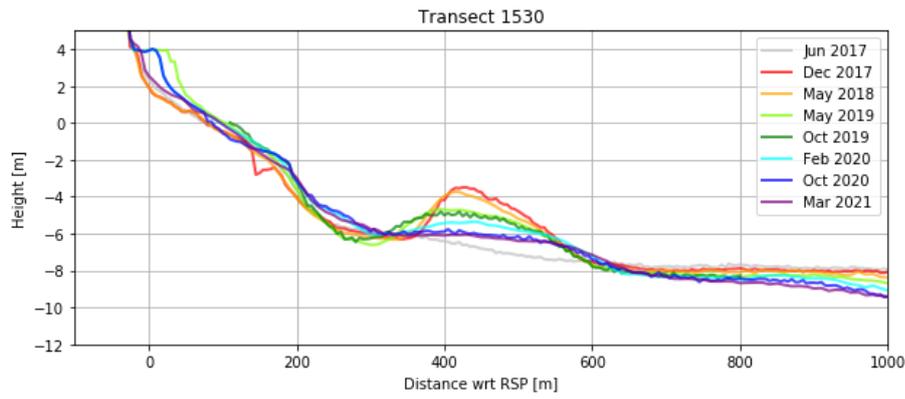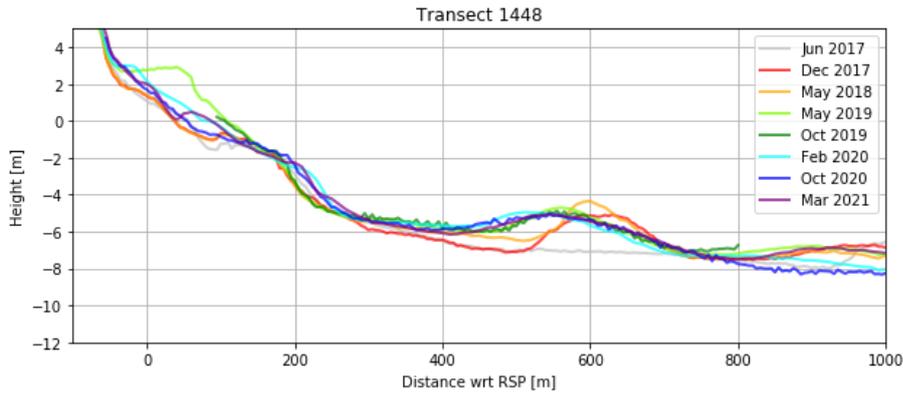
Transect 1448

B.3 East: transects 1448-1306

No nourishments were constructed in the East transects in the interval 2017-2021.

Transect 1428

Transect 1406

Transect 1386

Transect 1366

Transect 1346

Transect 1326

Transect 1306

x
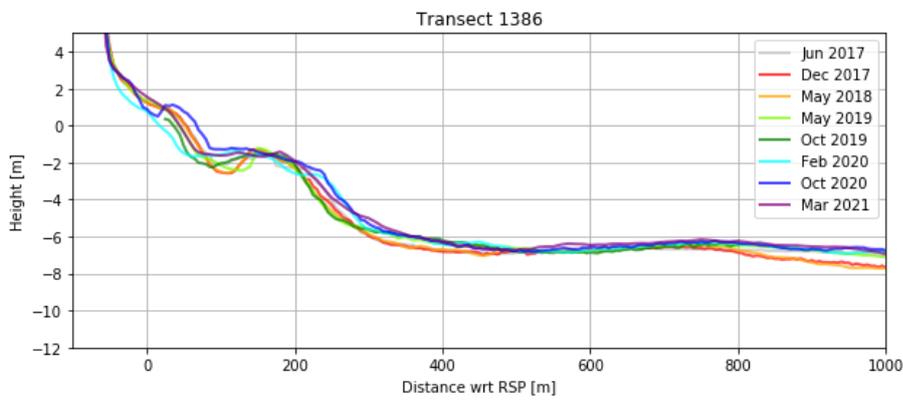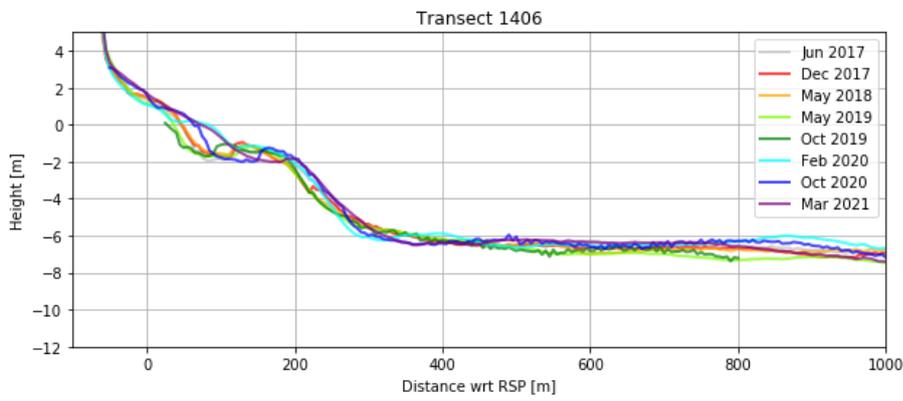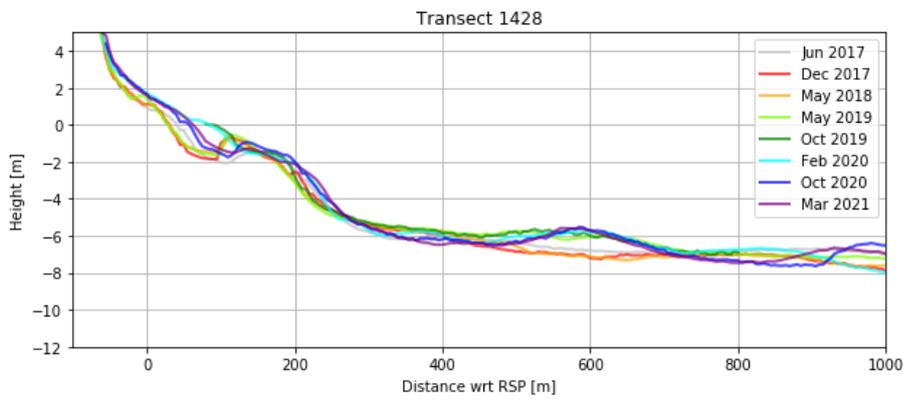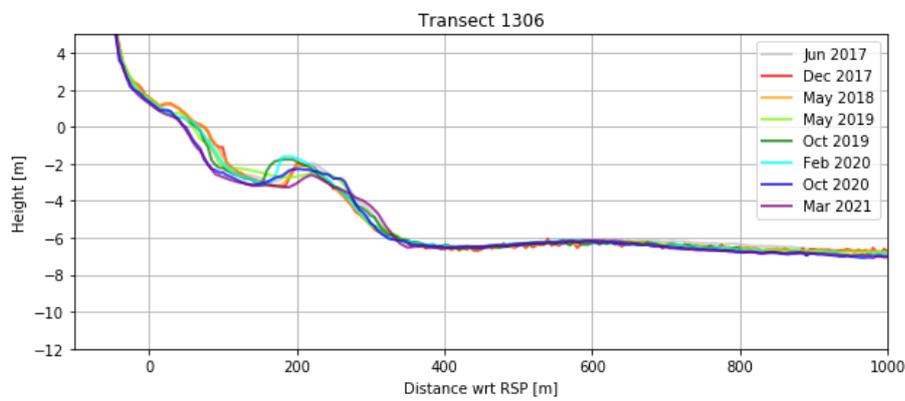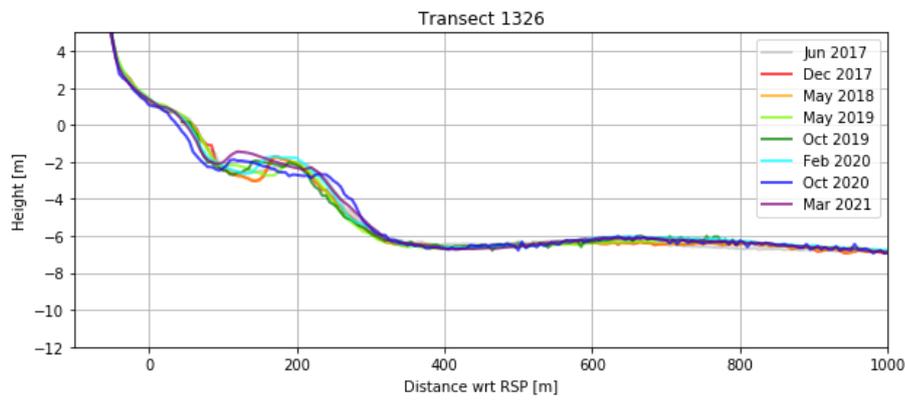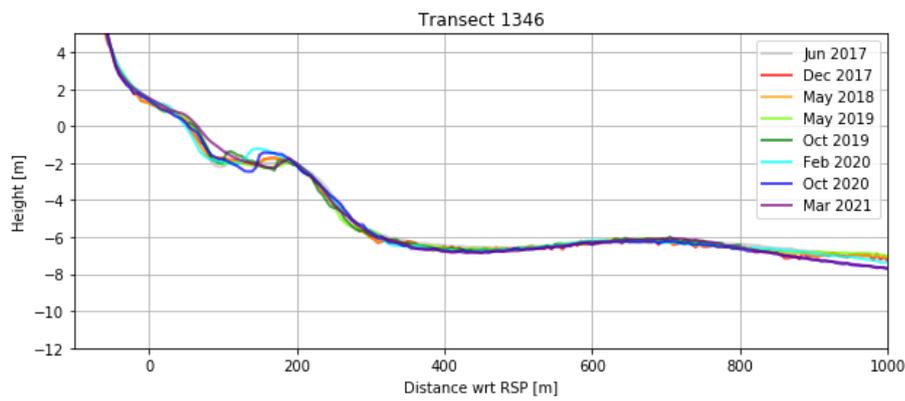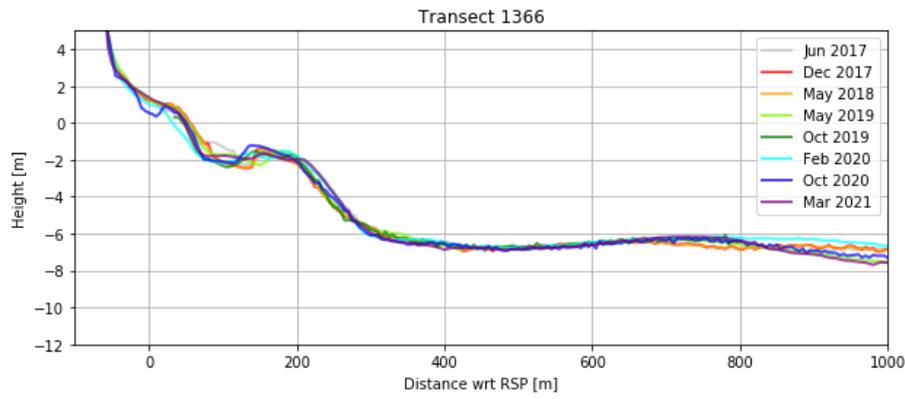
Appendix C

This Appendix present the numerical model input. It provides the settings for XBeach, the boundary conditions, grid and bathymetry.

C.1 XBeach settings

Table 16: Default XBeach settings according to the safety evaluations of the Dutch primary water defences (Huisman, 2019).

Type	Description	Keyword	Value	Unit
Physical processes		Wave model	Surfbeat	
Grid	grid resolution (2DH)	*dx & dy*	10 - 50	m
Waves	Wave skewness factor	*facSk*	0.375	
	Wave asymmetry factor	*facAs*	0.123	
	Depth breaking parameter	*gamma*	0.541	
	Steepness breaking parameter	*alpha*	1.262	
	Min. adaptation time scale	*Tsmin*	1	s
	Max. wave steepness	*maxbrsteep*	0.4	
	Max. wave height	*gammax*	2.364	
Roller	Breaker slope coefficient	*beta*	0.138	
	Roller dissipation power	*n*	10	
Friction	Bed friction formulation	*bedfriction*	Chezy	
Sediment	Median grain diameter	D_{50}	300	μm
	90th percentile grain diameter	D_{90}	400	μm

C.2 Boundary conditions

This section provides the input for the model boundaries: the offshore wave classes and the morphological tide.

C.2.1 Wave conditions at the Schouwenbank 2 buoy

Table 17: Offshore wave conditions outside the model boundaries at the Schouwenbank 2 wave buoy.

|	Wave class [°N]	H_s [m]	Θ_{wave} [°N]	T_p [s]	U_{wind} [m/s]	Θ_{wind} [°N]	P [%]	Weight [%]
	$0.25 \le H_s < 1.25$							
1.	210-300	0.75	253.61	4.53	6.38	230.52	24.73	6.79
2.	300-30	0.68	346.86	5.53	4.90	330.95	32.21	7.25
	$1.25 \le H_s < 2.0$							
3.	210-255	1.58	238.13	5.52	10.80	221.07	8.90	12.93
4.	255-300	1.58	273.83	5.68	9.29	262.90	2.87	4.21
5.	300-345	1.57	329.10	6.50	7.29	313.44	3.84	5.54
6.	345-30	1.53	365.90	6.11	8.78	386.54	3.24	4.37
	$2.0 \le H_s < 3.0$							
7.	210-300	2.35	251.87	6.47	13.28	242.22	5.48	21.45
8.	300-30	2.39	335.77	7.08	10.75	336.85	3.10	12.66
	$3.0 \le H_s$							
9.	210-300	3.45	260.05	7.50	16.85	256.25	1.00	10.23
	$3.0 \le H_s < 4.0$							
10.	300-30	3.35	334.86	7.97	13.81	341.31	0.68	6.36
	$4.0 \le H_s < 7.0$							
11.	300-30	4.55	322.57	8.89	16.77	328.85	0.16	3.19
	Total						**86.21**	**94.98**

C.2.2 Tidal signal
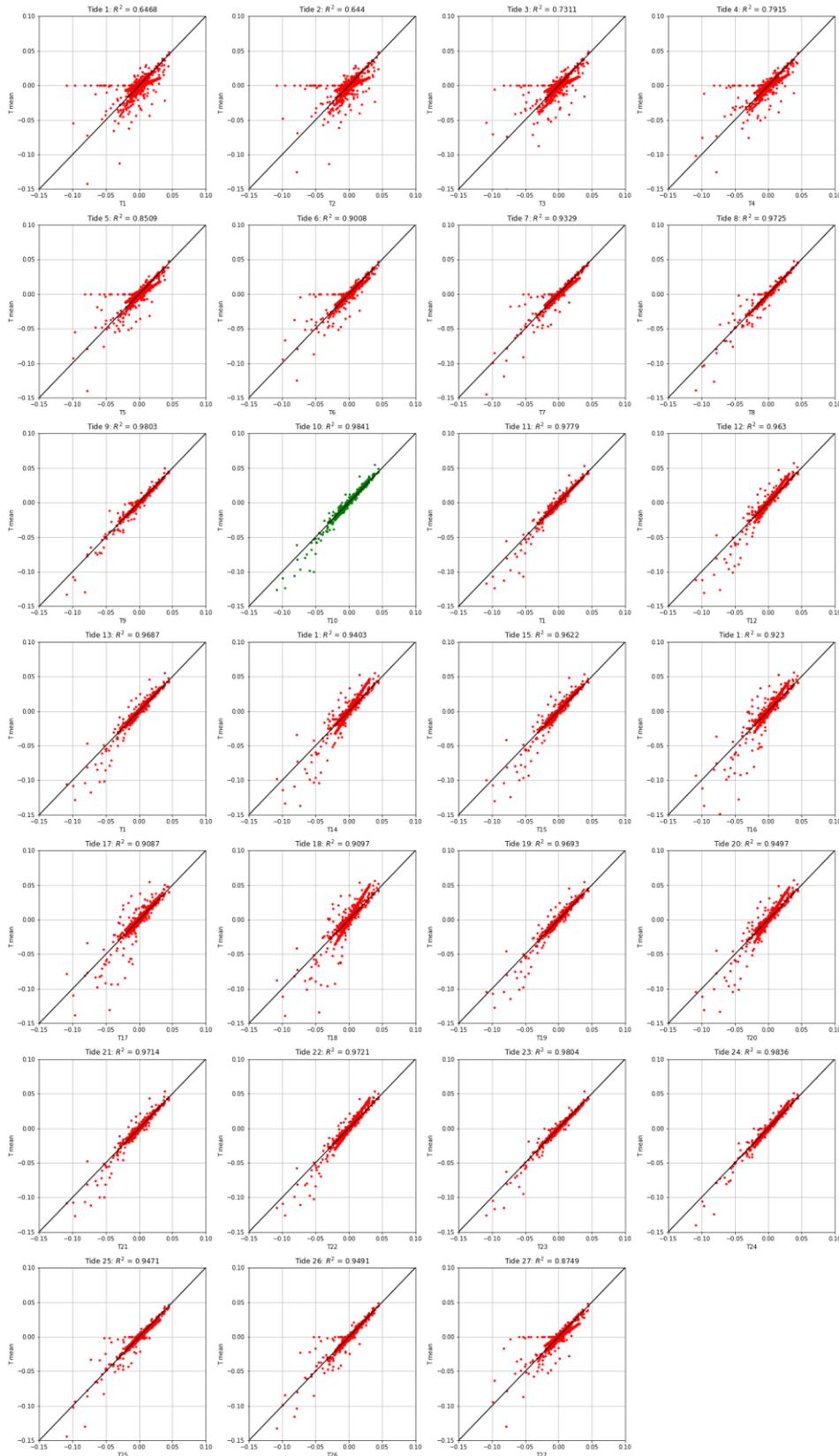
Figure 119: Correlation of the morphological change of a complete spring-neap tidal cycle with a single tide. Tide 10 has the largest coefficient of determination, and hence is used as the morphological tide.

Appendix D

Appendix D presents the numerical model input. It provides the settings for XBeach, the boundary conditions, grid and bathymetry.

D.1 Dissipation storm conditions

Table 18: Dissipation at nourished transects for wave conditions C9

Transect	D at bar [W/m]	D total T0, T1 [W/m]	D total T2, T3 [W/m]
1448	600	15000	15000
1469	1800	14800	15000
1489	3000	16000	16800
1509	2200	14800	15800
1530	2000	14700	15400
1550	100	16000	14300
1571	400	15600	15800
1591	1000	15000	15000
1612	1000	15000	17000
1632	1000	13200	13500
STD	**910**	**801**	**1061**
Mean	**1310**	**15010**	**15360**

Table 19: Dissipation at nourished transects for wave conditions C10

Transect	D at bar [W/m]	D total T0, T1 [W/m]	D total T2, T3 [W/m]
1448	5000	27000	28000
1469	8500	30000	32500
1489	8500	25000	30000
1509	6500	31000	27500
1530	8000	28000	30500
1550	1000	26500	22500
1571	5000	30000	30000
1591	5000	28000	28000
1612	4500	24500	27500
1632	4000	26500	28500
STD	**2343**	**2174**	**2646**
Mean	**5600**	**27650**	**28500**

D.2 Alternation of currents for different nourishment strategies
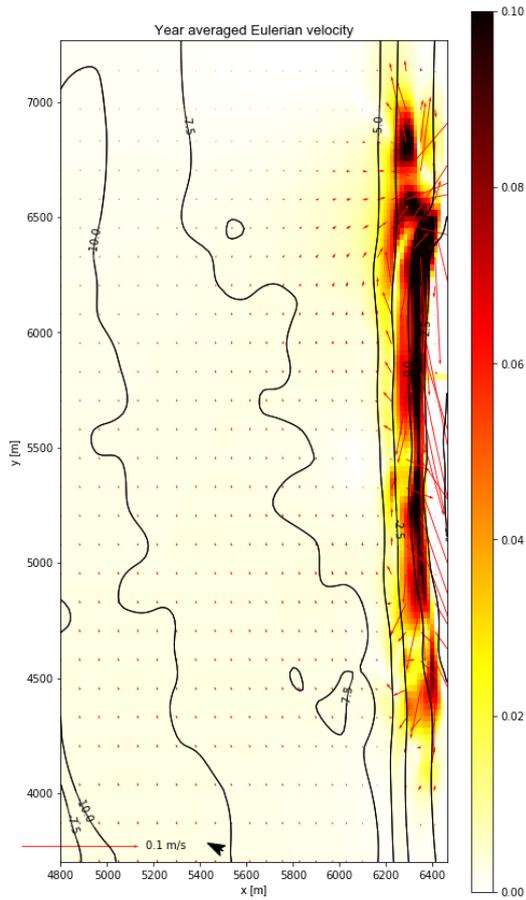
Figure 120: Year-averaged currents for T_1-T_0
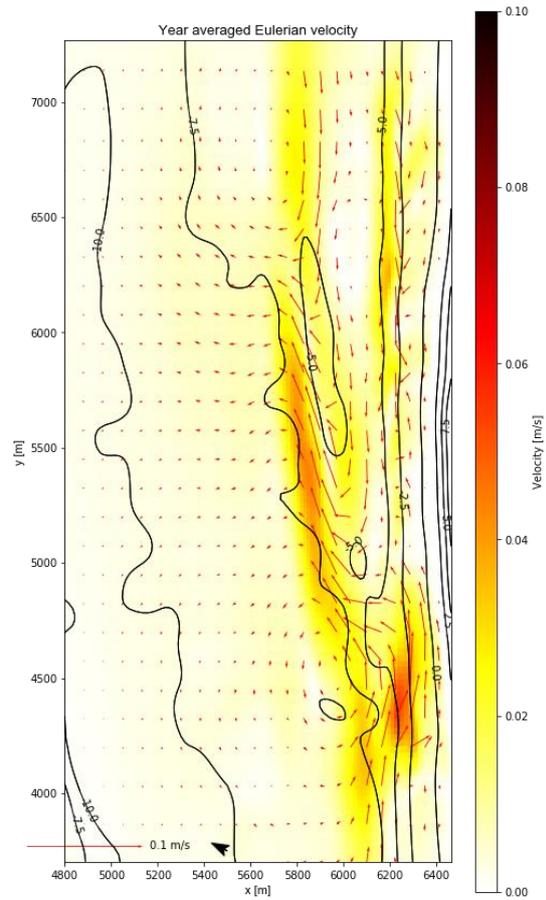
Figure 121: Year-averaged currents for T_2-T_0
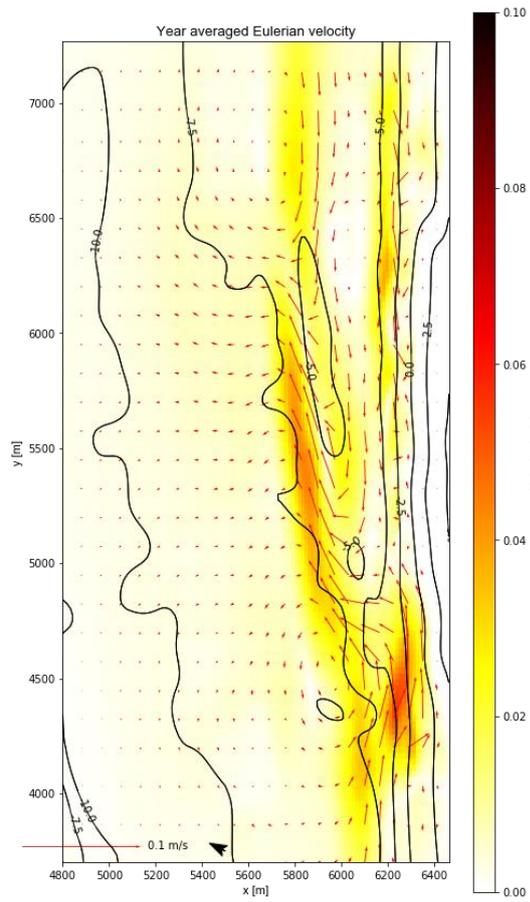
Figure 122: Year-averaged currents for T_3-T_1
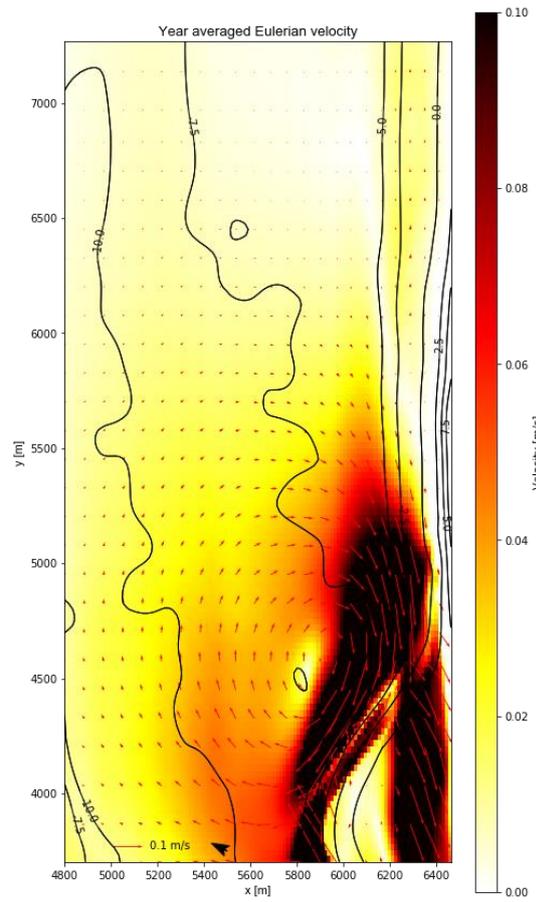

Figure 123: Year-averaged currents for T_4-T_0

D.3 Alternation of sediment transport for different nourishment strategies
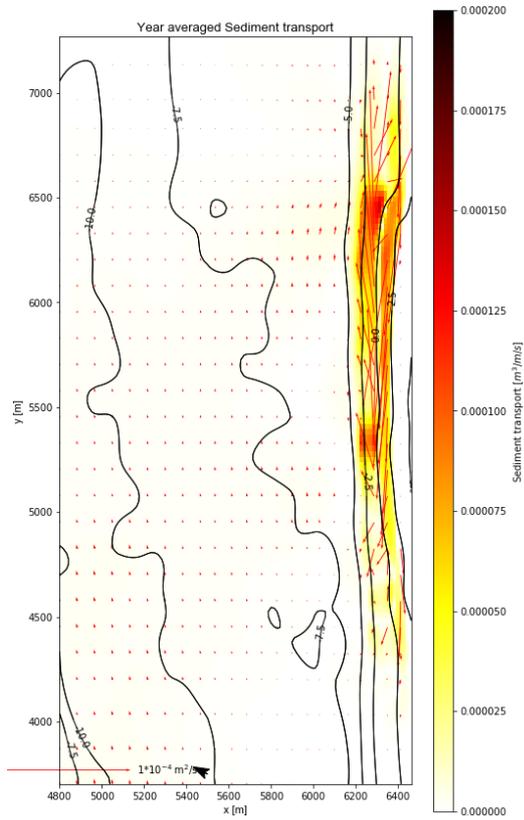
Figure 124: Year-averaged sediment transport for T_1 - T_0
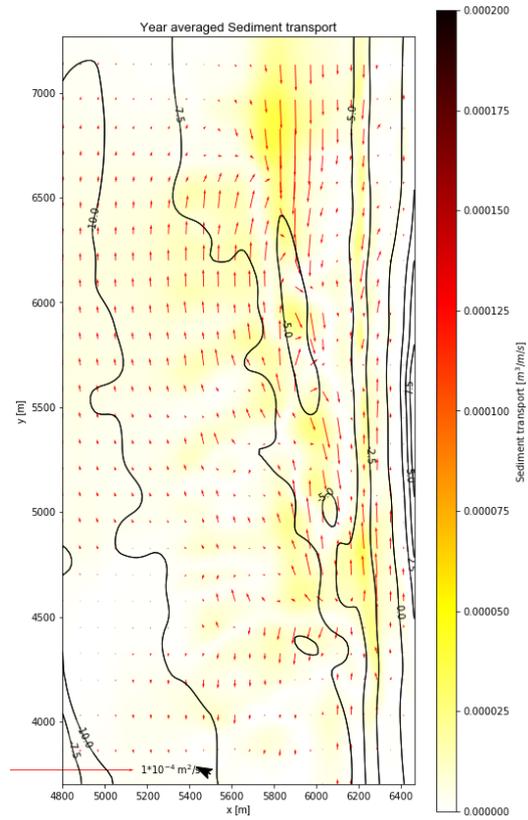
Figure 125: Year-averaged sediment transport for T_2 - T_0
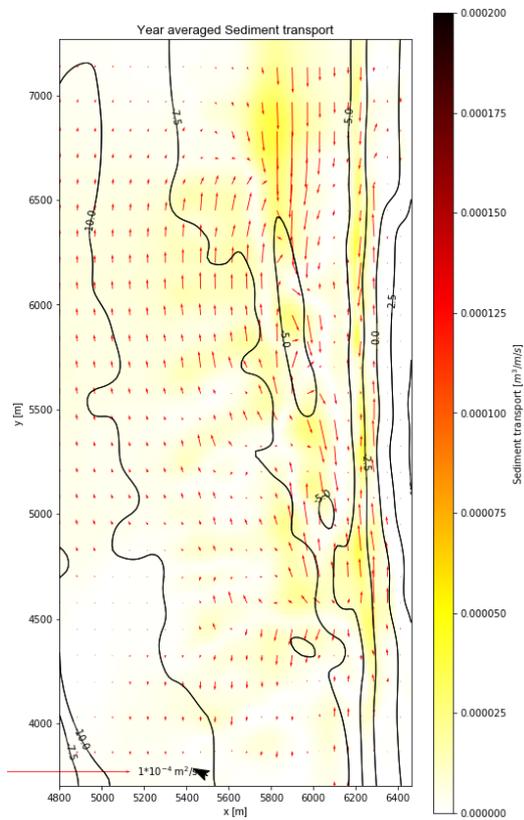
Figure 126: Year-averaged sediment transport for T_3 - T_1
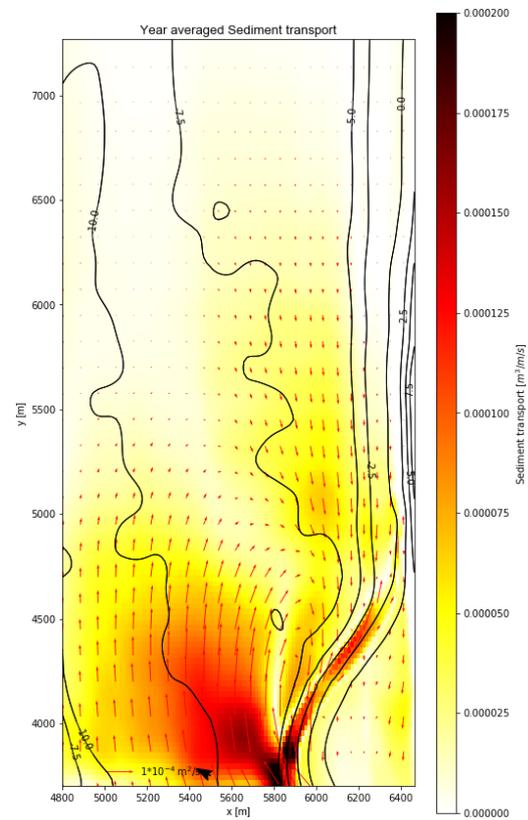
Figure 127: Year-averaged sediment transport for T_4 - T_0